Investigating the role of IL-4Rα mediated signalling on Foxp3^{+} T regulatory cells during cutaneous leishmaniasis

Rebeng Maine

Supervisor: Dr Ramona Hurdayal

Co-supervisor: Professor Frank Brombacher

Thesis presented for the degree of Master of Science in the Department of Molecular and Cell Biology University of Cape Town in fulfilment of the degree MSc in Molecular and Cell Biology

Department of Molecular and Cell Biology

Faculty of Science

University of Cape Town

January 2020

Plagiarism Declaration

‘I know the meaning of plagiarism and declare that all of the work in the dissertation (or thesis), save for that which is properly acknowledged, is my own’.

Signature: Signed by candidate

Acknowledgments

It is with sincerest gratitude that I would like to thank all those who contributed towards this MSc. thesis.

Firstly I would like to thank my supervisor Dr Ramona Hurdayal for being the best mentor, best tutor and best trainer. You provided me with strength during difficult moments, allowed me to work independently and work as part of team and were always there to provide a listening ear when I needed assistance. I will always cherish you and thank you for providing me with an environment to explore my passion for academic research. I would also like to thank Professor Frank Brombacher for all your assistance.

I would like to thank all the past and present members of the *Leishmania* research team. I would like to thank Dr Berenice Martinez-Salazar, Bernard Osero, Zama Cele, Raphael Aruleba, Fran Prenen, Aya Fouad, Bradley Wonderlink and Pamela Maimela for the hours spent together in the lab.

I would like to thank all the members of the Brombacher Group. I would to thank Julius Chia, and Dr Mumin Ozturk for the wisdom that they imparted, always going out their way to make sure I felt included as a member of the lab. To Shandré Pillay, Sibongiseni Poswayo and Martyna Scibiorek and Rachelle Van Der Colf thank you for all the memories.

I would like to offer my deepest gratitude to Dr Inssaf Berkiks and Dr Nada Abdel-Aziz for pushing me to explore beyond my limits. I would like thank all the Animal Unit staff for especially Dr Rodney Lucas for training me in mice handling. I would like to thank Munadia Ansari for genotyping the mice.

Lastly, this project would not have been completed without the support and love of my family and friends. Thank you to my Parents, Liyanda Lekalake and Potlaki Maine, my best friend Athi Welsh, my brother and sister, my two dogs, my cat and Khotso providing me with motivation

I dedicate this thesis to my late grandfather, Lawrence Lekalake.

Funding: This project was supported by the National Research Foundation (NRF),South Africa

Table of Contents

Plagiarism declaration 2
Acknowledgments 3
Table of contents 4
List of Figures and Tables 6
Abstract 8
1. Literature review 9
1.1 Leishmaniasis 9
1.2 Lifecycle of *Leishmania* parasites 10
1.3 Diagnosis and current treatment of cutaneous leishmaniasis 10
1.4 Use of murine models to understand immune polarization during cutaneous leishmaniasis 11
1.5 IL-4, IL-13 and the role of IL-4Rα chain 12
1.5.1 Defining the role of IL-4 and IL-13 during cutaneous leishmaniasis 12
1.5.2 The common IL-4Rα chain 13
1.6 Cell-specific IL-4Rα deletion mouse models in cutaneous leishmaniasis 14
1.7 The role of regulatory T cells in immunity 18
1.8 The role of regulatory T cells during cutaneous leishmaniasis 19
1.9 Project Rationale 21
1.10 Aim and Objectives 22
2. Material and Methods 23
2.1 Generation and genotyping of Foxp3^{cre}IL-4Rα$^{-/lox}$ mice 23
2.2 Ethics Statement 24
2.3 Preparation of *L. major* LV39 parasite culture from frozen stocks 24
2.4 *L. major* infections 24
2.4.1 Preparation of *L. major* culture growth curve and preparation for infection in mice 24
2.4.2 *L. major* footpad infection in mice 25
2.4.3 *L. major* ear infection in mice 25
2.4.4 Isolation of soluble *Leishmania* antigen from *L. major* cultures 26
2.5 Quantification of *L. major* parasite burden 26
2.5.1 Limiting Dilution Assay (LDA) to detect viable parasite burden 26
2.5.2 DNA extraction from *L. major* infected footpad samples 27
2.5.3 Endpoint PCR 28
2.6 Isolation and stimulation of draining lymph node cells 28
2.7 Flow cytometry analysis of lymph node cells 29
2.7.1 Extracellular surface staining 29
2.7.2 Intranuclear staining 29
2.7.3 Intracellular staining 30
2.8 Serum collection from blood samples 31
2.9 Nitric Oxide Synthase and Arginase activity 31
2.10 Enzyme-linked Immunosorbent Assay (ELISA) Analysis 32
2.10.1 Cytokine ELISA 32

2.10.2 Antibody ELISA 32
2.11 Statistical Analysis 33
3. Results 34
3.1 Preparation of *L. major* LV39 parasites for infection 34
3.2 Differential Cre-mediated deletion of IL-4Rα on Foxp3^{+} Treg cells between Foxp3^{cre}IL-4Rα$^{-/lox}$ male and female mice is maintained during *L. major* infection 34
3.3 Foxp^{3}IL-4Rα$^{-/lox}$ BALB/c male mice are hypersusceptible to *L. major* during footpad infection 37
3.3.1 Characterization of the clinical phenotype observed during *L. major* LV39 infection 37
3.3.2 Immunological responses observed at the cellular level 40
3.3.3 Immunological responses observed at the molecular level 42
3.4 An alternative infection route results in a similar disease outcome following *L. major* infection in experimental mice 46
3.4.1 Deletion of IL-4Rα signalling on T regulatory cells renders BALB/c male mice similarly hypersusceptible following inoculation of *L. major* parasites in the ear 46
3.4.2 Cytokine and antibody responses elicited in Foxp3^{cre}IL-4Rα$^{-/lox}$ male mice during *L. major* ear infection 47
3.5 Proposed mechanism in hypersusceptible *L. major*-infected Foxp3^{cre}IL-4Rα$^{-/lox}$ male mice 49
3.5.1 Enhanced IDO expression from dendritic cells is found in *L. major*-infected Foxp3^{cre}IL-4Rα$^{-/lox}$ male mice 49
3.5.2 PD-1 expression on Foxp3^{+} Treg cells is enhanced in *L. major*-infected Foxp3^{cre}IL-4Rα$^{-/lox}$ male mice 51
3.5.3 Differential IDO expression within *L. major*-infected Foxp3^{cre}IL-4Rα$^{-/lox}$ male mice could account for reduced T-bet^{+} Th1 cell recruitment 52
4. Discussion 54
5. References 65
6. Appendix 73
Supplementary Figures 75

Lists of Tables

1. Literature Review

Table 1.1: The number of reported cases of cutaneous leishmaniasis and visceral leishmaniasis in 2017

Table 1.2: The role of IL-4Rα signalling on various immune cell populations during *L. major* infection

Lists of Figures

2. Material and Methods

Figure 2.1: Schematic diagram representing the structure of the IL-4Rα gene on the Foxp3 promoter in IL-4Rα$^{-/lox}$ and Foxp3^{cre}IL-4Rα$^{-/lox}$ mice

3. Results

Figure 3.1: Growth curve of *L. major* LV39 promastigotes in preparation for infection

Figure 3.2: Efficient deletion of the IL-4Rα chain on T regulatory cells is maintained within Foxp3^{cre}IL-4Rα$^{-/lox}$ male mice during *L. major* infection

Figure 3.3: Deletion of the IL-4Rα chain is specific to T regulatory cells in *L. major* infected Foxp3^{cre}IL-4Rα$^{-/lox}$ female mice

Figure 3.4: Differential Cre-mediated deletion of the IL-4Rα chain on Foxp3^{+} Treg cells between female and male Foxp3^{cre}IL-4Rα$^{-/lox}$ mice is conserved during *L. major* infection

Figure 3.5: The absence of IL-4Rα signalling on T regulatory cells renders Foxp^{3}IL-4Rα$^{-/lox}$ male mice hypersusceptible to *L. major* infection; while Foxp^{3}IL-4Rα$^{-/lox}$ female mice remain as susceptible as their littermate control

Figure 3.6: The *L. major* parasite burdens are significantly increased in Foxp3^{cre}IL-4Rα$^{-/lox}$ male mice.

Figure 3.7: The *L. major* parasite loads are significantly increased in Foxp3^{cre}IL-4Rα$^{/lox}$ male mice.

Figure 3.8: Total cells in the lymph node of *L. major* infected male mice

Figure 3.9: Depletion of IL-4Rα signalling on Foxp3^{+} Treg cells alters Treg cell frequency and activity.

Figure 3.10: Enhanced Type 2 cytokine secretion occurs in Foxp3^{cre}IL-4Rα$^{-/lox}$ mice following *L. major* LV39 infection in the footpad.

Figure 3.11: Foxp3^{cre}IL-4Rα$^{-/lox}$ male mice display an elevated Type 2 humoral response following *L. major* LV39 footpad infection

Figure 3.12: Foxp3^{cre}IL-4Rα$^{-/lox}$ male mice display modulated killer-effector functions following *L. major* LV39 footpad infection.

Figure 3.13: Foxp3^{cre}IL-4Rα$^{-/lox}$ male mice following *L. major* LV39 ear inoculation display a hypersusceptible phenotype

Figure 3.14: Similar Type 2 immunity is enhanced in Foxp3^{cre}IL-4Rα$^{-/lox}$ male mice following ear inoculation with *L. major* LV39 promastigotes.

Figure 3.15: Dendritic cell populations within Foxp3^{cre}IL-4Rα$^{-/lox}$ mice show upregulated IDO, PDL-1 and CD80 expression following *L. major* infection

Figure 3.16: Deletion of IL-4Rα on Treg cells upregulates PD-1 expression following *L. major* infection

Figure 3.17: Deletion of IL-4Rα signalling on Treg cells enhances recruitment of Foxp3^{+} Treg cells and reduces recruitment of T-bet^{+} Th1 cells following *L. major* infection

4. Discussion

Figure 4.1 Deletion of the IL-4Rα chain on Foxp3^{+} Treg cells induces a Type 2 immune response during *L. major* infection.

Figure 4.2 Induced IDO production from dendritic cells concomitantly induces Treg cell production and reduces Th1 cell activity during *L. major* infection.

Abstract

In a murine model of *Leishmania major* infection, susceptible BALB/c mice develop a detrimental Type 2 immune response characterized by the production of interleukin (IL)-4 and IL-13, which single through a common receptor, the IL-4 receptor alpha chain (IL-4Rα). Forkhead box P3 (Foxp3^{+}) Regulatory T (Treg) cells are an unique subset of CD4^{+} T cells that play important immunomodulatory roles maintaining a balance between Type 1 and Type 2 immune responses. During *L. major* induced cutaneous leishmaniasis, Treg cells accumulation at the site of infection has been implicated in suppressing a detrimental Type 2 immune response by modulating early interleukin (IL)-4 production, however it remains unclear if IL-4Rα mediated signalling on Treg cells play a significant role in this process. To investigate this further, a novel BALB/c model was utilized in which the IL-4Rα chain was conditionally knocked out on Treg cells (Foxp3^{cre}IL-4Rα$^{-/lox}$ mice). We demonstrated that the differential IL-4Rα deletion efficiency in male (approximately 102 %) and female (approximately 32%) was maintained during *L. major* infection. Foxp3^{cre}IL-4Rα$^{-/lox}$ male mice, which had a greater degree of IL-4Rα deletion on Foxp3^{+} Treg cells, developed significant footpad swellings and ear swellings, increased parasitic burdens at the site of infection and within draining lymph nodes. This hypersusceptible phenotype observed in Foxp3^{cre}IL-4Rα$^{-/lox}$ BALB/c male mice was accompanied with an increased Treg cell activity and amplified Type-2 immune response with an increase in IL-4, IL-10 from *L. major*-infected lymph node samples and IgE antibody secretion in *L. major* infected serum samples. Flow cytometry analysis revealed that a *L. major*-induced Indoleamine 2,3 dioxygenase (IDO)-mechanism could allow for increased *Leishmania* replication. Collectively, these data suggest a protective role for IL-4Rα signalling on Treg cells in suppressing a detrimental Type 2 during cutaneous leishmaniasis.

1. Literature review

1.1 Leishmaniasis

Leishmaniasis is a highly prevalent vector-borne tropical disease, that is caused by parasites of the *Leishmania* genus and is transmitted to mammalian hosts by the bite of infected female sandflies (*Phlebotomus, Lutzymia)* [1, 2]. Globally, approximately 1.6 million new cases and 65000 deaths are estimated to occur annually and 1 billion people remain at risk of *Leishmania* infection [3]. Despite this high rate of morbidity and mortality, leishmaniasis is regarded as a disease of poverty as the majority of those affected are in less developed countries in South East Asia, Africa and South America [4]. The effects of urbanisation, deforestation and armed conflict have limited the diversity of mammalian hosts from which sandflies can take a blood meal, thus increasing the transmission to humans [5].

The disease exists as three main clinical manifestations. Cutaneous leishmaniasis, caused by *L. major*, *L. tropica* and *L. mexicana,* is the most prevalent form of the disease, as outlined in Table 1, leading to 1.2 million new infections annually and is characterised by the formation of disfiguring cutaneous lesions [2, 3, 6]. Mucocutaneous leishmaniasis, caused by *L. brazilensis* parasites, result in ulcer formation and destruction of the mucus membranes within the nose and mouse [7]. Visceral leishmaniasis, caused by *L. infantum* and *L. donovani* parasites, was prevalent in South East Asia, Africa, Eastern Mediterranean and the Americas (Table 1) and causes lethality if left untreated as parasites disseminate through the bloodstream and invade internal organs [3, 8].

Table 1.1: The number of reported cases of cutaneous leishmaniasis and visceral leishmaniasis in 2017 (WHO 2019) [3]

Region	**Cutaneous leishmaniasis cases in 2017**	**Visceral leishmaniasis cases in 2017**
Africa	13951	6050
Americas	49578	4422
Eastern Mediterranean	78040	5127
Europe	1056	180
South East Asia	3	6176
Western Pacific	7	190

1.2 Lifecycle of *Leishmania* parasites

Leishmania parasites have a digenetic lifecycle existing as flagellated promastigotes within the mid-gut of the infected sandfly and aflagellated amastigotes within the mammalian host [9]. Upon taking up of a blood meal by an infected sandfly, the promastigotes present within the microvilli of the midgut epithelium are ejected through the proboscis into the mammalian host [10]. Once within the mammalian host, promastigotes are subsequently phagocytosed by several antigen-presenting cells (APCs) including dendritic cells, macrophages and neutrophils. *Leishmania* promastigotes are able to overcome the microbicidal activity of the phagosome, preventing the formation of the phagolysosome, resulting in the formation of a parasitophorous vacuole [11]. The opportune conditions within the parasitophorous vacuole allow promastigotes to differentiate into amastigotes, which continue to replicate and upon cellular apoptosis are released to infect surrounding immune cells thus leading to the establishment of infection.

1.3 Diagnosis and current treatment of cutaneous leishmaniasis

The incidence of cutaneous leishmaniasis in human patients remains underreported as the development of a lesion may only occur after two weeks to three months post infection, therefore early disease diagnosis remains poor [12]. The disease is primarily diagnosed using parasitological techniques to detect amastigotes from biopsy specimen under a light microscope or immunohistochemistry [13]. However, the limitations of such techniques are that they have relatively low sensitivities , resulting in many *Leishmania* infections being misdiagnosed.

Consequently, molecular based methods have been utilised to amplify different target regions in *Leishmania* DNA. Different primer sequences to target repetitive Leishmania kinetoplast DNA (kDNA) or small subunit ribosomal RNA (SSU rRNA) via PCR have allowed for highly sensitive parasite detection as well as the identification of the particular *Leishmania* species in infected patients [13, 14].

There are currently no approved vaccines commercially available to prevent against cutaneous leishmaniasis and the front-line drug therapies available to reduce lesions include pentavalent antimonials, liposomal amphotericin B and miltefosine which target the *Leishmania* parasite [15]. Miltefosine treatment administered orally at a dose of 2mg/kg for 28 days has been shown

to have a 60-90% effectiveness rate [15]. Liposomal Amphoterin B deoxycholate administration intravenously at a dose of 25mg/kg significantly reduced lesion sizes following six days of treatment [16]. Pentavalent antimonials, such as Pentostam, are administered intramuscularly for a 20-day course at a dose of 20mg/kg/day; such compounds have a 90% effectiveness rate as they inhibit parasitic glycolysis and fatty acid oxidation [16]. However this drug treatment options have negative side effects associated which include cardiotoxicity, renal toxicity and nausea, and an increasing emergence of drug-resistant *Leishmania* populations [17, 18], therefore there remains a crucial need to understand the interaction between *Leishmania* parasites and their mammalian hosts to identify novel immunotherapeutic targets for effective disease management.

1.4 Use of murine models to understand immune polarization during cutaneous leishmaniasis

The introduction of *L. major* promastigotes into experimental mouse models has provided a robust model to investigate the immune evasion strategies utilized by *Leishmania* parasites, as well as immune response elicited in mammalian hosts during cutaneous leishmaniasis. BALB/c mice during *L. major* infection, display a susceptible phenotype that is characterized by parasite persistence and lesion development [19]. In contrast, C57BL/6 mice following 8 weeks of *L. major* infection, displayed a resistant phenotype showing a significant reduction in lesion size [20].

The resistant phenotype observed in C57BL/6 mice led to the *in vivo* characterization of a Type 1 immune response, defined by a reduction in IgG1 and IgE antibody serum levels and increased IgG2b and IgG3 antibodies. Interferon-gamma (IFN-γ) and IL-12 have been shown to directly enhance T helper 1 (Th1) cell development *in vitro* and *in vivo,* which are required for the resistant phenotype observed during *L. major* infection [21, 22]. Th1 cells, through the secretion of tumour necrosis factor (TNF), IL-12 and IFN-γ, activate the production of classically activated (M1) macrophages. M1 macrophages primarily regulate killing effector mechanisms through secretion of reactive oxygen species such as hydrogen peroxide (H_2O_2) and reactive nitrogen species intermediates such as nitric oxide (NO) that lead to the destruction of intracellular *Leishmania* parasites [11, 23].

In contrast, susceptibility to *L. major* infection observed in BALB/c mice has been attributed to the activation of Type 2 immune response. During a Type 2 immune response, IL-4 and IL-13 secretion have been shown to polarize naïve T cells towards Th2 cell development and directly inhibit IFN-γ production by Th1 cells. Th2 cells secretion of IL-4, IL-13 and IL-10, leads to the activation of alternatively activated (M2) macrophages that secrete arginase 1. Arginase 1 (Arg1) secretion depletes the common L-arginine substrate, that is required by induced nitric oxide synthase (iNOS) for NO production; this leads to an inhibition of M1 macrophage activation and a reduction in a Type 1 immune response. *L. major* parasites are able to evade the killing-effector mechanisms of M1 macrophages, by enhancing IL-4 and IL-13 secretion, leading to M2 macrophage activation thereby enabling sustained intracellular replication [11, 24]. The Type 2 immune response in infected BALB/c mice further differs from a Type 1 immune response, as higher levels of IgE and IgG1 serum antibodies have been reported [25].

1.5 IL-4, IL-13 and the role of IL-4Rα chain

1.5.1 Defining the role of IL-4 and IL-13 during cutaneous leishmaniasis

Murine IL-4 and IL-13 have been identified as canonical cytokines that maintain Type 2 immune response, observed in susceptible BALB/c mice during *L. major* infection. IL-4 has a molecular weight of 14-19 kDA and IL-13 has a molecular weight of 10-14 kDA and both are localised on chromosome 11 [26]. Although IL-4 and IL-13 are key immunoregulatory cytokines required for the initiation of a Type 2 immune response, they are initially secreted in both BALB/c mice and C57BL/6 mice during the early stages of infection [27, 28]. Various immune cells have been identified as producers of IL-4 and IL-13 such as innate immune cells including dendritic cells, basophils, natural killer T cells, mast cells and adaptive immune cells including Th2 cells and B effector 2 (Be2) B cells [26].

Despite this early IL-4 production in both strains, IL-4 signalling is short-lived in resistant C57BL/6 mice and is sustained in susceptible BALB/c mice [28]. The observed differences in IL-4 signalling between the two different strains of mice, led to the emergence of research centred around establishing a mechanism that could explain the contrasting disease phenotypes observed.

IL-13 signalling is critical for enhancing susceptibility during *L. major* infection. Matthew *et al.* (2000) showed that *L. major* infected IL-13 deficient BALB/c mice (IL-13$^{-/-}$) developed

significantly reduced footpad swellings similar to that of genetically resistant C57BL/6 mice, suggesting that IL-13 signalling is also required to inhibit the activation of Type 1 immune response which reduces *L. major* survival [9, 29].

On the other hand, IL-4 signalling during *Leishmania* infection seems to play a dual role in polarising the immune response. IL-4 is considered a key cytokine for the establishment of a Type 2 immune response, as it is able to downregulate the secretion of IFN-γ and IL-12, that leads to enhanced susceptibility to *L. major* infection [25, 30]. However, Bierdermann *et al.* (2001) provided a novel role that suggested that during *L. major* infection early IL-4 production is required initially to drive IL-12 production in dendritic cells, leading to the establishment of a Type 1 immune response [27].

During *L. major* infection, $V\beta4^+$ $V\alpha8^+$ $CD4^+$ T cell population have been identified as significant contributor's to early IL-4 production and sustaining IL-4 expression at the site of infection [31]. These $V\beta4^+$ $V\alpha8^+$ $CD4^+$ T cells specifically recognise and respond to the *Leishmania* homolog of receptors for activated C kinase (LACK) antigen from *L. major* parasites, leading to enhanced IL-4 production within 16 hours post infection, during which immune polarisation begins [32].

Notably however, although during *L. major* infection IL-4 is initially required by dendritic cells to establish a Type 1 immune response [27], early production of IL-4 from $V\beta4^+$ $V\alpha8^+$ $CD4^+$ T cells has been simultaneously shown to initiate a Type 2 immune response suggesting cell-specific differences for IL-4 signalling at the same time point [32].

1.5.2 The common IL-4Rα chain during cutaneous leishmaniasis

The IL-4 receptor alpha (IL-4Rα) chain is a 140kDA complex that has been found to be ubiquitously expressed on an array of immune cells including keratinocytes, macrophages, dendritic cells, B cells and T cells [6, 26]. The IL-4Rα chain serves as an integral monomer in both IL-4 and IL-13 receptors [33, 34]. The IL-4Rα chain integrates with the gamma common chain forming the Type 1 IL-4Rα or it integrates with the IL-13 binding receptor 1 (IL-13Rα1) forming the Type 2 IL-4α/IL-13Rα1 which binds to IL-13 with higher affinity [34, 35]. The IL-4Rα chain, in combination with signal activation of JAK/STAT6 pathway, have been shown to be crucial for IL-4 and IL-13 mediated functions [36]. Experiments using anti-IL-4Rα

antibodies, were found to inhibit IL-4 and IL-13 signalling via IL-4Rα chain, thereby inhibiting their ability to mediate a Type 2 immune response [37, 38].

Given that both IL-4 and IL-13 signal via the IL-4Rα and that these cytokines modulate a Type 2 immune response, that leads to parasite persistence during *L. major* infection, initial studies used global IL-4Rα deficient (IL-4Rα$^{-/-}$) BALB/c mice, to dissect the mechanism by which IL-4/IL-13 signalling directs the immune response [25, 39]. Despite the hypothesis that a Type 1 protective immune response would be elicited, IL-4Rα$^{-/-}$ BALB/c mice were only able to control acute *L. major* infection for 80 days post infection. Following 80 days post infection, these IL-4Rα$^{-/-}$ BALB/c mice developed increasing footpad lesions indicating that *L. major* parasites were able to dampen the host's immune system allowing for sustained parasite replication [25]. In contrast, IL-4-deficient and IL-13-deficient BALB/c mice displayed sustained resistant phenotypes, implicating that IL-4 and IL-13 as key cytokines in modulating susceptibility to *L. major* [25, 29]. Collectively, these studies indicated that susceptibility to *L. major* may be modulated by a combination of IL-4/IL-13 directed mechanisms and mechanisms acting independently of either cytokine.

The emergence of a sustained Type 2 immune response even in the absence of the IL-4Rα chain on all hematopoietic cells [25], led to the development of cell-specific IL-4Rα mice models to explore whether IL-4Rα signalling on different innate immune cells or adaptive immune cells has an effect on modulating immunity.

1.6 Cell-specific IL-4Rα deletion mouse models in cutaneous leishmaniasis

The utilisation of the cre/*lox*P genetic recombination system, originally identified within bacteriophages, has allowed for the generation of murine models in which to assess the IL-4R α chain at a cellular level [40]. During embryonic development cyclization recombinase (Cre) expression is directed by cell-specific promotors flanked by *lox*P sites, to selectively delete the IL-4Rα chain on specific cell populations under control of a cell-specific promoter [26]. The cre/*loxP* system has provided an efficient targeting strategy to establish the role of IL-4Rα signalling within particular cell populations.

As early produces of IL-4 and abundant innate-like cells contained in the skin, which serves as the primary site of infection during cutaneous leishmaniasis, keratinocytes provided a favourable cell population for further investigation [41]. A keratinocyte-specific deletion of IL-4Rα in KRT14^{cre}IL-4Rα$^{-/lox}$ BALB/c and C57BL/6 mice generated, to characterize whether

IL-4Rα signalling on this innate-like cell population contributes to susceptibility during *L. major* infection [42]. In *L. major* infected KRT14^{cre}IL-4Rα$^{-/lox}$ C57BL/6 mice and their littermate control mice developed similar lesion sizes accompanied by similar parasite burdens [43]. Similarly, KRT14^{cre}IL-4Rα$^{-/lox}$ BALB/c mice and their littermate control mice developed similar increased lesion sizes during *L. major* infection [42, 43]; this indicated that IL-4Rα signalling on keratinocytes does not contribute to the initiation of a Type 2 immune response in BALB/c or Type 1 immune response in C57BL/6 mice during *L. major* infection.

Following *Leishmania* inoculation innate macrophages, neutrophils and dendritic cells flux to the site of infection, are capable of phagocytosing invading parasites, and play key roles in determining Type 1 or Type 2 immune polarization [44]. The sustained Type 2 immune response observed in global IL-4Rα deficient mice, led to the proposition that IL-4Rα signalling on T cells did not solely drive Th2 cell polarization or lead to enhanced susceptibility to *L. major* infection [39, 45]. Subsequently, Holscher *et al.* (2006) proposed that the non-healing susceptible phenotype observed in BALB/c mice was driven by altering the polarization of macrophages, as they primarily regulate intracellular *Leishmania* parasite killing [45]. Previous studies have shown that neutrophils are also able to regulate intracellular *Leishmania* killing by forming neutrophil extracellular traps or by activating M1 macrophages killer effector functions through TLR4 recruitment [44, 46]. In order to assess if IL-4Rα signalling on macrophages and neutrophils played any role in modulating Type 1 or Type 2 immune response, BALB/c mice were genetically engineered in which the IL-4Rα chain was selectively deleted on macrophage and neutrophil populations (LysM^{cre}IL-4Rα$^{-/lox}$) [47]. The absence of IL-4Rα signalling on macrophages and neutrophils led to delayed establishment of *L. major* infection in BALB/c mice up to 13 weeks post infection, which was attributed to inhibition of M2 macrophage activation and enhanced NO production by M1 macrophages [45]. Collectively, this data suggested that IL-4Rα signalling modulates M2 macrophage activation allowing for initial *Leishmania* replication in BALB/c mice.

The functional ability of dendritic cells to serve as innate cells that are able to initiate adaptive immunity through antigen-presentation [48], provided them as a favourable cell population for further analysis. To characterize the functional role of IL-4Rα signalling on dendritic cells during *L. major* infection, dendritic-cell specific deletion of the IL-4Rα chain was generated in a murine model (CD11c^{cre}IL-4Rα$^{-/lox}$ BALB/c mice) [6]. A more susceptible phenotype was observed in CD11c^{cre}IL-4Rα$^{-/lox}$ mice, in comparison to the littermate control mice, that was

made evident by necrotic lesion development, up-regulation of a Type 2 immune response and *L. major* parasite dissemination into the brain [6]. The impairment of dendritic cells to activate NO killing effector mechanisms prevented the elimination of intracellular parasites in these infected mice [6]. This data gave new insight that indicated that signalling through the IL-4Rα chain is required for the activation of killing-effector mechanisms employed by dendritic cells [49], thus suggesting that IL-4Rα signalling on dendritic cells provides a protective role during *L. major* infection.

As part of the acquired immune cells, B lymphocytes were initially thought to only contribute towards host protection or susceptibility to *L. major* infection through immunoglobulin production [50, 51]. Subsequent studies have revealed that stimulated B cells, like T cells, can be defined as B effector 1 (Be1) cells and B effector 2 (Be2) cells that are able to produce a range of polarizing cytokines including IFN-γ, IL-12 and IL-4 and IL-13 respectively [52, 53]. Signals from Th2 cells and the IL-4/IL-4Rα signalling pathway have been reported to be critical for differentiation of IL-4 secreting Be2 cells, which in turn are able to maintain $CD4^+$ Th2-dependent immune responses [53], however the specific role of IL-4Rα signalling on cytokine-producing B cells during *L. major* infection remained unknown.

To dissect the role of IL-4Rα-responsive B cells during cutaneous leishmaniasis, a BALB/c murine model was utilized in which the IL-4Rα chain was selectively deleted on B cells ($mb1^{cre}$IL-4R$\alpha^{-/lox}$ mice) [54]. During *L. major* infection, $mb1^{cre}$IL-4R$\alpha^{-/lox}$ BALB/c mice showed enhanced control of the disease as they had reduced footpad swellings and a significant reduction in parasite burden in the footpad [55]. This improved resistant phenotype observed in the absence of IL-4Rα B cells was due to a reduced Type 2 immune response, indicated by significantly lower IL-4, IL-13 and IgE levels and consequently a shift towards a Type 1 immune response was observed to control parasite replication [55]. Collectively, this data indicated that IL-4Rα signalling on B cells has a detrimental function during *L. major* infection, as it contributes to enhancing a susceptible Type 2 immune response.

Murine models of *L. major* infection have delineated that the resistant phenotype observed in C57BL/6 mice is promoted by Th1 cells and the susceptible phenotype in BALB/c mice is counter-regulated by Th2 cells [19, 56]. Given that IL-4 signalling solely had been shown to have a crucial role in Th2 cell development [57, 58], a $CD4^+$ T cell specific deletion of the IL-4Rα chain was genetically engineered in BALB/c mice (Lck^{cre}IL-4R$\alpha^{-/lox}$ BALB/c) to elucidate

the role of IL-4Rα signalling on $CD4^+$ T cells [59]. Lck^{cre}IL-$4R\alpha^{-/lox}$ BALB/c mice had significantly reduced footpad swellings, reduced parasite burdens in the footpad and draining lymph nodes, accompanied with elevated IFN-γ and IL-12 levels similar to resistant C57BL/6 mice [59]. Subsequent studies showed that $iLck^{cre}$ IL-$4R\alpha^{-/lox}$ BALB/c mice, in which there was pan T cell-specific IL-4Rα deletion, where also able to control *L. major* infection similar to Lck^{cre}IL-$4R\alpha^{-/lox}$ BALB/c and C57BL/6 mice [60]. These data indicated that signalling via IL-4Rα on T cell populations ($CD4^+$, $CD8^+$, $\gamma\delta^+$ and natural killer T cells) has a detrimental role as it contributes to the susceptible phenotype observed in BALB/c mice; however since this pan T-cell specific IL-4Rα deletion model the specific contribution of T regulatory cells remained unclear.

Collectively, these IL-4Rα-deficient murine models have indicated that IL-4Rα signalling can modulate disease outcome during cutaneous leishmaniasis due to its differential role in immune cell populations (Table 1.2). This differential role of IL-4Rα signalling has prompted further investigation regarding the modes of action of IL-4/IL-13 signalling on an additional T cell population that plays a crucial modulatory role: the regulatory T cell population.

Table 1.2: The role of IL-4Rα signalling on various immune cell populations during *L. major* infection

Cell Type – IL-4Rα Deficient Mouse Strain	Role of IL-4Rα signalling (Protective or Detrimental)	Disease phenotype during IL-4Rα deficiency
All Cells (IL-4Rα $^{-/-}$)	Both	Resistant during acute phase of *L. major* infection; becomes susceptible eleven weeks post infection [25]
Keratinocytes (KRT14^{cre}IL-4Rα$^{-/lox}$)	Neither	Susceptible phenotype observed similar to littermate controls [42]
Macrophages and Neutrophils (LysM^{cre}IL-4Rα$^{-/lox}$)	Detrimental	Resistant phenotype driven by inhibition of M2 macrophage activation and increased NO production [45]
Dendritic Cells (CD11c^{cre}IL-4Rα$^{-/lox}$)	Protective	Hypersusceptible phenotype due to inhibition of dendritic cell mediated killer-effector mechanisms [6]
B Cells (*mb*1^{cre}IL-4Rα$^{-/lox}$)	Detrimental	Resistant phenotype driven by reduction in Type 2 immune response [55]
CD4^{+} T cells (Lck^{cre}IL-4Rα$^{-/lox}$)	Detrimental	Resistant phenotype driven by increased Th1 cytokine secretion [59]
Non CD4^{+} T cells (iLck^{cre} IL-4Rα$^{-/lox}$)	Detrimental	Increased resistant driven by activation of Type 1 immune response [60]

1.7.1 The role of regulatory T cells in immunity

Regulatory T (Treg) cells are a unique subset of CD4^{+} T cells whose immunosuppressive activities are crucial for maintaining immune homeostasis and tolerance to self-antigens [61]. Similar to other T cells, Treg cells are derived from progenitor cells in the bone marrow and require intermediate signalling via the TCR for successful development [62, 63]. Human Treg and mouse Treg cells were initially distinguished from other T cell populations by cluster of differentiation 4 (CD4) and CD25 [64, 65]. However, as other T cell population also co-express these markers, subsequent studies revealed that forkhead box P3 (Foxp3) expression can be used as a specialized marker to discriminate Treg cells from effector and memory T cells which are also CD4^{+} CD25^{+}, as Foxp3 acts as a master transcription factor that drives the development and function of Treg cells [66-68]. Foxp3 belongs to the forkhead/winged helix transcription factor family and is located on the X-chromosome [69]. The Foxp3 protein is 48kDA and

consists of 4 distinct domains: forkhead domain, leucine zipper, zinc-finger and repressor domains, which are required for Foxp3 transcriptional repressive activity [70, 71]. The importance of $Foxp3^+$ Treg cells as modulators of the immune system has been established in Scurfy mice and human patients with immunodysregulation, poly-endocrinopathy and enteropathy, X-linked syndrome (IPEX), as mutations in Foxp3 genes lead to a loss in functional Treg cells resulting in the development of fatal autoimmune disease that causes lethality in 4-5 week old mice [72, 73].

Several mechanisms are employed by $Foxp3^+$ T reg cells to achieve an immunosuppressive effect which include the production of suppressive cytokines- IL-10, IL-35 and transforming growth factor beta (TGF-β) [65]. Treg cell-derived IL-10 and TGF-β have been identified having crucial roles in mediating the host immune response during *Mycobacterium tuberculosis* (*Mtb*) infection, suppressing colitis in an Inflammatory Bowel Disease (IBD) mouse model and inhibiting airway allergic responses in sensitized mice [74-77]. Gondek *et al.* (2005) provided an additional suppressive mechanism by which Treg cell secretion of granzyme B induced cytolysis of effector T cells [78]. Subsequent studies have shown that Treg cell expression of granzyme B induces apoptosis of B cells, Natural killer (NK) cells and $CD8^+$ cytotoxic T cells [79, 80]. Treg cells, through their expression of inhibitory receptors such as co-stimulatory molecule cytotoxic T-lymphocyte antigen (CTLA-4), or programmed death-1 (PD-1) are additionally able to induce immunosuppression by modulating the function of dendritic cells [81]. CTLA-4 or PD-1 interaction with CD80/86 or programmed death ligand 1 (PD-L1) on dendritic cells, induces dendritic cells to produce immunosuppressive molecules such as Indoleamine 2,3 dioxygenase (IDO), thereby suppressing effector T cell activation [82]. IDO as an immunosuppressive enzyme promotes Treg cell differentiation and diminishes the levels of tryptophan, which has been reported to skew T helper polarization [83].

1.8 The role of regulatory T cells during cutaneous leishmaniasis

Although the suppressive functions of Treg cells had been well characterised, the role of Treg cells during cutaneous leishmaniasis remains unclear, as some studies have proposed a protective role, whilst others have suggested a detrimental role for Treg cells during *L. major* infection. Treg cells have been postulated to play a critical role in minimizing the levels of tissue damage during cutaneous leishmaniasis, due to their modulatory abilities that allow them to maintain homoeostasis between Th1 and Th2 cells [84, 85]. In a murine model of *L. major*

infection Foxp3$^+$ Treg cells were shown to accumulate at the site of infection and a similar finding was noted in skin lesions from human patients that were diagnosed with cutaneous leishmaniasis [84, 86].

Aseffa *et al.* (2002) showed that CD4$^+$CD25$^+$ T reg cells were able to control early IL-4 production by acting on the IL-4 secreting Vβ4 Vα8 CD4$^+$ T cell population [20]. Depletion of the CD4$^+$CD25$^+$ Treg cell population in BALB/c mice resulted in increased levels of IL-4 expression and rendered these mice more susceptible to *L. major* infection [20]. This data suggested that Treg cells have a protective role during cutaneous leishmaniasis, as they play an important role in inhibiting early IL-4 production thereby reducing the adverse effects of a Type 2 immune response.

In contrast, Suffia *et al.* (2005) showed that depletion of α_E chain (CD103), which is required for the homing of Treg cells to the site of infection, led to increased resistance in BALB/c mice during *L. major* infection [87]. In previously infected C57BL/6 mice, re-challenge with *L. major* parasites led to the aggregation of CD4$^+$CD25$^+$ Treg cells at the initial site of infection, where they inhibit effector T cells ability to control parasite replication [88]. Treg cells sustained inhibition of effector T cells could therefore lead to *Leishmania* parasite persistence and reactivation of infection [86, 88]. Collectively, these data suggest that Treg cells also play a detrimental role during *L. major* infection and this enables sustained *Leishmania* replication during cutaneous leishmaniasis.

Currently, there is no definitive role of Foxp3$^+$ Treg cells during cutaneous leishmaniasis as this T cell population is able to contribute to host protection against and lead to sustained *L. major* replication at the site of infection. While Treg cells are required to suppress a detrimental Type 2 response, excessive Treg cell accumulation leads to *L. major* persistence, which suggests that for effective protection against *L. major* infection a balance is required between Treg cells and effector T cells [20, 84, 87].

Research that focuses on Treg cell regulation has identified that IL-4, along with various other cytokines, are required to modulate Treg function [89]. Previous studies have found that reduced Foxp3 expression on Treg cells, lead to their reverting to Th2-like cells, which secrete cytokines such as IL-4 and IL-2 and express transcription factor gata binding protein 3

(GATA3); indicating evidence of plasticity between Th2 and Treg cell populations [90-92]. A previous study has shown that IL-4 signalling via STAT6 was required to maintain to Foxp3 expression in $CD4^+CD25^+$ Treg cells [36]; indicating that IL-4 has a stimulatory effect on Treg cell development. In contrast, Wei *et al.* (2007) showed that IL-4 secretion by Th2 cells can inhibit TGF-β-mediated Treg cell differentiation from naïve $CD4^+$ T cells [93]; indicating that IL-4 also has an inhibitory effect on Treg cell development. Given the apparent contradictory effects of IL-4 on Treg cell development, the effects of signalling via the IL-4Rα chain may provide further insight with regards to Treg cell development and modulation in *vivo*.

Although Treg cells act to inhibit early IL-4 production [20], IL-4 signalling via the IL-4Rα complex was required to drive Foxp3 expression, highlighting its importance in influencing the immunomodulatory activity of Treg cells [20, 36]. IL-4Rα mediated signalling was also shown to act on Th cells to increase their resistant to the suppressive activity of Treg cells; which further provides an undiscovered role for IL-4Rα signalling in modulating $Foxp3^+$ Treg cell function in different disease settings [36].

1.9 Project Rationale

The influence of IL-4Rα signalling on $Foxp3^+$ Treg cells has been limited as it has only been reported during the context of helminth infection [89]. Treg cells have been identified as a crucial $CD4^+$ T cell population involved in modulating the host's immune response during cutaneous leishmaniasis, however the influence of IL-4Rα signalling on $Foxp3^+$ Treg cells during *L. major* infection remains unknown. To enable further investigation into this signalling pathway, a *L. major* model of infection was established in BALB/c mice that were engineered, using the cre/*lox*P system, to selectively delete the IL-4Rα chain on Treg cells under the control of the *Foxp3*$^+$ locus ($Foxp3^{cre}$IL-$4R\alpha^{-/lox}$ mice) [89]. This present study attempted to provide a potential mechanism of action of IL-4Rα signalling that can be targeted to enhance mammalian host's immunity during cutaneous leishmaniasis

1.10 Aim and Objectives

The aim of this study is to dissect the role of IL-4Rα signalling on Treg cells during cutaneous leishmaniasis

To achieve this aim, we set forth the following objectives:

- To confirm efficient Cre-mediated deletion of IL-4Rα on Foxp3^{+} Treg cells during *L. major* infection
- To characterize the clinical phenotype observed between male and female Foxp3^{cre}IL-4Rα$^{-/lox}$ mice following *L. major* infection
- To characterize the immune responses at cellular and molecular levels elicited in male Foxp3^{cre}IL-4Rα$^{-/lox}$ male mice during footpad infection
- To characterize the immune response at a cellular and molecular elicited during an ear infection
- To provide a proposed mechanism for immune response generated in Foxp3^{cre}IL-4Rα$^{-/lox}$ male mice during *L. major* infection

2. Material and Methods

2.1 Generation and genotyping of Foxp3^{cre}IL-4Rα$^{-/lox}$ mice

T regulatory cell-specific IL-4Rα deficient (Foxp3^{cre}IL-4Rα$^{-/lox}$) BALB/c mice were generated using the cre/*lox*P system and characterised as previously described [89]. Briefly, Foxp3^{cre} mice were crossed with IL-4Rα$^{-/-}$ BALB/c mice [25] and IL-4Rα$^{lox/lox}$ BALB/c mice [47] to generate hemizygous Foxp3^{cre}IL-4Rα$^{-/lox}$ BALB/c mice. During cutaneous leishmaniasis experiments, the following mice groups were included as controls: IL-4Rα$^{-/lox}$ (hemizygous littermate), global IL-4Rα$^{-/-}$, wild type BALB/c mice and C57BL/6 mice. All mice were housed in specific-pathogen-free conditions in individually ventilated cages within the Animal Unit Facility of Health Science Faculty, University of Cape Town. All experimental mice were age and sex-matched and used between 8-10 weeks of age. Mice were genotyped using PCR, by Miss Munadia Ansarie (Division of Immunology), to confirm *il-4rα* exons 7-9 were removed (Figure 1) from the genome of Foxp3^{cre}IL-4Rα$^{-/lox}$ mice, as previously described [89], using specific primers: Forward 5'-CTG CTT CCT TCA CGA CAT TCA AC-3' and Reverse 5'-AAG TGC TTT GTG CGA GTG GAG AGC-3' (IDT, South Africa).

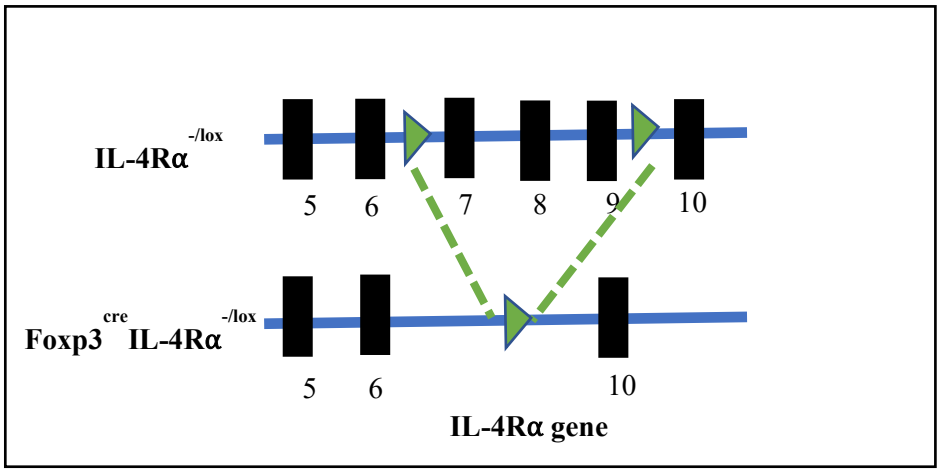

Figure 2.1: Schematic diagram representing the structure of the IL-4Rα gene on the Foxp3 promoter in IL-4Rα$^{-/lox}$ and Foxp3^{cre}IL-4Rα$^{-/lox}$ mice (Adapted from Abdel Aziz *et al.* 2018 [89])

2.2 Ethics Statement

This study was performed in strict accordance with recommendations of the South African National guidelines. All mice experiments were performed according to protocols approved by the Science Faculty Biological Safety Committee, BSC005_2016 and by the Animal Research Ethics Committee at the Faculty of Health Sciences, University of Cape Town (Permit numbers: 015/034 and 019/001; South African Veterinary Council Authorisation number: AR18/1696). All efforts were made to minimize the suffering of the animals.

2.3 Preparation of *L. major* LV39 parasite culture from frozen stocks

L. major LV39 (MRHO/SV/59/P) parasite stocks were stored in liquid nitrogen. A total of $2x10^8$ parasite pellet were stored in a 2 ml cryovial (Corning, USA) containing medium 199 (M199) (Gibco, USA) supplemented with 8% dimethyl sulphoxide (DMSO) (Sigma-Aldrich, USA) and 92% fetal bovine serum (FBS) (Thermofischer Scientific Pierce, USA). To generate a viable parasite culture, a *L. major* LV39 stock was defrosted at room temperature, resuspended in 8 ml 1x phosphate buffered saline (PBS), pH 7.4, and centrifuged at 23°C for 10 minutes at 3000rpm. The parasite pellet was resuspended in 10 ml 1xPBS and pelleted by centrifugation at 23°C for 10 minutes at 3000rpm. The parasite pellet was resuspended in 5 ml M199 supplemented with 10 % FBS, 50 units/ml penicillin and 50 µg/ml streptavidin (complete M199), transferred to a $25cm^3$ tissue culture flasks (Corning, USA) and subsequently incubated at 26°C. An equivalent volume of complete M199 was added to the $25cm^3$ tissue culture flasks once the parasites reached confluency.

L. major in vitro cultures were maintained by subculturing as previously described [25]. Briefly, parasite cultures were maintained by weekly subculturing 1:50 of *L .major* LV39 parasites into new tissue culture flask containing 10 ml complete M199 and incubated at 26°C.

2.4 *L. major* infections

2.4.1 Preparation of *L. major* culture growth curve and preparation for infection in mice

L. major in vitro cultures were subcultured as described above, however in preparation for infection *L. major* LV39 promastigotes were transferred from $25cm^3$ tissue culture flasks to 50 ml Falcon tube and centrifuged at 4000rpm for 10 minutes at 23°C. The parasite pellet was resuspended and washed twice in 1xPBS, and subsequently centrifuged at 3000rpm for 10 minutes at 23°C. Following resuspension in 3 ml 1xPBS, parasites were fixed in 4%

paraformaldehyde and counted using a Neubauer haemocytometer. To initiate a growth curve $10x10^6$ *L. major* promastigotes were transferred into 10 ml of M199 media and incubated at 26°C in a humified incubator. *L. major in vitro* cultures were counted daily and plotted as an exponential curve.

L. major LV39 parasites were prepared for infection as previously described [25]. Briefly, after 6 days at 26°C, stationary phase *L. major* parasites were centrifuged at 500rpm for 10 minutes at 23°C, to pellet out cell debris and lipids. The parasite solution was then pelleted by centrifugation at 3000rpm for 10 minutes at 23°C and washed twice in 1xPBS. Following resuspension in 1x PBS, the parasites were fixed with 4% paraformaldehyde, counted using a Neubauer haemocytometer and adjusted for infection studies. The concentration *of L. major* promastigotes were adjusted to $2x10^6$/50 µl of 1xPBS or $1x10^4$/10 µl 1x PBS for footpad or ear infections respectively. Prior to infection, experimental mice were anaesthetized by intraperitoneal (i.p) injection consisting of 12% ketamine and 8% xylavet made up in 1x PBS at a dose of 10 µl/gram.

2.4.2 *L. major* footpad infection in mice

Anaesthetized mice were subcutaneously injected in the left hind footpad with $2x10^6$ stationary phase *L. major* promastigotes in 50 µl of 1xPBS. Disease progression was monitored weekly, by measuring changes in infected footpad swellings using a Mitutoyo micrometer caliper (Brütsch-Rüegger, Switzerland).

To maintain *L. major in vitro* cultures, at 8 weeks post infection mice were sacrificed by halothane inhalation followed by cervical dislocation. 200µl 1x PBS was aspirated within the mouse infected footpad. An amastigote parasite solution was extracted, and transferred to 15ml Falcon tube containing 2 ml 1x PBS and centrifuged at 3000rpm for 5 minutes at 25°C. The parasite pellet was resuspended in 2 ml M199 media and transferred to a $25cm^3$ tissue culture flask containing 8 ml M199 media and incubated in 26°C humified incubator, to allow for efficient replication and differentiation into the promastigote form.

2.4.3 *L. major* ear infection in mice

Alternatively, anaesthetized mice were intradermally injected into the left ear with $1x10^4$ stationary phase *L. major* promastigotes in 10 µl of 1x PBS [94]. Disease progression was monitored weekly, by measuring changes in lesion diameter in an infected ear weekly using a

Vernier caliper (Massmart Holdings, South Africa). The mice were monitored daily and the weight of all experimental mice were recorded weekly to assess overall welfare until they reached the experimental endpoint. Mice infected *with L. major* LV39 were sacrificed at 8 weeks post infection.

2.4.4 Isolation of soluble *Leishmania* antigen from *L. major* cultures

Frozen *L. major* LV39 samples prepared from *in vitro* cultures, as described in Section 2.4.3 were thawed at 4°C and centrifuged at 3000rpm for 10 minutes at 4°C. The parasite pellet was resuspended in PBS-containing protease inhibitor cocktail (1:100) (Sigma-Aldrich, USA), to prevent protein degradation. The pellet sample was subsequently sonicated 4 times for 20 second cycles (amplitude 3) and the samples were stored at 4°C between sonication cycles. The suspensions were centrifuged at 8000rpm for 10 minutes at 4°C to pellet debris and the supernatant containing soluble *leishmania* antigen (SLA) was filtered through a 0.22µm filter. The protein concentration of the SLA samples were determined using a bicinchoninic acid protein assay (BCA) (Thermofischer Scientific Pierce, USA) according to the manufacturer's protocol. The SLA samples were aliquoted in 0.5 ml Eppendorf tubes and stored at -80°C.

2.5 Quantification of *L. major* parasite burden

2.5.1 Limiting Dilution Assay (LDA) to detect viable parasite burden

Following infection of mice with *L. major* LV39 parasites infected footpads, ears, spleens and draining lymph nodes were collected for further analysis. Detection of viable parasite burden was assessed by two-fold limiting dilution assay as previously described [25]. Briefly, footpads and spleens were collected in 2 ml complete M199 media and homogenized in complete M199 media, whilst popliteal and cervical lymph nodes were collected in 1 ml Dulbecco's modified eagle medium (DMEM) (Gibco, USA) supplemented with 10% FBS, 100 units/ml penicillin, 100 µg/ml streptomycin, 0.1% β-mercaptoethanol and 1% HEPES buffer (Lonza, Belgium). The samples were teased through a 40µm filter (Falcon, USA) to create single-cell suspensions in a final volume of 6.4 ml (100 µl= 2^6 parasites) by adding 5.4 ml complete DMEM. Two-fold serial dilutions from each tissue suspension were prepared in 96-well flat-bottom plates using complete M199 media in a final volume of 100 µl. The plates were incubated for 7 days at 26°C; thereafter each well was observed using an Olympus SC30 and the parasite burden was scored microscopically as being the lowest two-fold dilution (2^n) at which promastigotes were observed.

2.5.2 DNA extraction from *L. major* infected footpad samples

To extract DNA from the infected samples, 800 µl of footpad homogenate was transferred to 1.5 ml Eppendorf tubes and centrifuged at 5000rpm for 10 minutes at 4°C. The pellets, which contain murine and amastigote DNA, were then stored at -80°C until DNA extraction. As a positive control, stationary phase parasite cultures in 1x PBS were transferred to 1.5 ml Eppendorf tubes and centrifuged at 5000rpm for 10 minutes at 4°C. The pellets were stored at -20°C until DNA extraction.

Genomic DNA was isolated from the pellets as previously described [95] with modifications. The pellets were resuspended in 450 µl Saline/EDTA buffer (40mM NaCl and 10mM EDTA, pH 8) and 50 µl of 10% sodium dodecyl sulphate (SDS) was added to solubilise proteins. Following this 20 µl of 20 mg/ml proteinase K was added to digest contaminating nucleases and the Eppendorf tubes were vortexed briefly. Following this the samples were incubated for 2 hours at 56°C to lyse the cells. In order to precipitate out proteins, 225 µl of 5M NaCl was added and the samples were incubated at room temperature for 1 hour. The samples were centrifuged at 10 000rpm for 10 minutes at 4°C. The supernatant was then transferred to fresh 1.5 ml Eppendorf tubes and recentrifuged at 10 000rpm for 10 minutes at 4°C. The supernatant was then transferred to fresh 2 ml Eppendorf tubes, 1ml of ice cold isopropanol was added to each sample, and the samples were incubated overnight at -20°C to precipitate genomic DNA.

After this incubation to pellet the genomic DNA, the samples were centrifuged at 10 000rpm for 20 minutes at 4°C. The pellet was then washed in 1 ml of 70% Ethanol and centrifuged 10000rpm for 20 minutes at 4°C. The pellet was dried at room temperature for 1 hour to allow the excessive 70% Ethanol to evaporate. The pellet was resuspended in 30 µl of TE buffer (10mM Tris, 1mM EDTA, pH 8). The DNA yield for each sample was measured using a nanodrop ND1000 (Thermo Scientific, USA). The quality of DNA was further confirmed by loading 5 µl of sample and 1 µl of Tritrack loading dye (Thermofischer scientific, South Africa) in a 1.5% agarose gel (1.5 g agarose gel in 100 ml 1x Tris-Borate-EDTA buffer containing 5 µl of 10 mg/ml ethidium bromide stock). The gel was allowed to run for 20 minutes at a 100V and bands were visualized under UV light.

2.5.3 Endpoint PCR

To detect *Leishmania* kinetoplast DNA (kDNA) from DNA samples, as prepared in Section 2.5.2, endpoint PCR was performed as previously described [96, 97]. The following JW11/JW12 primers for *Leishmania* kDNA were used to amplify a 120bp fragment: Forward 5'-CCT ATT TTA CAC CAA CCC CCA GT-3' and Reverse 5'-GGG TAG GGGG CGT TCT GCG AAA-3' (IDT, South Africa). Briefly, 5 ng/µl extracted gDNA was amplified in a mix containing 0.2 µM of forward primer, 0.2 µM reverse primer, 1.5 mM $MgCl_2$, 0.2mM each deoxynucleotide triphosphate and 0.2 units of Taq DNA polymerase (KAPA Taq PCR Readymix KK1024; KAPA Biosystems, USA) in a 10 µl final volume. PCR was performed on an XP thermal cycler (Bioer Technology, China) under the following conditions: initial denaturation at 94°C for 4 minutes, followed by 30 cycles (denaturation for 1 min at 94°C, annealing for 30 seconds at 58°C, elongation for 30 seconds at 72°C) and conditions were terminated by a final extension for 10 minutes at 72°C. A volume of 5 µl from each PCR product was run at 100 volts for 30 minutes on 1.5% [w/v] agarose gel stained with ethidium bromide (5 µg/ml) in 1x Tris-EDTA buffer. The PCR products were visualised using a Syngene G box and images were captured using Genesnap software (Syngene Synoptics, UK). PCR product images were quantified using ImageJ software (National Institutes of Health, USA). The relative expression levels of amastigote kDNA, from equivalent 5 ng/µl DNA isolated from infected samples, was determined as the intensity from each band on the visualized gel normalized to the intensity from pure *L. major* parasite *in vitro* cultures as a positive control.

2.6 Isolation and stimulation of draining lymph node cells

Lymph nodes were isolated and prepared as described in Section 2.5.1. Lymph node cells were centrifuged at 1300rpm for 5 minutes at 4°C and the pellet was resuspended in 3 ml complete DMEM, re-filtered through a 40µm filter and the number of viable cells was determined by trypan blue staining using a 1:50 dilution. Cells were made up to $1x10^7$ cells in complete DMEM. The cells were plated at $1x10^6$/ml in 48-well flat-bottom plates (Corning, USA) and left unstimulated or stimulated with 20 µg/ml plate-bound α-CD3. The plates were placed in a 37°C incubator with 5%CO_2 for 72 hours. Following incubation, the plates were centrifuged at 1300rpm for 5 minutes at 4°C and the supernatants were stored at -20°C until used for detection of cytokines.

2.7 Flow cytometry analysis of lymph node cells

2.7.1 Extracellular surface staining

Lymph node cells were isolated, as described in Section 2.6, seeded at $2x10^6$ cells/well from each sample in 96-well v-bottom plates (Nalge Nunc International, USA) and centrifuged at 1500rpm for 5 minutes at 4°C. Following centrifugation, the supernatants were discarded and the pelleted cells were resuspended in 50 µl of antibody surface mix prepared in FACS buffer (0.5% BSA in 1xPBS, pH 7.4) supplemented with 1% heat-inactivated rat serum (iRS) and 10 µg/ml anti-FcγR (2.4G2). The plates were covered in tin foil and incubated for 20 minutes at 4°C. After incubation, 150 µl of FACS buffer was added to each sample to wash out unbound antibodies and the cells were centrifuged at 1200rpm for 5 minutes at 4°C. Following this, the supernatant was discarded and the stained cells were resuspended in 200 µl FACS buffer until acquisition.

2.7.2 Intranuclear staining

In preparation for cytokine staining, $2x10^6$ lymph node cells/well were seeded in a 96-well U bottom plate (Nalge Nunc International, USA) and stimulated for 2 hours at 37°C in 10 µl complete DMEM containing 50 ng/ml phorbol myristate acetate (PMA) (Sigma-Aldrich, USA) and 250 ng/ml ionomycin (Sigma-Aldrich, USA); this stimulation was done to enhance intracellular cytokine production [98]. After incubation, 10 µl complete DMEM with 200 µM monensin was added to each sample and the cells were furthered incubated for 4 hours at 37°C; this treatment was performed to block cytokine secretion out of the Golgi apparatus [99]. Following incubation, the re-stimulated cells were transferred to a new V-bottom plate and centrifuged at 1500rpm for 5 minutes at 4°C. The supernatant was discarded gently. T and B cells populations were identified by staining with extracellular antibodies for CD3, CD4, CD8, CD19, PD-1, IL-4Rα (Appendix 1), as described in Section 2.7.1. For intranuclear staining, Anti-mouse/Rat Foxp3 staining set (77-5775) (eBioscience, Thermofischer South Africa) was used as per the manufacturer's protocol with modifications; this allowed for detection of intracellular molecules and intranuclear transcription factors. Briefly following extracellular staining, cells were washed with 150 µl Foxp3 Permeabilization buffer (diluted 1:10 in distilled H_2O) and centrifuged at 1500rpm for 5 minutes at 4°C. The pelleted cells were fixed and permeabilized in 100 µl Fixation-Permeabilization working solution (1 part Fixation/Permeabilization concentrate: 3 parts Fixation/Permeabilization diluent) covered in

tin foil for 30 minutes at 4°C. Cells were centrifuged at 1500rpm for 5 minutes at 4°C and washed twice in 150 µl Foxp3 Permeabilization buffer. Cells were stained with 50 µl of antibody mixes, prepared in Foxp3 Permeabilization buffer supplemented with 2% iRS and 10 µg/ml anti-FcyR, against intracellular IFN-γ, IL-4, IL-13, IL-10, and intranuclear transcription factors: GATA3, T-bet, RoRγt and Foxp3 (Appendix 1). The plates were covered in tin foil and cells were stained for 50 minutes at 4°C. The cells were washed in 150 µl Foxp3 Permeabilization buffer, centrifuged at 1500rpm for 5 minutes at 4°C and subsequently resuspended in 200 µl FACS buffer at 4°C until acquisition.

2.7.3 Intracellular staining

For intracellular staining, lymph node cells were isolated, seeded at $2x10^6$ cells/well and dendritic cell populations were identified by staining with surface marker antibodies for CD11c, CD11b, MHC-II, B220, PD-L1 and CD80 (Appendix 1), as described in Section 2.7.1. Following staining, cells were washed with 150 µl FACS buffer and centrifuged at 1500rpm for 5 minutes at 4°C. The cell pellets were then fixed in 200 µl 2% paraformaldehyde for 20 minutes at 4°C. The cells were washed with 200 µl 1xPBS and centrifuged at 1500rpm for 5 minutes at 4°C. The cell pellets were subsequently permeabilized with 200 µl Permeabilization buffer (0.11% $CaCl_2$, 0.1% saponin, 0.1% BSA, 0.05% NaN_3, 0.0125% $MgSO_4$, 10mM Hepes in 1xPBS, pH 7.4) for 30 minutes at 4°C. The cells were centrifuged at 1500rpm for 5 minutes at 4°C, followed by intracellular staining with 50 µl per well of anti-mouse IDO (Appendix 1), prepared in Permeabilization buffer supplemented with 2% iRS and 10 µg/ml anti-FcyR, for 50 minutes at 4°C. Biotin-labelled antibodies were detected by staining with 50 µl of Streptavidin conjugated to PE-CF594 (Appendix 1). Cells were then washed with 150 µl Permeabilization buffer, centrifuged at 1500rpm for 5 minutes at 4°C and resuspended in 200 µl FACS buffer at 4°C until acquisition.

Cell acquisition was completed on BD LSRFortessa Machine (BD Biosciences, USA) and data was analysed using FlowJo software v10.5.3 (Treestar, USA).

2.8 Serum collection from blood samples

Following sacrifice, blood samples were collected from each mouse by cardiac puncture using an insulin syringe and transferred to serum separator tubes (BD Bioscience, USA). The samples were centrifuged at 8000rpm at 4°C for 10 minutes and stored at -80°C until further analysis.

2.9 Nitric Oxide Synthase and Arginase activity

Lymph node cells collected and seeded at $2x10^6$ cells/ml, as described in section 1.4.3, were stimulated with 10 ng/ml LPS in 37°C incubator with 5%CO_2 for 72 hours. Following incubation, the plates were centrifuged at 1300rpm for 5 minutes at 4°C and the supernatants were collected for quantification of nitrite production as an indication of iNOS activity as previously described [100]. Briefly, a Griess reagent standard (1 mM $NaNO_2$) was serially diluted 2-fold in DMEM in a 96-well flat-bottom plate and 50 µl of supernatants were added. Following this 25 µl Griess Reagent 1 (1 % sulphanilamide in 2.5% phosphoric acid) was added per well and the plate was incubated for 5 minutes in the dark. An equal volume Griess Reagent 2 (0.1% naphthyl-ethylenediamine in 2.5% phosphoric acid) was added per well and the plate was incubated for 10 minutes in the dark until a pink colour develops across the standard wells. The optical density was measured at 540nm on a VersaMax™ microplate reader using Softmax pro software (Molecular Devices, Germany).

Arginase activity within infected cell lysates was determined as previously described. Briefly, 100 µl 0.1% Triton X-100 per well was used to lyse infected cells. After lysis, 50 µl of lysed cells were transferred to a new 96-well flat-bottom plate and 50 µl Arginase buffer (50 mM Tris-HCl and 10 mM $MnCl_2$ pH 7.5) was added per well. Arginase activity was then activated by heating for 10 minutes at 55°C. Following incubation, 25 µl of activated lysate and 25µl of 0.5 M arginine pH 9.7 were added in combination and the plate was incubated at 37°C for 1 hour to induce arginine hydrolysis. As a measure of arginase activity, Urea (5 mg/ml) was added and diluted as 2-fold dilution series in distilled H_2O to generate a standard curve. The reaction was stopped by adding 200 µl of H_2SO_4: H_3PO_4: H_2O (1:3:7). Following this 12.5 µl of 9% isonitrosopropiophenone (dissolved in 100% Ethanol) was added and the plates were heated at 100°C for 45 minutes. The optical density was measured at 540nm on a VersaMax™ microplate reader to measure the concentration of urea produced.

2.10 Enzyme-linked Immunosorbent Assay (ELISA) Analysis

2.10.1 Cytokine ELISA

Cytokine secretion in *L. major* infected lymph node supernatants (as prepared in Section 2.6) was detected by sandwich ELISA as previously described [25]. Briefly, 96-well flat bottom plates (Nalge Nunc International, USA) were coated with primary coating antibodies specific for each cytokine of interest (Appendix 2), diluted in carbonate coating buffer (1.5 mM Na_2CO_3, 35 mM $NaHCO_3$ and 71 mM NaCl, pH 9.5) and incubated at 4°C overnight. The plates were then washed 4 times in washing buffer and blocked with 2% BSA for 2 hours at 37°C. The plates were then washed 4 times in washing buffer and recombinant cytokine standards (Appendix 2) or lymph node supernatants were added in 3-fold serial dilutions and incubated at 4°C overnight. Following overnight incubation, the plates were washed 4 times in washing buffer. Biotinylated secondary anti-mouse antibodies for each cytokine were then added and the plates were incubated at 4°C overnight. The plates were then washed 5 times in washing buffer and streptavidin substrate conjugated with alkaline phosphatase (AP) (1:1000) or horse-radish peroxidase (HRP) (1:5000) was added and incubated for 1 hour at 37°C.

The plates treated with HRP-conjugated streptavidin were incubated with TMB peroxidase substrate (KPL, USA) and the reaction was stopped with 1M H_2PO_4. The optical density was recorded at 450nm-540nm on a VersaMax™ microplate reader. The plates treated with AP-labelled streptavidin were developed by adding 4-Nitrophenyl phosphate (1 mg/ml PNP in AP substrate buffer: 9.7% $C_4H_{11}NO_2$, 0.02% NaN_3 and 0.8% $MgCl_2.6H_2O$, pH 9.8) and incubated for 15 minutes at room temperature. Absorbance was recorded on a VersaMax™ microplate reader at 405-492nm.

2.10.2 Antibody ELISA

Antibody response was measured in mouse serum samples collected as described in Section 1.4.4. Antigen-specific IgG1 and IgG2b were measured by indirect ELISA and total IgE was measured by sandwich ELISA as previously described [25]. Briefly, 96 well plates (Nalge Nunc International, USA) were coated with 5 µg/ml *L. major* SLA or 1 µg/ml IgE clone 84.1C (Southern Biotechnology, USA) in PBS coating buffer (pH 9.5) and incubated at 4°C overnight. Following overnight incubation, the wells were washed 4 times in 1x washing buffer and blocked with 2% BSA for 2 hours at 37°C. The plates were washed 4 times and serum

(diluted 1:10 in dilution buffer) was added in a 3-fold dilution series. For Total IgE ELISA plates, 100 ng/ml IgE standard (BD Pharmingen, USA) was added in a 3-fold serial dilution. The plates were then incubated overnight at 4°C. After washing 4 times, alkaline phosphatase-conjugated goat anti-mouse IgG1, IgG2b and IgE secondary antibodies (Southern Biotechnology, USA) were added and the plates were incubated at 4°C overnight. The plates were developed following incubation with PNP substrate as described in Section 1.5.1 and the absorbance was recorded at 405-492nm on a VersaMax^{TM} microplate reader.

2.11 Statistical Analysis

Statistical analyses were performed using Graphpad Prism v6.2 (GraphPad Software, USA). The data were calculated as mean ± Standard error of the mean (SEM). Statistical analysis was calculated using unpaired student t-test (two-tailed with unequal variance) between 2 groups or one-way Analysis of Variance (ANOVA) with a Bonferroni multiple comparison post-hoc test was used to compare more than 2 groups. Differences to IL-4Rα$^{-/lox}$ mice were defined as significant (*, $p < 0.05$; **, $p < 0.01$; ***, $p < 0.001$; ****, $p < 0.0001$).

3. Results

3.1 Preparation of *L. major* LV39 parasites for infection

In preparation for infection in experimental mice, *L. major* LV39 promastigotes were cultured at a fixed parasite number and promastigote numbers were counted daily, following fixation in 4% paraformaldehyde (Figure 3.1). During days 2 to 4 post culturing, logarithmic growth was initially observed; following this on day 6 the *L. major* promastigote numbers plateaued as they reached stationary phase (Figure 3.1). Subsequently these stationary-phase *L. major* promastigotes, now at their most virulent infectious stage [101], were prepared for infection.

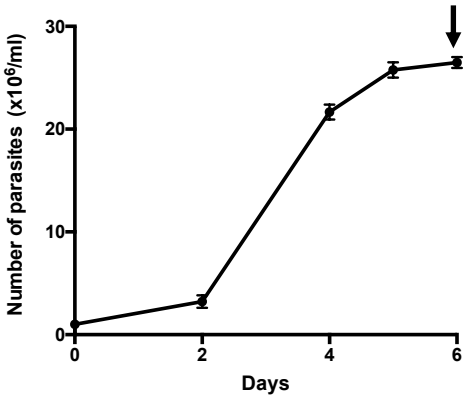

Figure 3.1: Growth curve of *L. major* LV39 promastigotes in preparation for infection. $1x10^6$ parasites/ml of complete M199 medium were subcultured into $25cm^3$ tissue culture flasks and parasite numbers were counted daily to determine the stationary growth phase (depicted by arrow). Consequently, on day 6 *L. major* LV39 (MRHO/SV/59/P) promastigotes were used for infection. Results are the mean parasite counts ± SEM from 5 pooled LV39 cultured flasks.

3.2 Differential Cre-mediated deletion of IL-4Rα on Foxp3$^+$ Treg cells between Foxp3^{cre}IL-4Rα$^{-/lox}$ male and female mice is maintained during *L. major* infection

Previous studies have reported that IL-4Rα chain is a complex, expressed on an array of cell types including hematopoietic, endothelial, epithelial, hepatocyte and brain tissue [34, 102]. Following *L. major* LV39 infection, surface expression of the IL-4Rα chain on various immune cell populations was initially assessed at a protein level by flow cytometry analysis (Figure 3.2 and Figure 3.3). The CD19$^+$ B cell and CD4$^+$ T cell populations were gated as shown in Supplementary Figure 1. The total IL-4Rα expression at an individual cell level was defined as the geometric mean fluorescent intensity (GMFI). In line with trends found in a previous study, CD19$^+$ B cell and CD4$^+$ Foxp3$^-$ T cell populations from Foxp3^{cre}IL-4Rα$^{-/lox}$ mice and their littermate controls had comparable IL-Rα GFMI expression (Figure 3.2 and Figure 3.3) [89]. The significant reduction in IL-4Rα GMFI on CD4$^+$ Foxp3$^+$ Treg cells observed in IL-

4Rα$^{-/-}$ mice, which are deficient of the IL-4Rα chain on all hematopoietic cells [39], corresponded to a similar reduction observed in Foxp3^{cre}IL-4Rα$^{-/lox}$ male and female mice (Figure 3.2 and Figure 3.3), indicating successful depletion of the IL-4Rα chain within CD4^{+} Foxp3^{+} Treg cells within both mice strains.

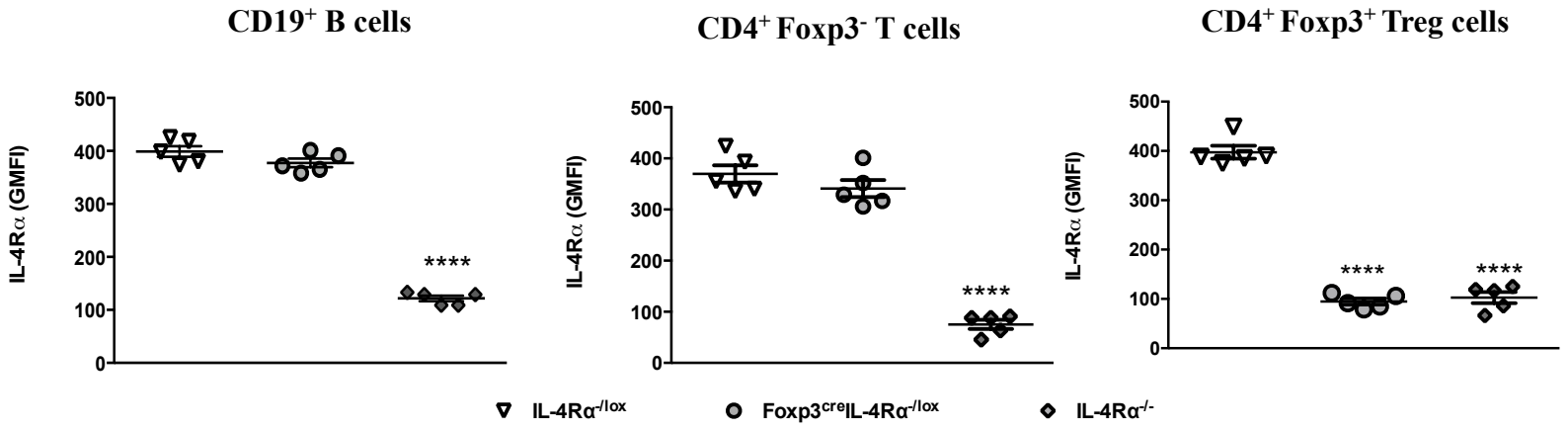

Figure 3.2: Efficient deletion of the IL-4Rα chain on T regulatory cells is maintained within Foxp3^{cre}IL-4Rα$^{-/lox}$ male mice during *L. major* infection. Experimental male mice were subcutaneously infected with 2x10^{6} stationary phase *L. major* LV39 promastigotes into the left hind footpad. At 8 weeks post infection, geometric mean fluorescent intensity (GMFI) of IL-4Rα expression was determined by flow cytometry analysis from the popliteal lymph nodes of *L. major* infected IL-4Rα$^{-/lox}$, Foxp3^{cre}IL-4Rα$^{-/lox}$ and IL-4Rα$^{-/-}$ male mice. B cells were CD19^{+}CD3^{-}, non-Treg T cells were CD4^{+}Foxp3^{-} and Treg cells were CD4^{+}Foxp3^{+}. Results are representative of two independent experiments with 5 mice per group expressed as mean±SEM. Statistical significance was determined in comparison to IL-4Rα$^{-/lox}$ mice (*, p≤0.05; **, p≤0.01; ***, p≤0.001, **** p≤0.0001).

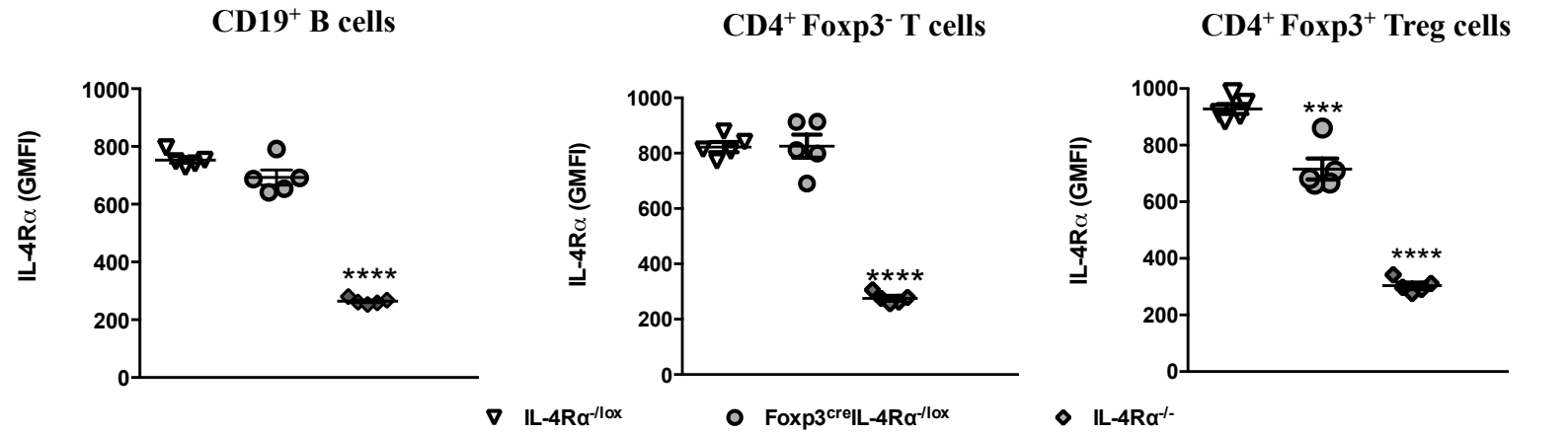

Figure 3.3: Deletion of the IL-4Rα chain is specific to T regulatory cells in *L. major* infected Foxp3^{cre}IL-4Rα$^{-/lox}$ female mice. Experimental male mice were subcutaneously infected with 2x10^{6} stationary phase *L. major* LV39 promastigotes into the left hind footpad. At 8 weeks post infection, geometric mean fluorescent intensity (GMFI) of IL-4Rα expression from the popliteal lymph nodes of *L. major* infected IL-4Rα$^{-/lox}$, Foxp3^{cre}IL-4Rα$^{-/lox}$ and IL-4Rα$^{-/-}$ female mice. B cells were CD19^{+}CD3^{-}, non-Treg T cells were CD4^{+}Foxp3^{-} and Treg cells were CD4^{+}Foxp3^{+}. Results are representative of two independent experiments with 5 mice per group expressed as mean±SEM. Statistical significance was determined in comparison to IL-4Rα$^{-/lox}$ mice (*, p≤0.05; **, p≤0.01; ***, p≤0.001, **** p≤0.0001).

A previous study had reported that at naïve level, in the spleen and mesenteric lymph node (MLN), a difference in deletion efficiency of IL-4Rα chain on $CD4^+$ $Foxp3^+$ Treg cells was noted between $Foxp3^{cre}IL\text{-}4R\alpha^{-/lox}$ male mice and female mice [89]. To assess whether the deletion efficiencies were maintained during *L. major* infection, popliteal lymph nodes were isolated from *L. major* infected male and female mice following 8 weeks of infection and the deletion efficiency was quantified using a previously derived formula [89]. The deletion efficiency of the IL-4Rα chain in $CD4^+$ $Foxp3^+$ Treg cells was significantly reduced in $Foxp3^{cre}IL\text{-}4R\alpha^{-/lox}$ female mice (Average Efficiency of deletion(Ed) = 32,48%) compared to $Foxp3^{cre}IL\text{-}4R\alpha^{-/lox}$ male mice (Ed=102,73%). Collectively, these data suggest that the Cre-mediated deletion of IL-4Rα signalling is specific to the $CD4^+$ $Foxp3^+$ Treg cell population and that the differential deletion efficiency observed between $Foxp3^{cre}IL\text{-}4R\alpha^{-/lox}$ male and female mice is conserved during *L. major* LV39 infection.

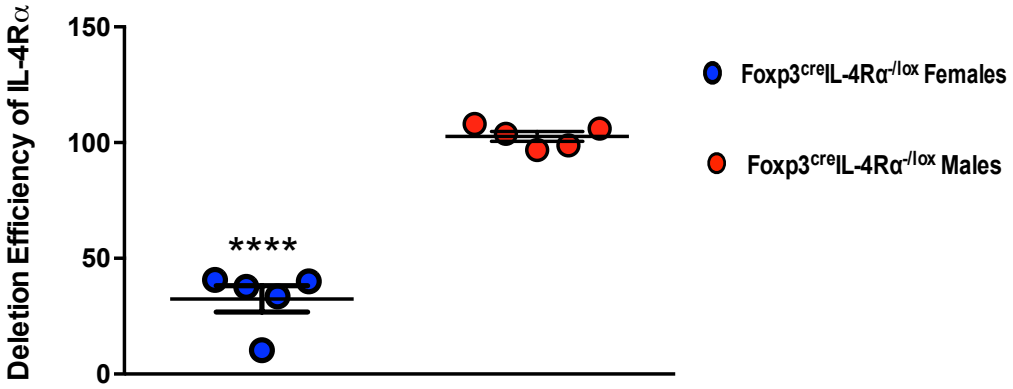

Figure 3.4: Differential Cre-mediated deletion of the IL-4Rα chain on $Foxp3^+$ Treg cells between female and male $Foxp3^{cre}IL\text{-}4R\alpha^{-/lox}$ mice is conserved during *L. major* infection. Experimental mice were subcutaneously infected with $2x10^6$ stationary phase *L. major* LV39 promastigotes into the left hind footpad. At 8 weeks post infection, the deletion efficiency of the IL-4Rα chain on $CD4^+Foxp3^+$ Treg cells was calculated in the popliteal lymph nodes of *L. major* infected female and male $Foxp3^{cre}IL\text{-}4R\alpha^{-/lox}$ mice. Results are representative of two independent experiments with 5 mice per group expressed as mean±SEM. Statistical significance was determined in comparison to $Foxp3^{cre}IL\text{-}4R\alpha^{-/lox}$ male mice (*, $p\leq0.05$; **, $p\leq0.01$; ***, $p\leq0.001$, **** $p\leq0.0001$).

3.3 Foxp^{3}IL-4Rα$^{-/lox}$ BALB/c male mice are hypersusceptible to *L. major* during footpad infection

3.3.1 Characterization of the clinical phenotype observed during *L. major* LV39 infection

In order to investigate the role of IL-4Rα signalling on Foxp3$^+$ Treg cells during cutaneous leishmaniasis, experimental mice were infected subcutaneously in the left hind footpad with 2x10^6 stationary phase *L. major* promastigotes. Footpad swellings were measured weekly over as an indication of disease progression (Figure 3.5, A-B). Similar to previous studies, susceptible IL-4Rα$^{-/lox}$ littermate control female and male mice developed enhanced footpad swellings during the course of *L. major* LV39 infection (Figure 3.5, A-B) [47, 59]. Notably, Foxp3^{cre}IL-4Rα$^{-/lox}$ BALB/c female mice developed enhanced footpad swellings, similar to their littermate control (IL-4Rα$^{-/lox}$) (Figure 3.5A), which correlated with similar parasite burdens in infected footpads (Figure 3.6A), draining popliteal lymph nodes (Figure 3.6B) and spleens (Figure 3.6C). The PCR products of *Leishmania* amastigote kDNA isolated from infected footpad samples were electrophoresed on a 1.5% agarose gel and visualized by UV illumination using a Syngene G box (Supplementary Figure 2). Similar to the results observed during LDA parasite burdens, no significant difference was identified in the relative amastigote kDNA expression levels between Foxp3^{cre}IL-4Rα$^{-/lox}$ female footpad samples and their littermate controls (Figure 3.7A).

In contrast, Foxp3^{cre}IL-4Rα$^{-/lox}$ BALB/c male mice developed significantly larger footpad swellings and early necrosis was noted for a greater number of mice, in comparison to their littermate controls during *L. major* infection (Figure 3.5B). This increased disease progression observed in *L. major* infected Foxp3^{cre}IL-4Rα$^{-/lox}$ BALB/c male mice was associated with significantly greater parasite burdens in infected footpads (Figure 3.6D), lymph nodes (Figure 3.6E) and enhanced parasite dissemination to the spleen (Figure 3.6F). The significantly enhanced relative amastigote kDNA expression levels of Foxp3^{cre}IL-4Rα$^{-/lox}$ male footpad samples (Figure 3.7B), provided further evidence of increased parasite loads at the site of infection. In line with previous studies [25, 59], resistant C57BL/6 female and male mice were able to resolve lesion development during the 8 week *L.* major LV39 infection period (Figure 3.5, A-B); accompanied with significantly lower parasite burdens in the infected footpads, lymph nodes and spleens (Figure 3.6, A-F). Collectively, these results suggest that the greater

efficiency of deletion of the IL-4Rα chain on Treg cells, the more susceptible Foxp3^{cre}IL-4Rα$^{-/lox}$ mice strain appeared to be to *L. major* infection; thus suggesting that IL-4Rα signalling on T reg cells provides a protective role to control against *L. major* disease progression.

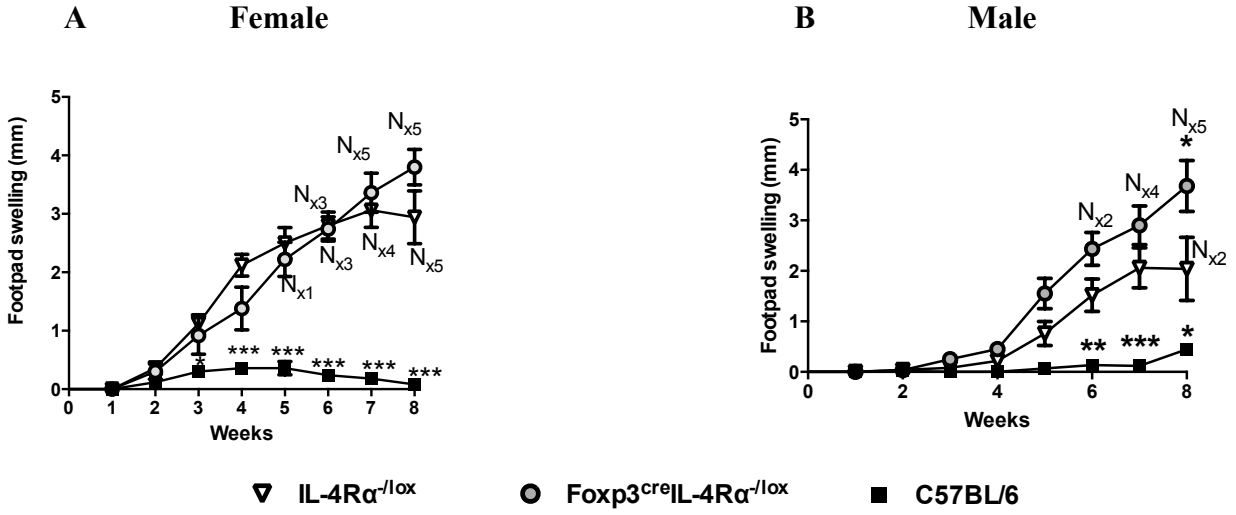

Figure 3.5: The absence of IL-4Rα signalling on T regulatory cells renders Foxp^{3}IL-4Rα$^{-/lox}$ male mice hypersusceptible to *L. major* infection; while Foxp^{3}IL-4Rα$^{-/lox}$ female mice remain as susceptible as their littermate control. Experimental mice were subcutaneously infected with 2x10^6 stationary phase *L. major* LV39 promastigotes into the left hind footpad. Changes in diameter at the site of infection was measured weekly as footpad swelling (mm). Footpad swelling for female (A) and male mice (B) was measured over an 8 week period. Necrosis is indicated by "N" per number of mice in which it was observed. Results are representative of two independent experiments with 5 mice per group expressed as mean±SEM. Statistical significance was determined in comparison to IL-4Rα$^{-/lox}$ mice (*, p≤0.05; **, p≤0.01; ***, p≤0.001).

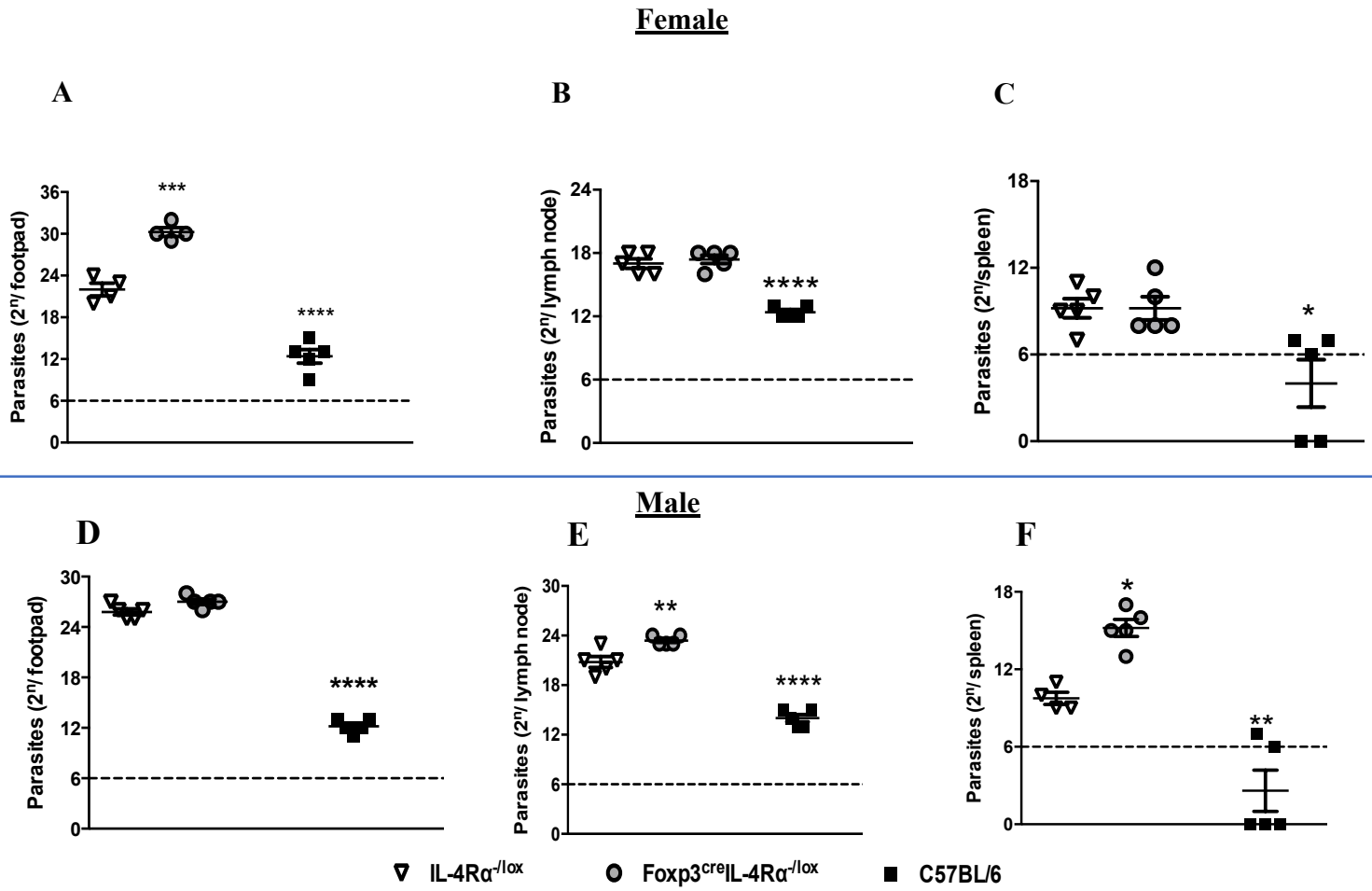

Figure 3.6: The *L. major* parasite burdens are significantly increased in Foxp3^{cre}IL-4Rα$^{-/lox}$ male mice. Experimental mice were subcutaneously infected with 2x10^6 stationary phase *L. major* LV39 promastigotes into the left hind footpad. The parasite burden (2^n) within female mice footpads (A), lymph nodes (B) and spleens (C) at week 8 post infection with *L. major* was determined by limiting dilution assays. Similarly, limiting dilution assays were used to determine parasite burden within male mice footpads (D), lymph nodes (E) and spleens (F). The limit of detection (2^6) is indicated as a dashed line. Results are representative of two independent experiments with 5 mice per group expressed as mean±SEM. Statistical significance was determined in comparison to IL-4Rα$^{-/lox}$ mice (*, p≤0.05; **, p≤0.01; ***, p≤0.001, **** p≤0.0001).

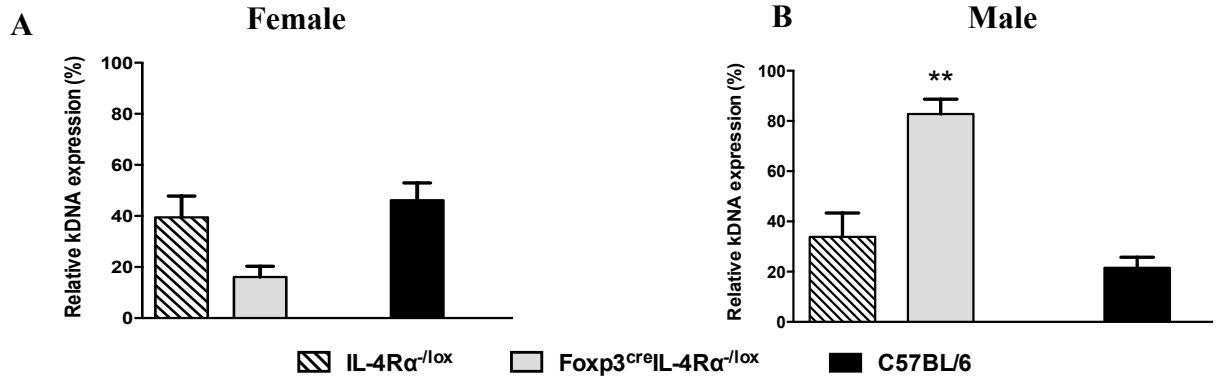

Figure 3.7: The *L. major* parasite loads are significantly increased in Foxp3^{cre}IL-4Rα$^{-/lox}$ male mice. Experimental mice were subcutaneously infected with 2x10^6 stationary phase *L.major* LV39 promastigotes into the left hind footpad. At 8 weeks post *L. major* infection the relative amastigote kinetoplast DNA from DNA samples extracted from female (A) and (B) male homogenized footpads, were quantified by densitometry using ImageJ software. The relative expression levels were normalized to *L. major in vitro* cultures. Results are representative of one independent experiment with 5 mice per group expressed as mean±SEM. Statistical significance was determined in comparison to IL-4Rα$^{-/lox}$ mice (*, p≤0.05; **, p≤0.01).

3.3.2 Immunological responses observed at the cellular level

As Foxp3^{cre}IL-4Rα$^{-/lox}$ male mice showed greater *L. major* parasite dissemination, indicative of enhanced susceptibility during *L. major* LV39 infection, we sought to assess the recruitment of cells in the isolated draining lymph nodes. At 8 weeks post infection, the total number of lymph node cells were comparable between the three mice strains (Figure 3.8). (Foxp3^{cre}IL-4Rα$^{-/lox}$, IL-4Rα$^{-/lox}$ littermate control and C57BL/6 resistant control mice).

Previous studies have elucidated that mechanisms employed by Treg cells to modulate the host immune response involve cytokine production [61, 74]. Given this, we sought to determine the effect on Treg cell population cytokine levels following the deletion of IL-4Rα signalling on Foxp3$^+$ Treg cells. The intracellular cytokine staining and gating of Foxp3$^+$ Treg cell population by flow cytometry (Supplementary Figure 3), allowed for the frequency of Foxp3$^+$ Treg cells and their cytokine activity within the infected popliteal lymph nodes to be determined. Following *L. major* infection, the frequency of CD4$^+$ Foxp3$^+$ Treg cells infiltrating the draining lymph nodes was significantly increased in Foxp3^{cre}IL-4Rα$^{-/lox}$ male mice in comparison to IL-4Rα$^{-/lox}$ male mice (Figure 3.9A). CD4$^+$Foxp3$^+$ Treg cell cytokine production revealed similar levels of IFN-γ expression between Foxp3^{cre}IL-4Rα$^{-/lox}$ male mice and their littermate control (Figure 3.9B). In contrast, the frequencies of IL-4, IL-10, and IL-13 CD4$^+$Foxp3$^+$ Treg cells were significantly increased in Foxp3^{cre}IL-4Rα$^{-/lox}$ male mice compared to littermate mice (Figure 3.9C, Figure 3.9D and Figure 3.9E). Infected C57BL/6 mice displayed lower frequencies of these Type 2 cytokine producing Treg cells (Figure 3.9C, Figure 3.9D and Figure 3.9E). Collectively, these results suggest that despite the inability of IL-4 and IL-13 to signal to these Treg cells, the deletion of IL-4Rα chain within this cell population favours enhanced CD4$^+$Foxp3$^+$ Treg cell recruitment and increased Treg-specific Type 2 cytokine production.

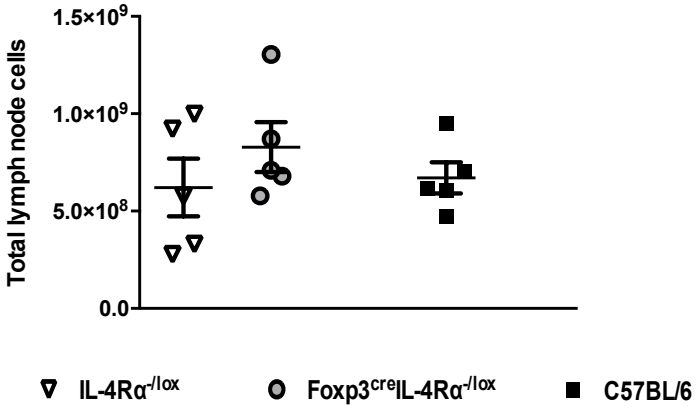

Figure 3.8: Total cells in the lymph node of *L. major* infected male mice. Experimental male mice were subcutaneously infected with $2x10^6$ stationary phase *L. major* LV39 promastigotes into the left hind footpad. The total number of cells within the popliteal lymph node were quantified following an 8-week *L. major* infection of experimental male mice in the left hind footpad. Results are representative of two independent experiments with 5 mice per group expressed as mean±SEM. Statistical significance was determined in comparison to IL-4Rα$^{-/lox}$ mice (*, p≤0.05).

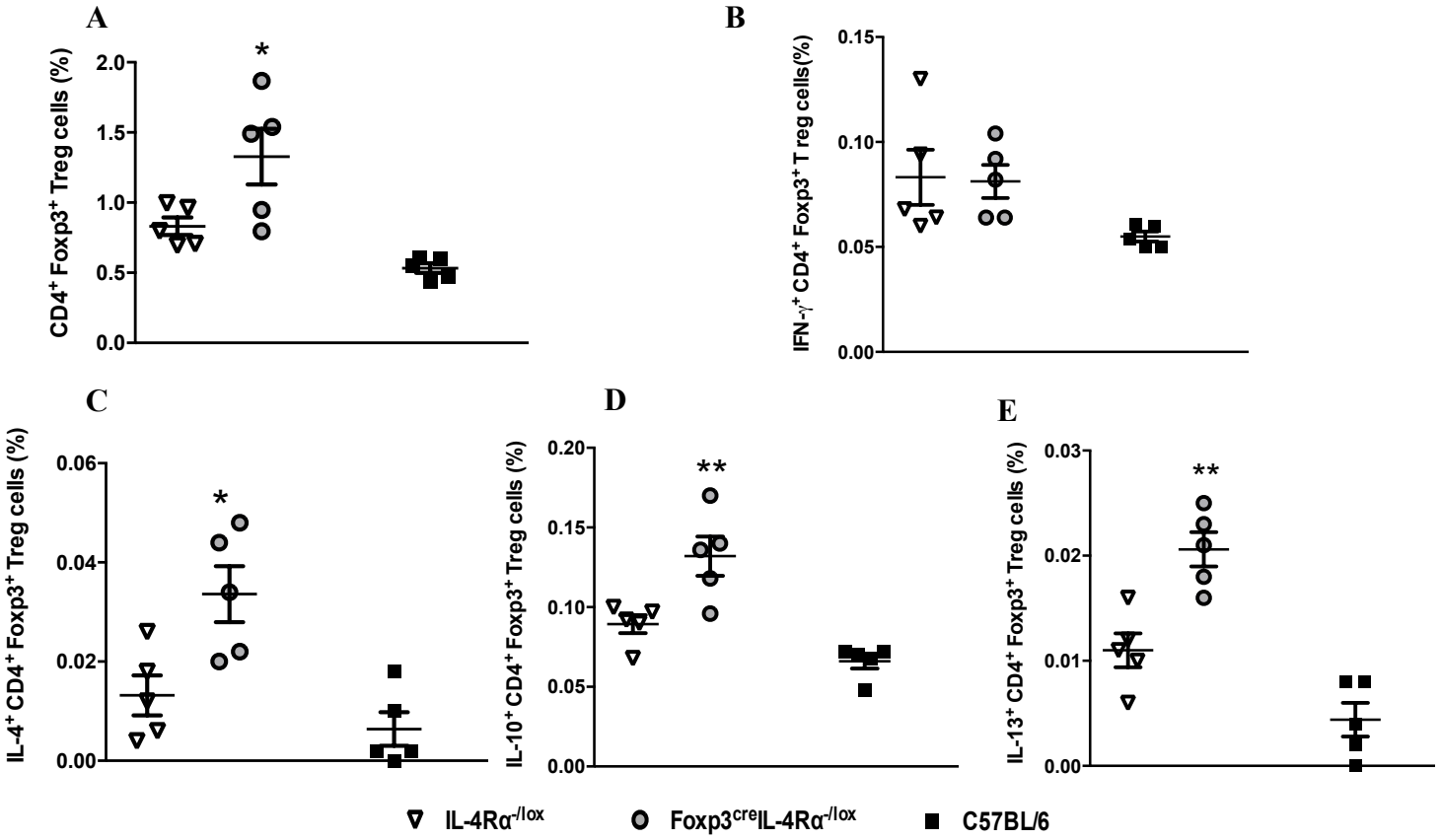

Figure 3.9: Depletion of IL-4Rα signalling on Foxp3$^+$ Treg cells alters Treg cell frequency and activity. Experimental male mice were subcutaneously infected in the left hind footpad with $2x10^6$ stationary phase *L. major* LV39 promastigotes for 8 weeks. The frequency of CD4$^+$ Foxp3$^+$ T regulatory cells within the popliteal lymph nodes (A) were assessed by flow cytometry analysis. The frequency of CD4$^+$ Foxp3$^+$ Treg cells producing IFN-γ (B), IL-4 (C), IL-13 (D) and IL-10 (E) were determined by flow cytometry analysis Results are representative of two independent experiments with 5 mice per group expressed as mean±SEM. Statistical significance was determined in comparison to IL-4Rα$^{-/lox}$ mice (*, p≤0.05).

3.3.3 Immunological responses observed at the molecular level

The activation of a Type 2 immune response has been associated with increased susceptibility to *L. major* induced cutaneous leishmaniasis, while induction of Type 1 immune response provides the host with protection against *L. major* infection [9, 11]. In order to determine whether the hypersusceptible phenotype observed in Foxp3^{cre}IL-4Rα$^{-/lox}$ male was associated with an altered immune response, the cytokine and humoral Type 1 or Type 2 immune responses were assessed following *L. major* infection. Cytokine production was measured within infected supernatants following T cell mitogenic (anti-CD3) re-stimulation of total lymph node cells at 8 weeks post infection [25]. Similar concentrations of IFN-γ where secreted between Foxp3^{cre}IL-4Rα$^{-/lox}$ mice and their littermate control IL-4Rα$^{-/lox}$ mice (Figure 3.10A); while resistant C57BL/6 mice, similar to previous studies, secreted significantly higher levels of this Type 1 cytokine [21, 25]. In contrast, the levels of Type 2 cytokine IL-4 were significantly higher in Foxp3^{cre}IL-4Rα$^{-/lox}$ mice compared to their littermate controls (Figure 3.10B). Due to the suppressive activity of CD25^{+} Treg cells being attributed to the secretion of IL-10 and TGF-β [103], and the contribution of IL-10 towards the activation of a Type 2 immune response [104], the concentrations of these cytokines were measured. The levels of IL-10 and TGF-β secretion were found to be 2.5 fold greater in the Foxp3^{cre}IL-4Rα$^{-/lox}$ mice relative to littermate controls (Figure 3.10, C-D). Thus, the deletion of IL-4Rα signalling on Treg cells resulted in the elevated production of Type 2 cytokines (IL-4, IL-10) and cytokines associated with increased Treg cell suppression (IL-10 and TGF-β), while Type 1 cytokine secretion (IFN-γ) remained unaltered.

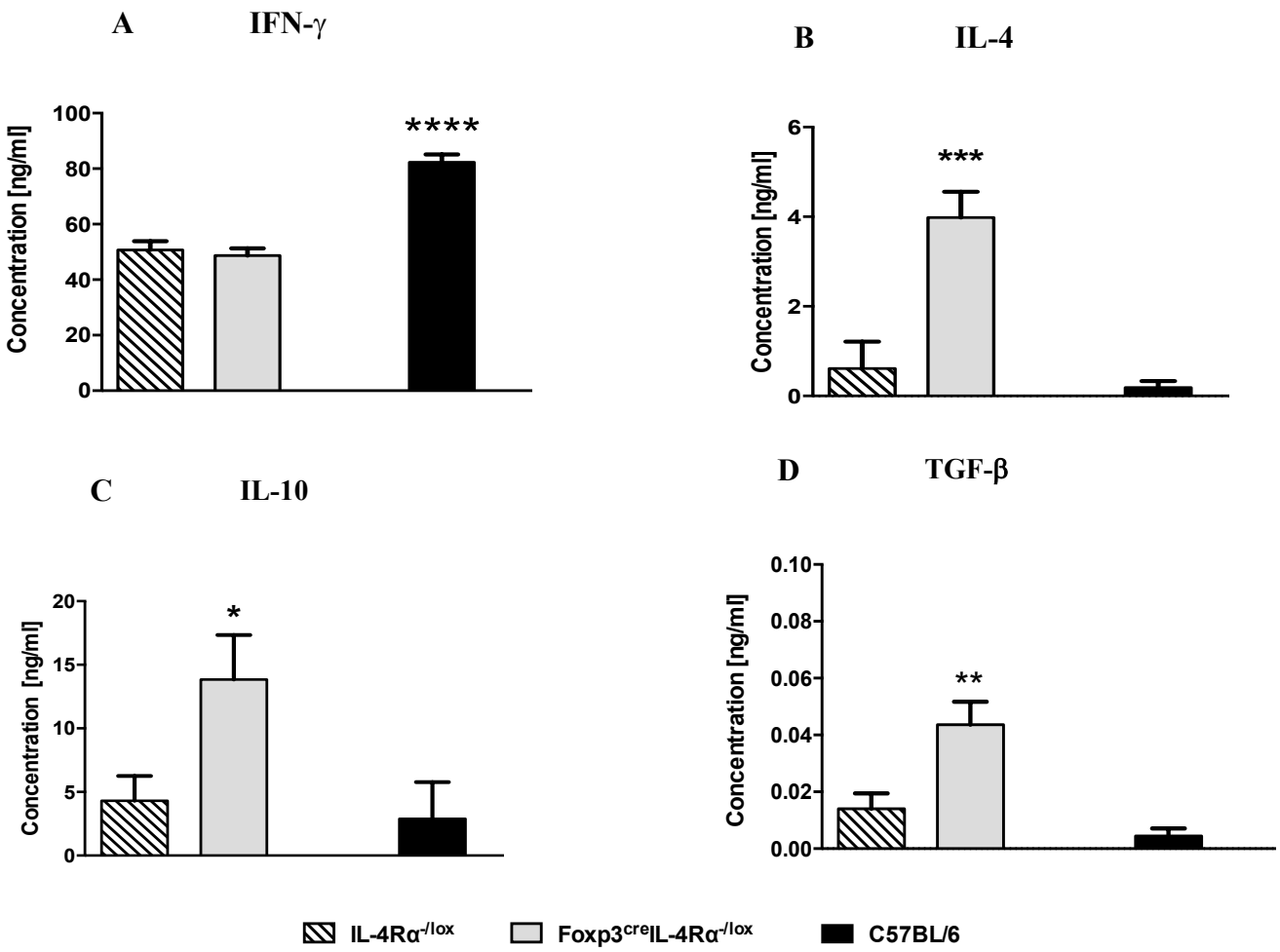

Figure 3.10: Enhanced Type 2 cytokine secretion occurs in Foxp3^{cre}IL-4Rα$^{-/lox}$ mice following *L. major* LV39 infection in the footpad. Experimental male mice were subcutaneously infected in the left hind footpad with 2x10^6 stationary phase *L. major* LV39 promastigotes. At 8 weeks post infection, popliteal lymph node cells were re-stimulated for 72 hours with anti-CD3. IFN-γ (A), IL-4 (B), IL-10 (C) and TGF-β (D) cytokine production within lymph node cell supernatants was measured by cytokine ELISA. Results are representative of two independent experiments with 5 mice per group expressed as mean±SEM. Statistical significance was determined in comparison to IL-4Rα$^{-/lox}$ mice (*, p≤0.05; **, p≤0.01; ***, p≤0.001).

The observed shift towards the activation of a Type 2 immune response in Foxp3^{cre}IL-4Rα$^{-/lox}$ mice was further evaluated by assessing the antibody responses within serum samples following 8 weeks of *L. major* infection. The sera of C57BL/6 mice displayed lower levels of Type 1 antibodies (antigen-specific IgG2b) and Type 2 antibodies (antigen-specific IgG1 and Total IgE) (Figure 3.11, A-C), similar to previous results, as by 8 weeks post infection C57BL/6 mice had healed from *L. major* infection [25]. In contrast, Foxp3^{cre}IL-4Rα$^{-/lox}$ mice displayed significantly elevated concentrations of total IgE (Figure 3.11C), indicating augmentation towards a Type 2 humoral response, however antigen-specific IgG1 levels were similar in comparison to littermate control IL-4Rα$^{-/lox}$ mice (Figure 3.11B). Therefore, the deletion of IL-4Rα signalling on Treg cells resulted in isotype switching in B cells, leading to elevated total IgE production.

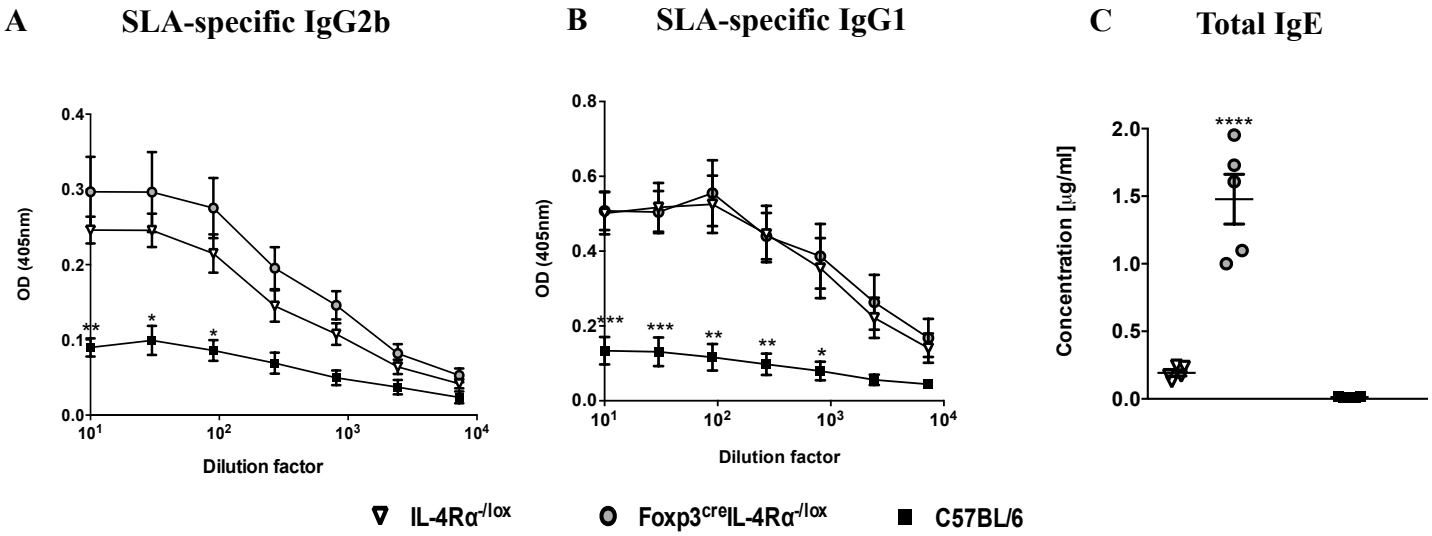

Figure 3.11: Foxp3^{cre}IL-4Rα$^{-/lox}$ male mice display an elevated Type 2 humoral response following *L. major* LV39 footpad infection. Experimental male mice were subcutaneously infected in the left hind footpad with 2x10^6 stationary phase *L. major* LV39 promastigotes. At 8 weeks post infection *L. major* antigen-specific IgG2b (A), IgG1 (B), and total IgE (C) antibody production within infected sera were quantified by ELISA. Results are representative of two independent experiments with 5 mice per group expressed as mean±SEM. Statistical significance was determined in comparison to IL-4Rα$^{-/lox}$ mice (*, p≤0.05; **, p≤0.01; ***, p≤0.001, **** p≤0.0001).

The augmentation towards a Type 2 immune response within Foxp3^{cre}IL-4Rα$^{-/lox}$ mice during *L. major* infection, was further evaluated through the production of nitrite and urea. Previous studies have shown that iNOS mediated nitrite production by M1 macrophages induces a Type 1 killer-effector mechanism that eliminates *L. major* parasites; in contrast M2 macrophage secretion of Arg1 resulted in urea production that induces a Type 2 immune response that sustains *L. major* parasite persistence [24]. The expression of these enzymes from M1 and M2 macrophages was determined by iNOS and arginase assays executed on LPS stimulated lymph nodes. At 8 weeks post infection, similar levels of nitrite production (Figure 3.12A) were observed between Foxp3^{cre}IL-4Rα$^{-/lox}$ male mice in comparison to littermate control IL-4Rα$^{-/lox}$ mice. Notably, a significant increase in urea production (Figure 3.12B) was observed in Foxp3^{cre}IL-4Rα$^{-/lox}$ male mice, indicating that deletion of IL-4Rα signalling on Treg cells leading to an increase in M2 macrophage Arg1 activity associated with activation of a Type 2 immune response, which may have contributed to sustained *L. major* parasite persistence.

Collectively, these results demonstrated that Foxp3^{cre}IL-4Rα$^{-/lox}$ mice display preferential activation of a Type 2 immune response which accounted for sustained *L. major* parasite replication and led to the hypersusceptible phenotype observed following subcutaneous infection in the footpad.

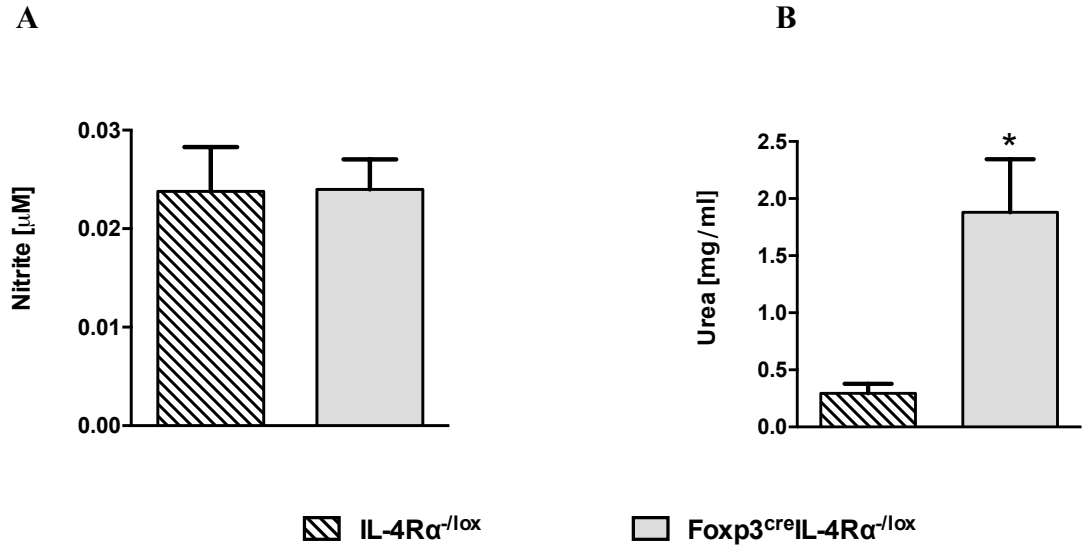

Figure 3.12: Foxp3^{cre}IL-4Rα$^{-/lox}$ male mice display modulated killer-effector functions following *L. major* LV39 footpad infection. Experimental male mice were subcutaneously infected in the left hind footpad with 2x10^6 stationary phase *L. major* LV39 promastigotes. At 8 weeks post infection lymph node cells were re-stimulated with 10 ng/ml LPS for 72 hours. Nitrite production (A) in cell supernatants were measured by Griess assay and urea production (B) in cell lysates were measured by Arginase activity assay. Results are representative of one independent experiment with 5 mice per group expressed as mean±SEM. Statistical significance was determined in comparison to IL-4Rα$^{-/lox}$ mice (*, p≤0.05).

3.4 An alternative infection route results in a similar disease outcome following *L. major* infection in experimental mice

3.4.1 Deletion of IL-4Rα signalling on T regulatory cells renders BALB/c male mice similarly hypersusceptible following inoculation of *L. major* parasites in the ear

Previous studies in murine models have provided significant evidence that suggests that alternatives routes of *L. major* infection may lead to differential immune response outcomes [94, 105]. Initially, the high parasite dose (10^5-10^7) subcutaneous inoculation of the footpad was used to examine response to *L. major* infection. However recent studies have established that the intradermal infection of the pinna of the ear with a lower dose of parasites (10^2-10^4) provides a more physiologically relevant infection model, as it mimics the low dose inoculation that occurs at the dermal site by an infected sandfly during natural transmission [94, 106]. To determine whether using an alternative route of infection and parasite dose would alter the observed phenotype and associated immune responses of Foxp3^{cre}IL-4Rα$^{-/lox}$ mice, experimental mice were intradermally inoculated with 1x10^4 *L. major* promastigotes in the left ear. Similar to previous studies [42, 107], C57BL6 mice had significantly reduced ear swellings (Figure 3.13A) accompanied with reduced parasite burdens in the ears (Figure 3.13B) and cervical lymph nodes (Figure 3.13C), in comparison to IL-4Rα$^{-/lox}$ mice, following *L. major* LV39 infection. Notably during intradermal *L. major* ear inoculation Foxp3^{cre}IL-4Rα$^{-/lox}$ male mice developed significantly increased ear swellings and greater parasite burdens were observed in the ear and cervical lymph node, compared to littermate control IL-4Rα$^{-/lox}$ male mice (Figure 3.13, A-C). These data suggest that similar to the hypersusceptible phenotype observed using the subcutaneous route of infection in the footpad, intradermal ear inoculation of *L. major* promastigotes led to enhanced disease progression in Foxp3^{cre}IL-4Rα$^{-/lox}$ male mice.

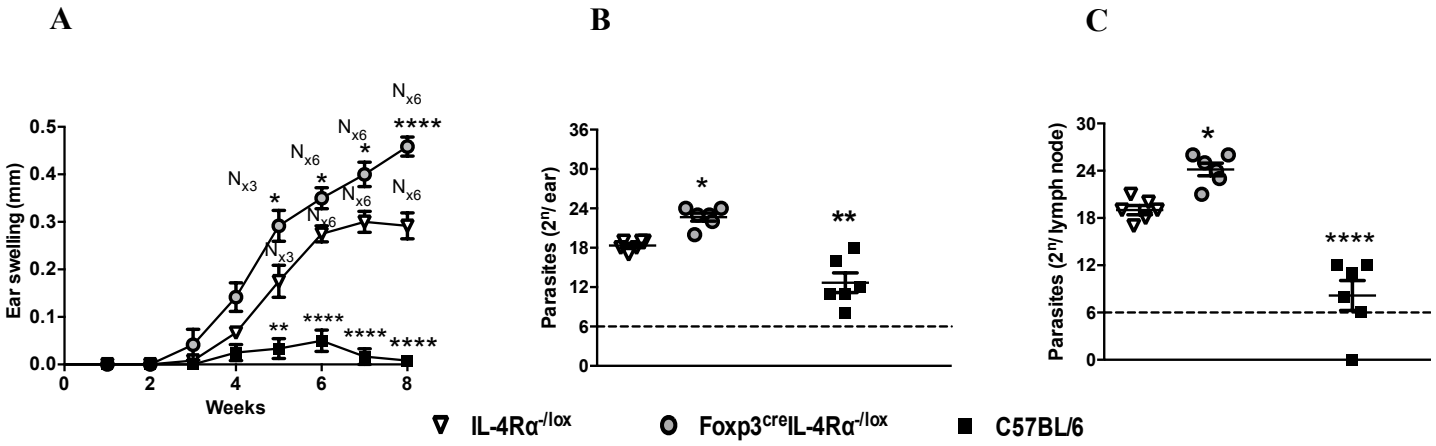

Figure 3.13: Foxp3^{cre}IL-4Rα$^{-/lox}$ male mice following *L. major* LV39 ear inoculation display a hypersusceptible phenotype. Experimental male mice were intradermally inoculated in the left ear with 1x10^4 stationary phase *L. major* LV39 promastigotes. Changes in diameter at the site of infection was measured weekly as ear swelling (mm) (A). Necrosis is indicated by "N" per number of mice in which it was observed. At 8 weeks post infection, the parasite burden (2^n) within infected ears (B) and lymph nodes (C) was determined by limiting dilution assay. The limit of detection (2^n) is indicated as a dashed line. Results are representative of one independent experiment with 6 mice per group expressed as mean±SEM. Statistical significance was determined in comparison to IL-4Rα$^{-/lox}$ mice (*, p≤0.05; **, p≤0.01; ***, p≤0.001, **** p≤0.0001).

3.4.2 Cytokine and antibody responses elicited in Foxp3^{cre}IL-4Rα$^{-/lox}$ male mice during *L. major* ear infection

Following 8 weeks of *L. major* infection, cytokine production within infected lymph node supernatants and antibody titres from sera samples were measured by ELISA. Although statistical significance was not observed, the biological concentrations of Type 2 cytokines IL-4 (Figure 3.14A) and IL-10 (Figure 3.14B) were greater in Foxp3^{cre}IL-4Rα$^{-/lox}$ male mice compared to littermate control IL-4Rα$^{-/lox}$ mice following intradermal ear infection. Similar to antibody titre production observed during subcutaneous footpad infection (Figure 3.11C), Foxp3^{cre}IL-4Rα$^{-/lox}$ male mice produced significantly greater total IgE levels (Figure 3.14C) in comparison to littermate control IL-4Rα$^{-/lox}$ mice. Collectively, these data suggest that despite changing the route of infection, the intradermal infection route in the ear results in a similar shift towards a Type 2 immune response and enhanced disease progression in Foxp3^{cre}IL-4Rα$^{-/lox}$ mice.

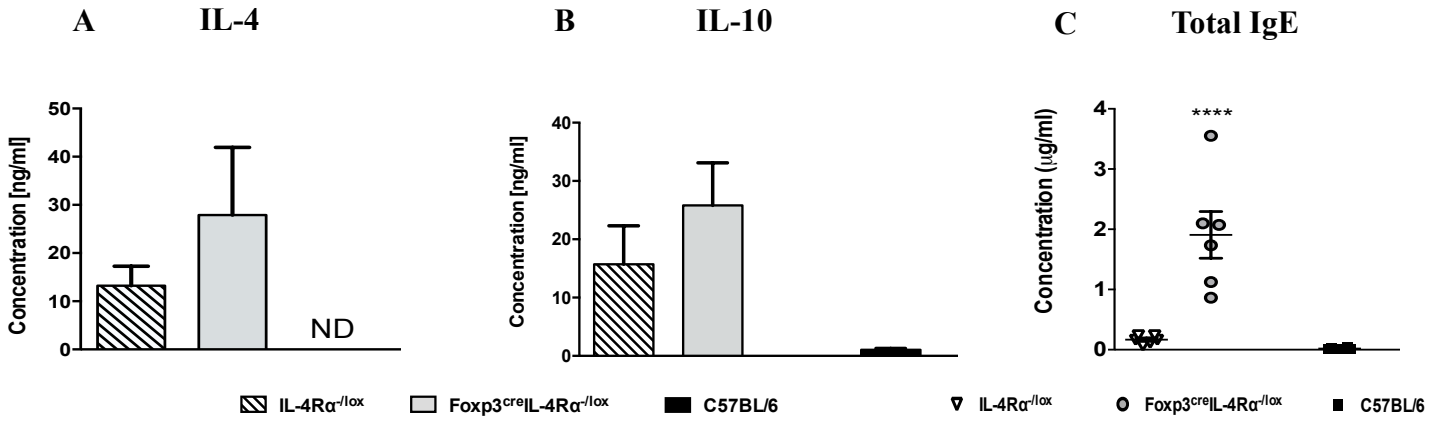

Figure 3.14: Similar Type 2 immunity is enhanced in Foxp3^{cre}IL-4Rα$^{-/lox}$ male mice following ear inoculation with *L. major* LV39 promastigotes. Experimental male mice were intradermally inoculated in the left ear with 1x10^4 stationary phase *L. major* LV39 promastigotes. At 8 weeks post infection, cervical lymph node cells were re-stimulated for 72 hours with anti-CD3. The production of IL-4 (A) and IL-10 (B) within lymph node cell supernatants were measured by ELISA. At 8 weeks post infection total IgE (C) antibody production within infected sera were quantified by ELISA. Results are representative of one independent experiment with 6 mice per group expressed as mean±SEM. Statistical significance was determined in comparison to IL-4Rα$^{-/lox}$ mice (*, p≤0.05; **, p≤0.01; ***, p≤0.001, **** p≤0.0001).

3.5 Proposed mechanism in hypersusceptible *L. major*-infected Foxp3^{cre}IL-4Rα$^{-/lox}$ male mice

3.5.1 Enhanced IDO expression from dendritic cells is found in *L. major*-infected Foxp3^{cre}IL-4Rα$^{-/lox}$ male mice

Previous studies have found that *L. major* parasites enhance the expression of an Indoleamine 2,3 dioxygenase (IDO) from dendritic cells to allow for successful replication within the infected host [108, 109]. IDO expression has further been shown to activate Treg cell activity by cell-mediated interactions via the B7 (CD80/86)/CTLA-4 or PD-L1/PD-1 pathways [110, 111]. Given the increased parasite burdens observed in *L. major*-infected Foxp3^{cre}IL-4Rα$^{-/lox}$ male mice (Figures 3.6, D-F, Figure 3.7B and Figure 3.13, B-C), we decided to examine whether elevated IDO expression contributed to the hypersusceptible phenotype observed in this model. The gating of various dendritic cell subpopulations by flow cytometry allowed for the expression of IDO, PD-L1 and CD80 to be assessed at a protein level (Supplementary Figure 4). Under naïve conditions, conventional dendritic cells (cDCs) and plasmacytoid dendritic cells (pDCs) within popliteal lymph nodes from Foxp3^{cre}IL-4Rα$^{-/lox}$ male mice and their L-4Rα$^{-/lox}$ littermate control had comparable levels of IDO GMFI expression (Supplementary Figure 5, A-B). Similarly, there were no differences in frequencies of IDO^{+}, PD-L1^{+}, CD80^{+} cDCs and IDO^{+}, PD-L1^{+}, CD80^{+} pDCs within popliteal lymph nodes from Foxp3^{cre}IL-4Rα$^{-/lox}$ male mice and their littermate controls (Supplementary Figure 5C). Following 8 weeks of *L. major* infection, cDCs and pDCS with popliteal lymph nodes from Foxp3^{cre}IL-4Rα$^{-/lox}$ male mice showed significantly elevated IDO expression compared to L-4Rα$^{-/lox}$ littermate control mice (Figure 3.15, A-B). The frequencies of IDO^{+}, PD-L1^{+}, CD80^{+} cDCs and IDO^{+}, PD-L1^{+}, CD80^{+} pDCs infiltrating the draining lymph nodes was significantly higher in Foxp3^{cre}IL-4Rα$^{-/lox}$ male mice in comparison to IL-4Rα$^{-/lox}$ male mice (Figure 3.15C). These results suggest that within Foxp3^{cre}IL-4Rα$^{-/lox}$ male IDO expressing dendritic cells are activated and concomitantly PD-L1 and CD80 molecules are engaged.

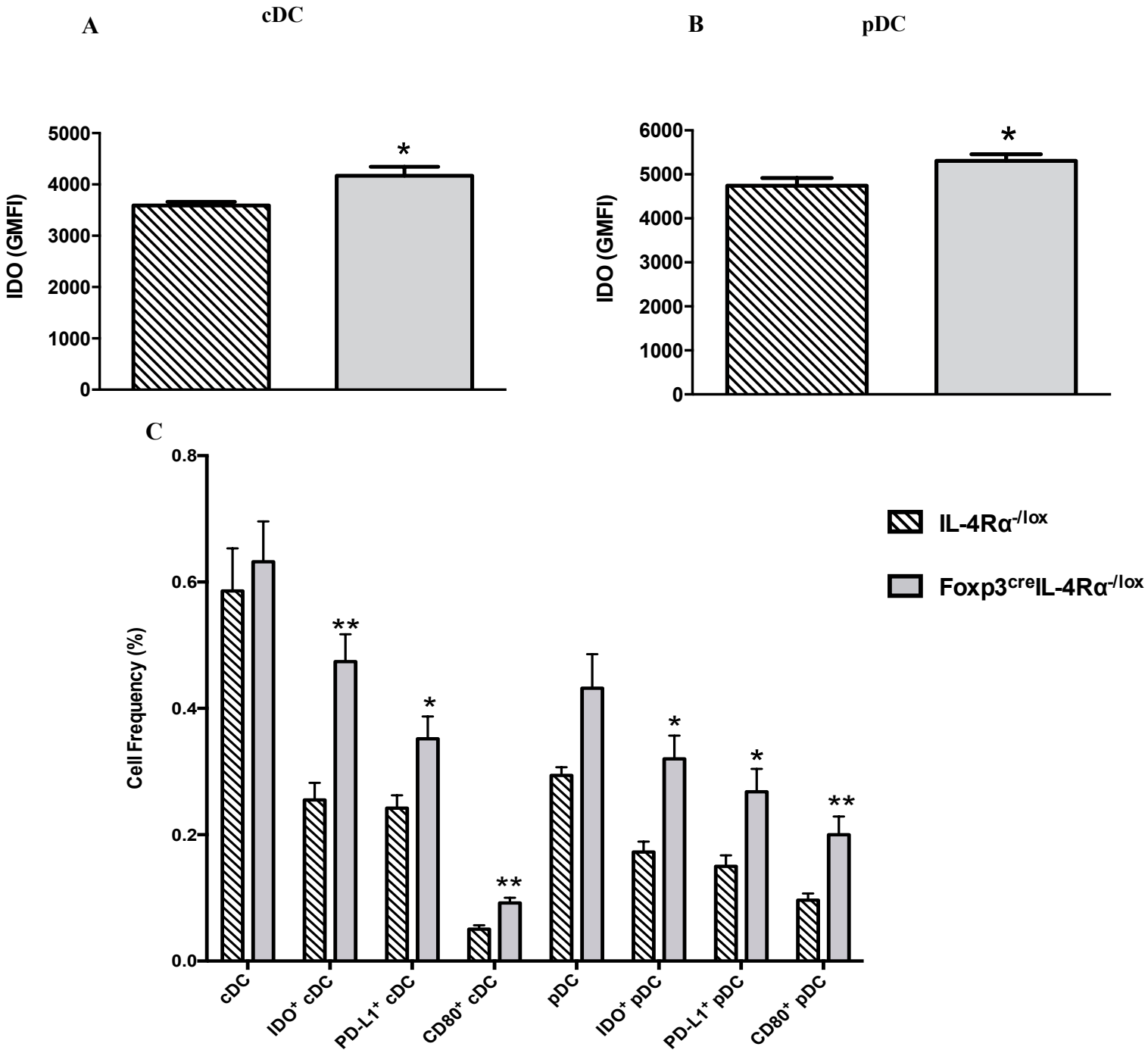

Figure 3.15: Dendritic cell populations within Foxp3^{cre}IL-4Rα$^{-/lox}$ mice show upregulated IDO, PDL-1 and CD80 expression following *L. major* infection. Foxp3^{cre}IL-4Rα$^{-/lox}$ and littermate control mice were infected subcutaneously with 2×10^6 stationary phase *L. major* LV39 promastigotes into the left hind footpad. At 8 weeks post infection, geometric mean fluorescent intensity (GMFI) of IDO expression was determined by flow cytometry analysis from the popliteal lymph nodes of *L. major*-infected IL-4Rα$^{-/lox}$ and Foxp3^{cre}IL-4Rα$^{-/lox}$ male mice. (A) IDO GMFI in conventional dendritic cells (cDCs; CD19$^-$CD11b$^+$CD11c$^+$MHCII$^+$), (B) IDO GMFI in plasmacytoid DCs (pDCs; CD11c$^+$MHCII$^+$B220$^+$), (C) Frequency of IDO expressing, PD-L1 and CD80 expressing dendritic cell subpopulations from the popliteal lymph nodes of IL-4Rα$^{-/lox}$ and Foxp3^{cre}IL-4Rα$^{-/lox}$ male mice following *L. major* infection. The following analyses are representative of 1 independent experiment with 5 mice per group expressed as mean±SEM. Statistical significance was determined in comparison to IL-4Rα$^{-/lox}$ mice (*, $p\leq0.05$; **, $p\leq0.01$).

3.5.2 PD-1 expression on Foxp3^{+} Treg cells is enhanced in *L. major*-infected Foxp3^{cre}IL-4Rα$^{-/lox}$ male mice

Previous studies have shown that during antigen presentation IDO expression in dendritic cells activates the PD-L1 or CD80/CD86 molecules that in turn ligate to the PD-1 or CTLA-4 molecules on Treg cells, activating their suppressive activity [82, 110, 112]. Given that in *L. major*-infected Foxp3^{cre}IL-4Rα$^{-/lox}$ male mice dendritic cells displayed elevated IDO levels associated with increased PD-L1 and CD80/CD86 expression (Figure 3.14, A-C and Figure 3.15, A-C), the expression of PD-1 on Treg cells was subsequently evaluated by flow cytometry analysis. Unfortunately at the time of the experiment, a fluorescently conjugated anti-CTLA-4 antibody was unavailable and therefore the expression of CTLA-4 on Treg cells could not be evaluated. The gating of CD4^{+}Foxp3^{+} Treg cells by flow cytometry allowed for expression of PD-1 to be assessed (Supplementary Figure 6). Under naïve conditions, comparable PD-1 GMFI on CD4^{+} Foxp3^{+} Treg cells and frequency of PD-1^{+} Treg cells were observed between Foxp3^{cre}IL-4Rα$^{-/lox}$ male mice and their IL-4Rα$^{-/lox}$ littermate control (Supplementary Figure 7, A-B). Notably following 8 weeks of *L. major* infection, the frequency of PD-1^{+} CD4^{+} Foxp3^{+} Treg cells infiltrating the draining lymph nodes significantly increased in Foxp3^{cre}IL-4Rα$^{-/lox}$ male mice in comparison to IL-4Rα$^{-/lox}$ male mice (Figure 3.16A). Furthermore, Foxp3^{cre}IL-4Rα$^{-/lox}$ male mice had significantly increased PD-1 GMFI expression, in comparison to L-4Rα$^{-/lox}$ littermate controls (Figure 3.16B). These results suggest that within Foxp3^{cre}IL-4Rα$^{-/lox}$ male mice IDO^{+} dendritic cells and Treg cell interact via PD-L1/PD-1 ligation during *L. major* infection.

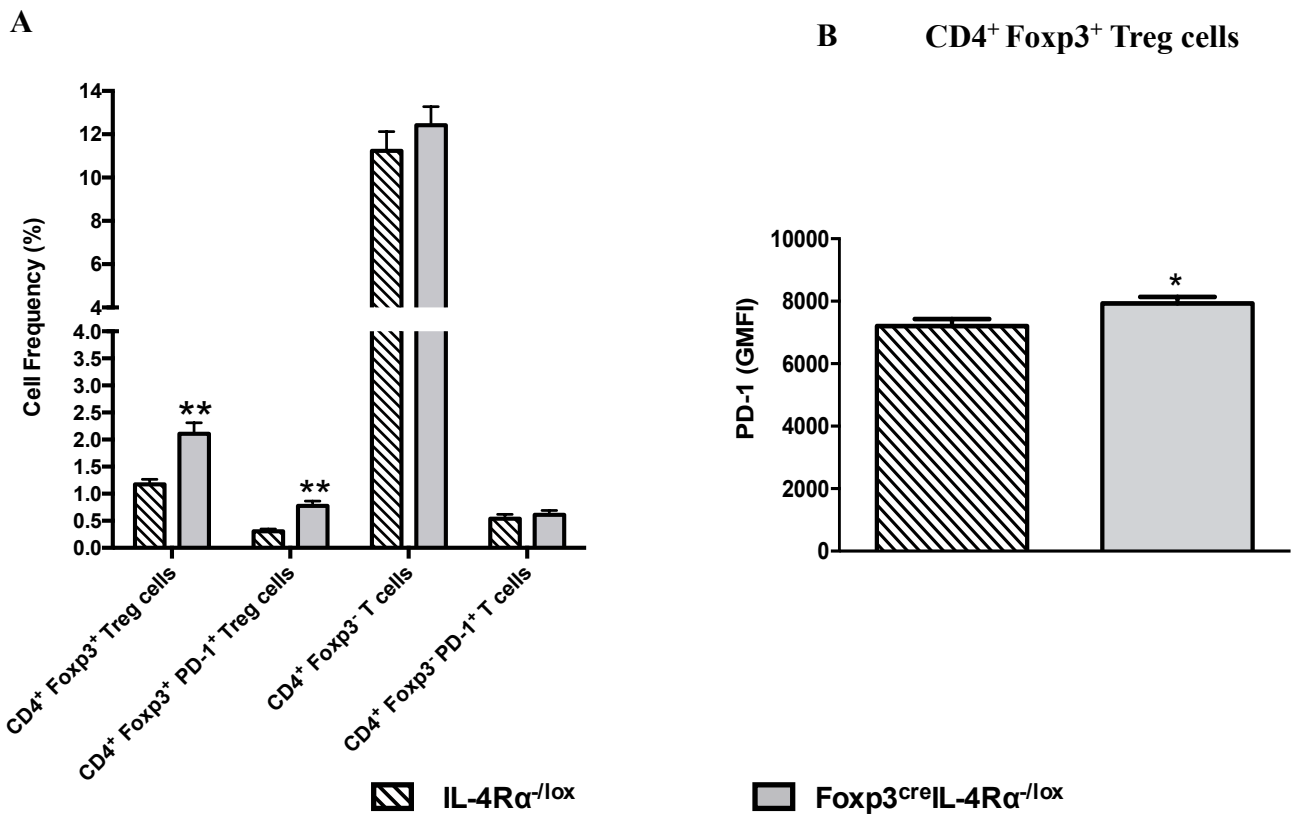

Figure 3.16: Deletion of IL-4Rα on Treg cells upregulates PD-1 expression following *L. major* infection. Foxp3^{cre}IL-4Rα$^{-/lox}$ and littermate control mice were infected subcutaneously with 2×10^6 stationary phase *L. major* LV39 promastigotes into the left hind footpad. (A) The frequency of PD-1 expressing T cells in the popliteal lymph node at 8 weeks post *L. major* infection. (B) PD-1 GMFI in CD4$^+$Foxp3$^+$ Treg cells in the popliteal lymph node at 8 weeks post *L. major* infection. The following analyses are representative of 1 independent experiment with 5 mice per group expressed as mean±SEM. Statistical significance was determined in comparison to IL-4Rα$^{-/lox}$ mice (*, p≤0.05; **, p≤0.01).

3.5.3 Differential IDO expression within *L. major*-infected Foxp3^{cre}IL-4Rα$^{-/lox}$ male mice could account for reduced T-bet$^+$ Th1 cell recruitment

Along with its role in activating Treg cell activity, previous studies have shown that IDO oxidation of L-tryptophan along the kynurenine pathway produced metabolites that induced T-cell apoptosis, specifically downregulating Th1 cells [83, 113]. Given that dendritic cells expressed elevated IDO levels within *L. major*-infected Foxp3^{cre}IL-4Rα$^{-/lox}$ male mice (Figure 3.15, A-C), we next examined by intranuclear staining the recruitment of transcription factor expressing T cell subsets. Following *L. major* infection, the frequencies of CD4$^+$ GATA3$^+$ Th2 cells and CD4$^+$RORγt Th17 cells infiltrating the popliteal lymph nodes was comparable between Foxp3^{cre}IL-4Rα$^{-/lox}$ male mice and their littermate controls (Figure 3.17). Similar to the results in Figure 3.9A, a significantly greater frequency of CD4$^+$Foxp3$^+$ Treg cell infiltrated the draining lymph nodes in Foxp3^{cre}IL-4Rα$^{-/lox}$ male mice (Figure 3.17). Notably, the frequency of CD4$^+$ T-bet$^+$ Th1 cells infiltrating the draining lymph nodes was significantly

reduced in Foxp3^{cre}IL-4Rα$^{-/lox}$ male mice in comparison to their littermate controls (Figure 3.17). These data provide supporting evidence that supports a mechanism whereby *L. major* parasites enhancing dendritic cell mediated IDO expression within infected Foxp3^{cre}IL-4Rα$^{-/lox}$ male mice, concomitantly resulted in increased Treg cell activity and increased selective apoptosis of Th1 cells; allowing for successful parasite replication [108, 113].

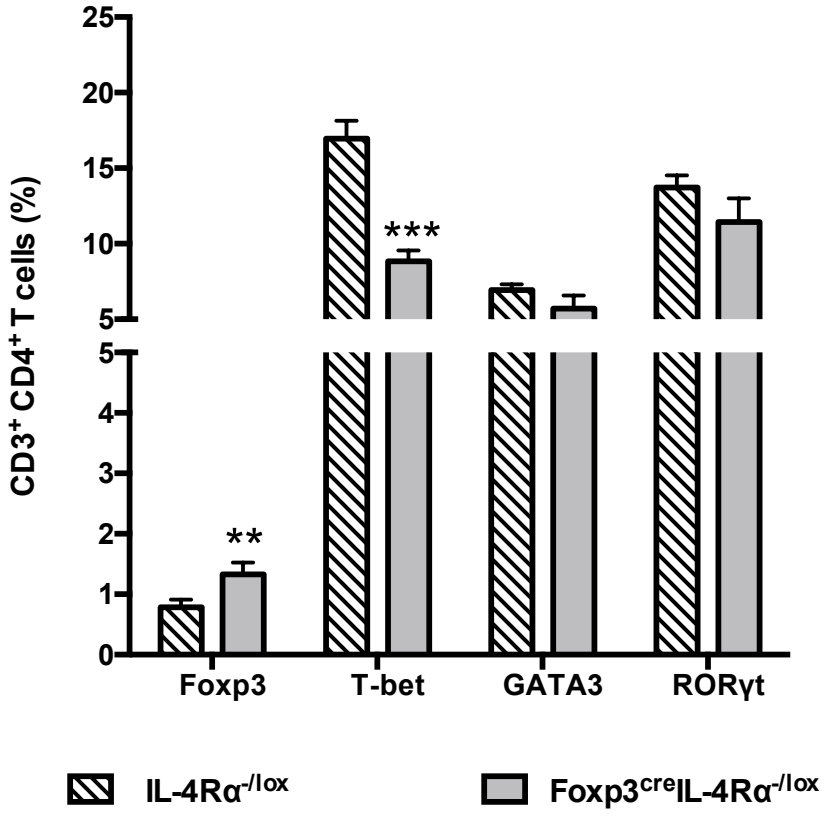

Figure 3.17: Deletion of IL-4Rα signalling on Treg cells enhances recruitment of Foxp3^{+} Treg cells and reduces recruitment of T-bet^{+} Th1 cells following *L. major* infection. Foxp3^{cre}IL-4Rα$^{-/lox}$ and littermate control mice were infected subcutaneously with 2×10^{6} stationary phase *L. major* LV39 promastigotes into the left hind footpad. (A) The frequency of transcription factor expressing CD3^{+}CD4^{+} T cells in the popliteal lymph node at 8 weeks post *L. major* infection. The following analyses are representative of 1 independent experiment with 5 mice per group expressed as mean±SEM. Statistical significance was determined in comparison to IL-4Rα$^{-/lox}$ mice (*, $p\leq0.05$; **, $p\leq0.01$).

4. Discussion

The ability of *L. major* parasites to persistent within a mammalian host is primarily based on immune response polarization in response to infection. Given that currently there are no commercially available vaccines against cutaneous leishmaniasis, the use of experimental murine models has been utilized as a robust system to elucidate the immune evasion strategies utilized by *Leishmania* parasites in order to identify novel immunotherapeutic targets for effective disease management [114]. During the first 72 hours post *L. major* infection, the decision between mounting a protective Type 1 immune response or susceptible Type 2 immune response occurs [115].

IL-4 and IL-13 were initially identified as canonical cytokines in initiating a Type 2 immune response during *L. major* infection, as its early secretion by $V\beta4^+$ $V\alpha8^+$ $CD4^+$ T cells caused elevated Th2 cell development and downregulated the secretion of Th1 cytokines IFN-γ and IL-12, resulting in enhanced susceptibility to *L. major* infection [25, 32]. Given the key roles of IL-4 and IL-13 in modulating Type 2 immune response, the impact of signalling via their common IL-4Rα chain was further examined.

As the IL-4Rα chain is ubiquitously expressed on an array of immune cells including keratinocytes, macrophages, dendritic cells, B cells and T cells, various cell-specific IL-4Rα deficient murine models have been established using the cre/*loxP* system to investigate IL-4Rα signalling on specific cell populations [26, 31]. The use of cell-specific IL-4Rα-deficient murine models during *L. major* infection has provided novel roles on specific cell populations through which IL-4Rα signalling has a detrimental effect leading to sustained parasite persistence or IL-4Rα signalling induces a protective effect leading to a reduction in parasite survival. In murine models IL-4Rα signalling on neutrophils, macrophages, B cells and total T cells were shown to favour *L. major* replication [45, 55, 59, 60]. In contrast, IL-4Rα signalling on dendritic cells was shown to be required to initiate NO-driven killer effector mechanism that reduces *L. major* survival within an infected host [6].

$Foxp3^+$ Treg cells are a unique $CD4^+$ T cell subset whose immunosuppressive activities are crucial for maintaining homeostasis between Type 1 or Type 2 immune responses and tolerance to self-antigens [61, 84]. IL-4 signalling has been shown to have both inhibitory and stimulatory effects on Treg cell development [36, 93].

During *L. major* infection, aggregation of $CD4^+CD25^+$ Treg cells at the site of infection has been found to have a detrimental effect, as they inhibit effector T cells ability to control parasite replication [87, 88]. In contrast, Treg cells have been shown to have a protective role in host immunity as they inhibit early IL-4 production in BALB/c mice, thereby reducing activation of a Type 2 immune response and allowing for *L. major* survival [20].

Treg cells therefore appear to contribute to host protection against and lead to sustained *L. major* replication at the site of infection, indicating that for effective protection against *L. major* infection a balance is required between Treg cells and effector T cells [20, 84, 87]. Given their critical role in regulating host immunity and the apparent dual roles of IL-4 signalling in their development, Treg cells have provided a novel $CD4^+$ T cell population in which to explore further. In this study, Treg cell-specific ($Foxp3^{cre}$IL-$4R\alpha^{-/lox}$) BALB/c mice generated using the cre/*lox*P system[89] were utilized to investigate whether IL-4Rα signalling on Treg cells influences disease outcome during cutaneous leishmaniasis.

Following *L. major* LV39 infection $Foxp3^{cre}$IL-$4R\alpha^{-/lox}$ mice were found to have depletion of the IL-4Rα chain specifically on $CD4^+$ $Foxp3^+$ Treg cells, while IL-4Rα expression was maintained in other cell populations. In naïve $Foxp3^{cre}$IL-$4R\alpha^{-/lox}$ mice, Cre-mediated deletion on Treg cells resulted in the partial deletion of the IL-4Rα chain in females and a quasi-complete deletion of the IL-4Rα chain in males [89]; this may have occurred as a result of random inactivation of genes along the X chromosome that occurs within females only [116]. During this study, it was determined that the differential deletion efficiency of the IL-4Rα chain on Treg cells observed between $Foxp3^{cre}$IL-$4R\alpha^{-/lox}$ female and male mice was conserved during *L. major* infection.

A previous study showed that specific deletion of the IL-4Rα chain on $Foxp3^+$ Treg cells resulted in mice developing enhanced tissue inflammation during *Schistosoma mansoni* and *Nippostrongylus brasiliensis* infections [89]; however the effects during cutaneous leishmaniasis were unknown.

In order to determine the role of IL-4Rα signalling on Foxp3 disease outcome during cutaneous leishmaniasis, $Foxp3^{cre}$IL-$4R\alpha^{-/lox}$ female and male mice were infected with *L. major* LV39 promastigotes subcutaneously in the footpad. Infection of $Foxp3^{cre}$IL-$4R\alpha^{-/lox}$ female with *L. major* promastigotes revealed similar footpad swellings, accompanied with similar parasite

burdens in the footpads, popliteal lymph nodes and spleens in comparison to IL-4Rα$^{-/lox}$ female littermate controls. In contrast, *L. major* infection of Foxp3^{cre}IL-4Rα$^{-/lox}$ male mice revealed a protective role for IL-4Rα signalling on Treg cells in controlling *L. major* disease progression. In comparison to IL-4Rα$^{-/lox}$ male littermate controls, Foxp3^{cre}IL-4Rα$^{-/lox}$ male mice developed greater footpad swellings and earlier necrosis. The hypersusceptible phenotype observed in Foxp3^{cre}IL-4Rα$^{-/lox}$ male mice was associated with significantly greater parasite loads which were analysed using LDA and endpoint PCR techniques. The endpoint PCR technique was utilised to quantify amastigote kDNA levels within infected footpad samples, however viable and non-viable parasites cannot be distinguished using this technique, so the results were compared to the LDA technique which allowed for the quantification of viable parasites within infected tissues following transformation from amastigote form within a mammalian host to *in vitro* promastigote form [25, 95]. Foxp3^{cre}IL-4Rα$^{-/lox}$ male mice developed significantly greater parasite burdens in the infected footpads, popliteal lymph nodes and spleens as well as significantly enhanced relative amastigote kDNA expression levels in comparison to IL-4Rα$^{-/lox}$ male littermate controls. In line with previous studies, genetically resistant C57BL/6 mice showed reduced footpad swelling and parasite burdens in the footpads and popliteal lymph nodes indicating effective control of *L. major* infection [25, 26]. Collectively, the difference in phenotype observed between Foxp3^{cre}IL-4Rα$^{-/lox}$ female and male suggests that a greater IL-IL-4Rα deletion efficiency on Treg cells enhances susceptibility of the Foxp3^{cre}IL-4Rα$^{-/lox}$ murine strain to *L. major* infection.

Foxp3^{+} T reg cells are able to maintain immune homeostasis by modulating cytokine production [65]. Flow cytometry analysis revealed significantly greater frequencies of CD4^{+}Foxp3^{+} Treg cell which produced IL-4, IL-10 or IL-13 were recruited in Foxp3^{cre}IL-4Rα$^{-/lox}$ male mice compared to their IL-4Rα$^{-/lox}$ littermate controls (Figure 4.1); which suggests that deletion of the IL-4Rα signalling on Treg cells augments these cells to increase Type 2 cytokine production during *L. major* infection. The increased CD4^{+}Foxp3^{+} Treg cell frequencies observed in *L. major*-infected Foxp3^{cre}IL-4Rα$^{-/lox}$ male mice were in line with a previous study that also showed increased CD4^{+}Foxp3^{+} Treg cell frequencies in the ear dermis of *L. major*-infected IL-4Rα$^{-/-}$ BALB/c mice [117]; which suggests that a global deletion or Treg cell specific deletion of IL-4Rα signalling in BALB/c mice results in a similar increase in CD4^{+}Foxp3^{+} Treg cell recruitment during *L. major* infection.

The results of this study support a previous study that suggested IL-4 signalling via STAT6 was required to maintain to Foxp3 expression in $CD4^+CD25^+$ Treg cells [36], as despite deletion of IL-4 signalling via the IL-4Rα chain, $CD4^+Foxp3^+$ Treg cell were able to increase IL-4 production which had a stimulatory effect on Treg cell differentiation.

Previous studies have determined that activation of Type 1 immune response within an infected mammalian host is detrimental to *L. major* survival, while induction of Type 2 immune response is favourable for *L. major* persistence [9, 39]. To determine the type of immune response elicited as a result of deleting the IL-4Rα chain on Treg cells, cytokine and antibody levels were compared following subcutaneous *L. major* infection. Treg cells secretion of suppressive cytokines, IL-10 and TGF-β has been shown to inhibit Th1 cell and Th2 cell activity and inhibit macrophages ability to kill intracellular *Leishmania* parasites [103, 118]. Analysis of T-cell specific cytokine production in $Foxp3^{cre}IL\text{-}4R\alpha^{-/lox}$ male mice revealed elevated production of IL-4, IL-10 and TGF-β, which suggested that increased Th2 and Treg cell cytokine activity contributes to the hypersusceptible phenotype observed during *L. major* infection (Figure 4.1).

Analysis of antibody production by B cells in $Foxp3^{cre}IL\text{-}4R\alpha^{-/lox}$ male mice showed significantly increased total IgE levels, accompanied with increased IL-4 and IL-10 secretion, indicated the shift towards an elevated Type 2 immune response occurred followed *L. major* footpad infection (Figure 4.1). Notably comparable of levels of SLA-specific IgG1, another Type 2 antibody, were detected within $Foxp3^{cre}IL\text{-}4R\alpha^{-/lox}$ male mice and their $IL\text{-}4R\alpha^{-/lox}$ littermate controls. Meiler *et al.* (2008) showed that increased IL-4 levels induce class-switching in B cells to enhance IgE production [119], which could account for the specific elevated levels of IgE detected in $Foxp3^{cre}IL\text{-}4R\alpha^{-/lox}$ male mice following *L. major* infection.

During *L. major* infection activation of a Type 1 immune response results in activation of M1 macrophages and leads to the destruction of intracellular *Leishmania* parasites by iNOS production [11]. The initiation of a Type 2 immune response enhances *Leishmania* survival as Th2 cells secretion of IL-4, IL-13 and IL-10 activate M2 macrophages to secrete Arginase 1 that depletes the common L-arginine substrate thereby subverting the NO-driven killer effector mechanism and allowing for *L. major* replication [9, 24]. The augmentation towards a Type 2 immune response within $Foxp3^{cre}IL\text{-}4R\alpha^{-/lox}$ mice during *L. major* infection was further examined by iNOS and Arg1 activity. Following *L. major* footpad infection, similar expression

of iNOS was detected, indicated by comparable nitrite production levels, between Foxp3^{cre}IL-4Rα$^{-/lox}$ male mice and their IL-4Rα$^{-/lox}$ littermate controls. In contrast, the significant increase in Arg1 activity indicated by increased urea production observed in Foxp3^{cre}IL-4Rα$^{-/lox}$ mice, indicated a shift towards M2 macrophage activation probably as a result of increased IL-4 and IL-10 production (Figure 4.1).

Previous studies in murine models have provided significant evidence that suggests that alternatives routes of *L. major* infection may lead to differential immune response outcomes [94, 105]. The subcutaneous footpad route of infection has been shown to require a high parasite dose (10^5-10^7) to induce *L. major* persistence within BALB/c mice; while the intradermal ear route of infection has provided an effective alternative model as it mimics natural sandfly infection with a lower parasite dose (10^2-10^4) [94, 120]. Similar to a previous study genetically resistant C57BL/6 mice developed reduced ear swellings and decreased parasite burden following *L. major* ear inoculation [42]. Foxp3^{cre}IL-4Rα$^{-/lox}$ male mice inoculated with 1x10^4 *L. major* promastigotes developed significantly increased ear swellings and parasite burdens, associated with elevated IL-4, IL-10 and total IgE levels, compared to their IL-4Rα$^{-/lox}$ littermate controls (Figure 4.1). These results suggested that both the subcutaneous footpad and intradermal ear routes of infections led to the induction of a Type 2 immune response that contributed towards the hypersusceptible phenotype observed in Foxp3^{cre}IL-4Rα$^{-/lox}$ male mice following *L. major* infection.

Collectively, these data suggest that efficient deletion of IL-4Rα signalling on Treg cells renders BALB/c mice hypersusceptible to *L. major* infection associated with augmentation towards a Type 2 immune response that allows for sustained parasite persistence.

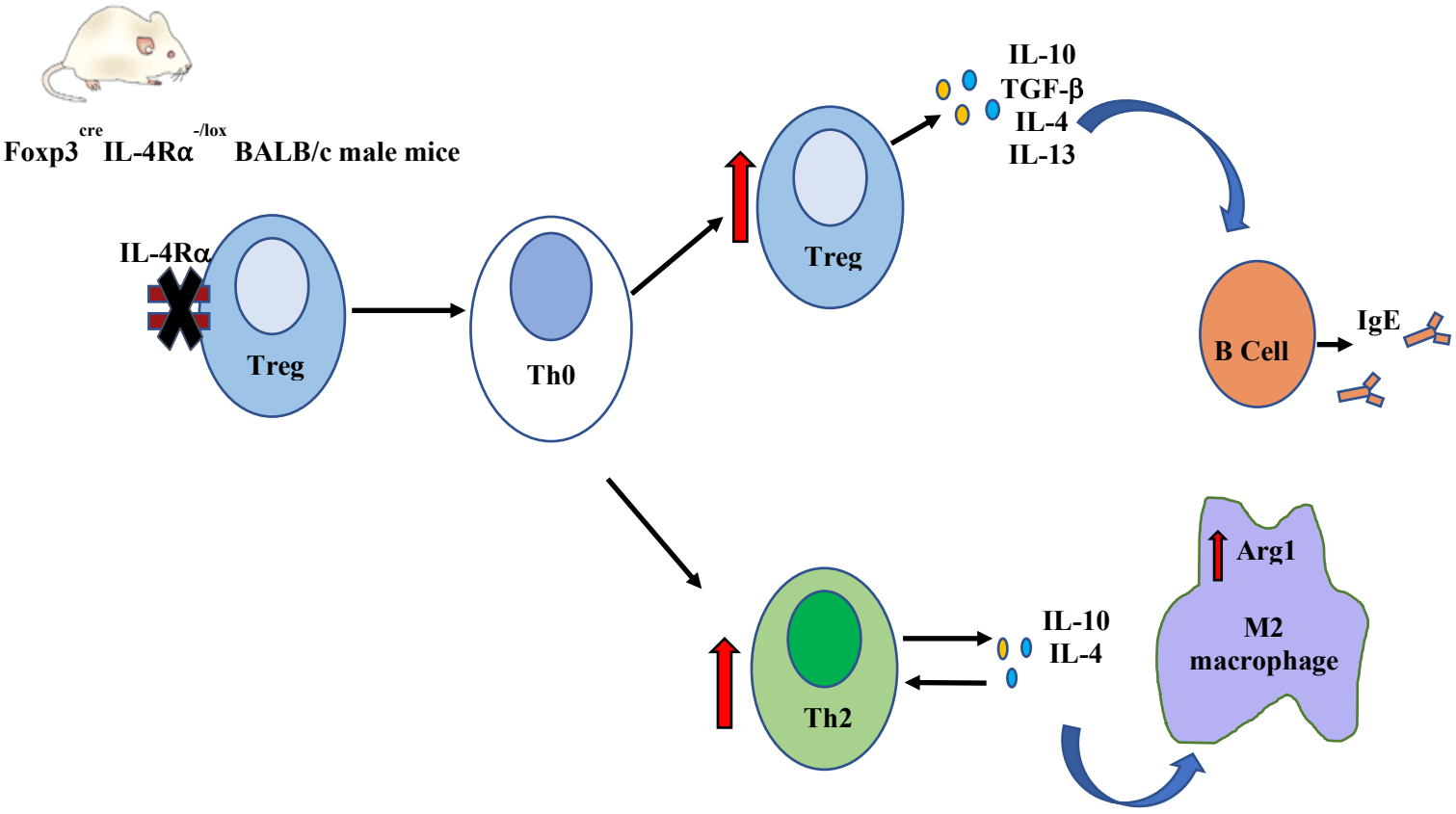

Figure 4.1 Deletion of the IL-4Rα chain on Foxp3^{+} Treg cells induces a Type 2 immune response during *L. major* infection. Within Foxp3^{cre} IL-4Rα$^{-/lox}$ BALB/c male mice, deletion of the IL-4Rα signalling on CD4^{+} Foxp3^{+} Treg cells primes, through cytokine signalling, the differentiation of naïve T cells into Treg cells. This resulted in increased production of Th2 and Treg cytokines (IL-4, IL-10, IL-13 and TGF-β). Elevated IL-4 levels can induce Th2 cell differentiation, direct M2 macrophage activation which leads to increased Arg1 activity and class switching of B cells to favour IgE antibody production; this apparent shift towards a Type 2 immune response favours *L. major* replication.

This current study has provided an additional host immune cell population in which IL-4Rα signalling has a protective role against *L. major* infection. Contrary to other *L. major*-infected cell-specific IL-4Rα conditional knockout models that developed a resistant phenotype [45, 55, 59], deletion of IL-4Rα signalling on dendritic cells [6] and Treg cells lead to BALB/c mice developing a hypersusceptible phenotype. A previous study showed IL-4Rα$^{-/-}$ BALB/c mice were only able to control acute *L. major* infection for 80 days, then they succumbed to infection [25]; suggesting that the deletion of IL-4Rα signalling on a particular subset of host cells may be detrimental to the host as this allows for sustained *Leishmania* replication. This may imply

that signal exists between dendritic cells and Treg cells, through which IL-4Rα signalling has a protective role against *L. major* infection.

IDO is an immunosuppressive enzyme primarily expressed by dendritic cells that has been shown to promote Treg cell differentiation and maintain Treg cell suppressive activity [83, 111]. IDO expression by dendritic cells has shown to promote Treg cell suppressive activity by CD80/86 or PD-L1 ligating to CTLA-4 or PD-1 respectively on Treg cells [82].

A previous study showed that to prevent against lethality during *Schistosoma mansoni* infection IL-4Rα$^{-/-}$ mice induced elevated IDO levels within the liver and intestine [121]; which proposed a link between IL-4Rα signalling and IDO expression. Makala *et al.* (2001) showed that IDO$^{-/-}$ mice had significantly reduced footpad swellings and footpad parasite burdens following *L. major* infection, which suggested that *L. major* parasites enhance IDO expression within an infected host to enhance their survival [108]. Flow cytometry analysis was utilised to determine whether the hypersusceptible phenotype observed in *L. major*-infected Foxp3^{cre}IL-4Rα$^{-/lox}$ male mice was driven by potential IDO-mediated mechanism.

Previous studies had suggested that the dendritic cell subset that expressed the greater level of IDO were pDCs (CD11c^{+}MHCII^{+}B220^{+}) [108, 122]. Increased frequencies of IDO^{+}, PD-L1^{+}, CD80^{+} cDCs and IDO^{+}, PD-L1^{+}, CD80^{+} pDCs infiltrated the popliteal lymph nodes Foxp3^{cre}IL-4Rα$^{-/lox}$ male mice during *L. major* infection; this suggested that the increased IDO expression observed was associated with up-regulation of PD-L1 molecules on activated dendritic cells. This observed elevated IDO expression within *L. major*-infected Foxp3^{cre}IL-4Rα$^{-/lox}$ male mice was associated with elevated PD-1 expression on Treg cells specifically; which correlated with increased Treg cell recruitment and secretion of Treg cell cytokines IL-10 and TGF-β. In the future, CTLA-4 expression will be examined at a protein level by flow cytometry analysis to examine whether CTLA-4/CD80 pathway is also activated. These results supported a hypothesis proposed in a previous study that suggests that elevated PD-L1/PD-1 engagement induces the expression of IDO by dendritic cells which in turn inhibits the mTOR/Akt pathway that destabilizes Treg cell function, allowing Treg cells to maintain their suppressive activity [111].

Previous studies have shown that increased IDO production leads to an accumulation of tryptophan metabolites such as kynurenine, quinolinic acid and picolinic acid, which induce apoptosis in $CD4^+$ Th1 cells and have no effect on Th2 cells [83, 113]. *In vitro* analysis revealed that increased IDO production prevents the conversion of Treg cells to $Ror\gamma t^+$ Th17-like cells [123]. To determine whether the observed increase in IDO production observed in *L. major*-infected $Foxp3^{cre}IL\text{-}4R\alpha^{-/lox}$ male mice affected $CD4^+$ T cell differentiation, transcription-factor expressing $CD4^+$ T cells were stained intranuclearly. A significant decrease in the frequency of $CD4^+T\text{-}bet^+$ Th1 cells was observed while the frequencies of $CD4^+GATA3^+$ Th2 cells and $CD4^+Ror\gamma t^+$ Th17 cells recruited to the popliteal lymph nodes remained unchanged in *L. major*-infected $Foxp3^{cre}IL\text{-}4R\alpha^{-/lox}$ male mice; which may suggest that observed increase in IDO production observed $Foxp3^{cre}IL\text{-}4R\alpha^{-/lox}$ male mice may reduce Th1 cell recruitment while simultaneously preventing the conversion of Treg cells into Th17, which in turn favours activation of Type 2 immune response.

Collectively, the results from this study suggest that deletion of IL-4Rα signalling on Treg cells in BALB/C mice lead to *L. major* parasites increasing IDO expression from dendritic cells, which in turn upregulates PD-L1 molecule to ligate to PD-1 on Treg cells, resulting in increased Treg cell activity (Figure 4.2). Concomitantly, increased IDO expression may have reduced Th1 cell recruitment at the site of infection (Figure 4.2), which in turn allowed for the induction of an elevated Type 2 immune response that favours *L. major* replication.

In order to validate whether the proposed mechanism outlined by the data from *L. major*-infected $Foxp3^{cre}IL\text{-}4R\alpha^{-/lox}$ male mice has translational potential, further studies will need to be conducted in cutaneous leishmaniasis diagnosed human patients. In a previous study qRT-PCR analysis on RNA extracted from human skin biopsies have shown significant increases in FOXP3 expression and elevated IDO expression in *L. vianna*-infected patients diagnosed with chronic cutaneous leishmaniasis as compared to asymptotically infected individuals [124]. Immunohistochemical analysis of stained human skin biopsies revealed higher intensities of Foxp3 expression in *L. brazilensis*-infected patients diagnosed with cutaneous leishmaniasis compared to healthy controls [84]. In the future, in line with these previous experiments, we would like to conduct immunohistochemistry and extract RNA from skin lesions of patients infected with *L. major*-causing cutaneous leishmaniasis and conduct qRT-PCR to analyse whether there is differential expression of IL-4Rα, FOXP3 and IDO; which may provide a

novel mechanism to explain sustained *Leishmania* replication and lesion development in human patients.

A previous study has identified that human patients diagnosed with chronic dermal leishmaniasis, caused by *L. vianna*, showed a 2-fold increase in $CD4^{+}CD25+Foxp3^{+}$ Treg cell recruitment in peripheral blood-mononuclear samples (PBMCs) [124]. In the future, in line with this approach we will analyse via flow cytometry whether PBMCs isolated from *L. major*-infected patients display differential $CD4^{+}Foxp3^{+}$ Treg cell and $CD4^{+}T\text{-}bet^{+}$ Th1 cell recruitment, similar to the data observed in $Foxp3^{cre}IL\text{-}4R\alpha^{-/lox}$ male mice.

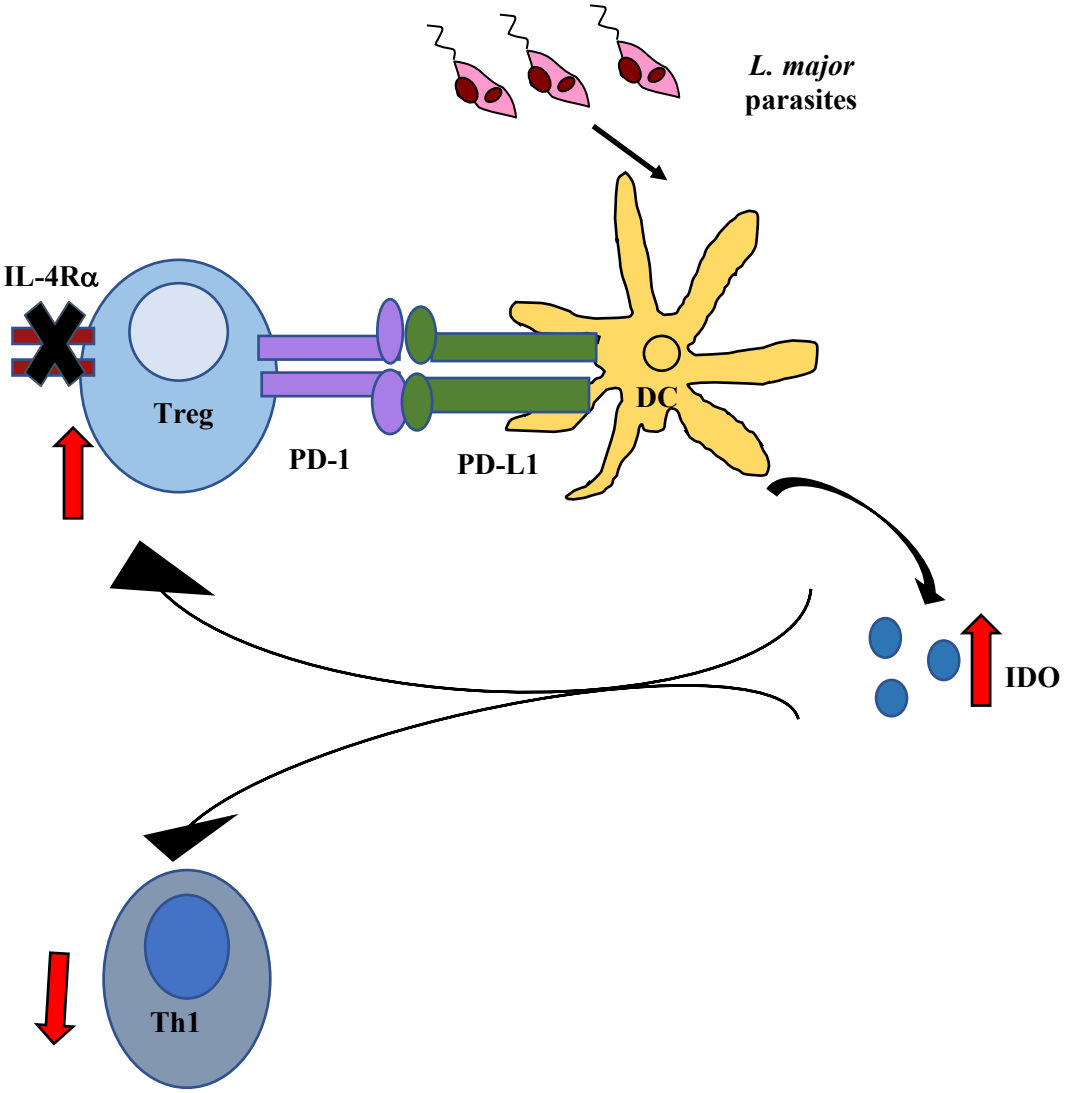

Figure 4.2: Induced IDO production from dendritic cells concomitantly induces Treg cell production and reduces Th1 cell activity during *L. major* infection. *L. major* parasites enhance IDO production from dendritic cells, which in turn upregulates PD-L1 expression which signals PD-1 expression on Treg cell and increases Treg cell production. IDO expression from dendritic cells leads to the apoptosis of Th1 cells, which in turn favours a Type 2 immune response and leads to increased *L. major* replication.

In conclusion, this study has provided a novel outcome of IL-4Rα signalling on a $CD4^+$ T cell subpopulation during cutaneous leishmaniasis. Deletion of the IL-4Rα chain on $Foxp3^+$ Treg cells enhanced BALB/c mice susceptibility to *L. major* infection; This resulted in enhanced disease progression and increased parasite dissemination from the infection site, This study has further proposed a novel mechanism by which enhanced IDO production within $Foxp3^{cre}$IL-$4R\alpha^{-/lox}$ male mice may contribute to the elevated Type 2 immune response induced following *L. major* infection. The protective role of IL-4Rα signalling on $Foxp3^+$ Treg cells during cutaneous leishmaniasis will now have to be considered carefully for future drug-based or vaccine-based strategies.

5. References

1. Kamhawi, S., Belkaid, Y., Modi, G., Rowton, E., Sacks, D. (2000). Protection against cutaneous leishmaniasis resulting from bites of uninfected sand flies. Science. **290**: 1351-1354.
2. Stockdale, L., and Newton, R. (2013). A review of preventative methods against human leishmaniasis infection. PLoS Negl Trop Dis. **7** (6): 1-15.
3. WHO (2019). Leishmaniasis. (World Health Organization: https://www.who.int/en/news-room/fact-sheets/detail/leishmaniasis).
4. Hotez, P., Remme, J.H.F., Buss, P., Alleyne, G., Morel, C., Breman, J.G. (2004). Combating Tropical Infectious Diseases: Report of the Disease Control Priorities in Developing Countries Project. Clinical Infectious Diseases. **38** (6): 871-878.
5. Reithinger, R., Dujardin, J.C,. Louzir, H,. Pirmez, C,. Alexander, B,. Brooker, S. (2007). Cutaneous leishmaniasis. The Lancet Infectious Diseases. **7** (9): 581-596.
6. Hurdayal, R., Nieuwenhuizen, N.E., Revaz-Breton, M., Smith, L., Hoving, J.C., Parihar S.P., Boris, R., Brombacher, F. (2013). Deletion of IL-4 receptor alpha on dendritic cells renders BALB/c mice hypersusceptible to *Leishmania major* infection. PLoS Pathog. **9** (10): 1-15.
7. Cabrera, M., Shaw, M.A., Sharpies, C., Williams, H., Castes, M., Convit, J., Blackwell, J.M. (1995). Polymorphism in Tumor Necrosis Factor Genes Associated with Mucocutaneous Leishmaniasis. J Exp Med **182** (11): 1259-1264.
8. Antoine, J.C., Prina, E., Courret, N., Lang, T. (2004). *Leishmania* spp.: on the Interactions They Establish with Antigen-Presenting Cells of their Mammalian Hosts. Advances in Parasitology **58** (4): 1-68.
9. Sacks, D., and Noben-Trauth, N. (2002). The immunology of susceptibility and resistance to Leishmania major in mice. Nat Rev Immunol. **2** (11): 845-58.
10. Sunter, J.D., Yanase, R., Wang, Z., Catta-Preta, C.M.C., Moreira-Leite, F., Myskova, J., Pruzinova, K., Volf, P., Mottram, J.C., Gull, K. (2019). *Leishmania* flagellum attachment zone is critical for flagellar pocket shape, development in the sand fly, and pathogenicity in the host. Natl Acad Sci **116** (13): 6351-60.
11.Duque, G.A., and Descoteaux, A. (2014) Macrophage cytokines: involvement in immunity and infectious diseases. Front Immunol. **5** (491): 1-12.
12. Machado, P., Araujo, C., da Silva, A.T., Almeida, R.P., D'Oliveira, A., Bittencourt, A., Carvalho, E.M. (2002). Failure of Early Treatment of Cutaneous Leishmaniasis in Preventing the Development of an Ulcer. Clinical Infectious Diseases. **34** (12): e69-e73.
13. Goto, H., and Lindoso, J.A. (2010) Current diagnosis and treatment of cutaneous and mucocutaneous leishmaniasis. Expert Review Anti-Infective Therapy. **8** (4): 419-33.
14. Bruijn, M.H.L., and Barker, D.C. (1992). Diagnosis of New World leishmaniasis: specific detection of species of the *Leishmania braziliensis* complex by amplification of kinetoplast DNA. Acta Tropica. **52**: 45-58.
15. WHO Expert Committee on the control of the Leishmaniases and World Heath Organization (2010). Control of the leishmaniases: report of a meeting of the WHO Expert Committee on the Control of Leishmaniases (World Health Organization https://apps.who.int/iris/bitstream/handle/10665/44412/WHO_TRS_949_eng.pdf?sequence=1&isAllowed=y).
16. Yardley, V., and Croft, S.L. (1997). Activity of Liposomal Amphotericin B against Experimental Cutaneous Leishmaniasis. Antimicrobial Agents and Chemotherapy. **41** (4): 752-756.
17. Ponte-Sucre, A., Gamarro, F., Dujardin, J.C., Barrett, M.P., Lopez-Velez, R., Garcia-Hernandez, R., Pountain, A.W., Mwenechanya, R., Papadopoulou, B. (2017). Drug resistance and treatment failure in leishmaniasis: A 21st century challenge. PLos Negl Trop Disease. **11** (12): 1-24.

18. Croft, S.L., Sundar, S., Fairlamb, A.H. (2006). Drug resistance in leishmaniasis. Clinical Microbiology Reviews. **19** (1): 111-126.
19. Heinzel, F.P., Sadick, M.D., Holaday, B.J., Coffman, R.L., Locksley, R.M. (1989) Reciprocal expression of interferon gamma or interleukin 4 during the resolution or progression of murine leishmaniasis. Evidence for expansion of distinct helper T cell subsets. J Exp Med. **169** (1): 59-72.
20. Aseffa, A., Gumy, A., Launois, P., MacDonald, H.R., Louis, J.A., Tacchini-Cottier, F. (2002). The early IL-4 response to *Leishmania major* and the resulting Th2 cell maturation steering progressive disease in BALB/c mice are subject to the control of regulatory CD4+CD25+ T cells. J Immunol. **169** (6): 3232-41.
21. Scharton-Kersten, T., Afonso, L.C., Wysocka, M., Trinchieri, G., Scott, P. (1995). IL-12 is required for natural killer cell activation and subsequent T helper 1 cell development in experimental leishmaniasis. J Immunol. **154** (10): 5320-5330.
22. Weng, M., Huntley, D., Huang, I.F., Foye-Jackson, O., Wang, L., Sarkissian, A., Zhou, Q., Walker, W.A., Cherayil, B.J., Shi, H.N. (2007). Alternatively activated macrophages in intestinal helminth infection: effects on concurrent bacterial colitis. J Immunol. **179** (7): 4721-
23. Mosser, D.M., and Edwards, J.P. (2008). Exploring the full spectrum of macrophage activation. Nat Rev Immunol. **8** (12): 958-969.
24. Rath, M., Muller, I., Kropf, P., Closs, E.I., Munder, M. (2014). Metabolism via Arginase or Nitric Oxide Synthase: Two Competing Arginine Pathways in Macrophages. Front Immunol. **5** (532): 1-10.
25. Mohrs, M., Ledermann, B., Köhler, G., Dorfmüller, A., Gessner, A., Brombacher, F. (1999). Differences Between IL-4- and IL-4 Receptor alpha-Deficient Mice in Chronic Leishmaniasis Reveal a Protective Role for IL-13 Receptor Signaling. J Immunol. **162** (12): 7302-7308.
26. Hurdayal, R., and Brombacher, F. (2017). Interleukin-4 Receptor Alpha: From Innate to Adaptive Immunity in Murine Models of Cutaneous Leishmaniasis. Front Immunol. **8** (1354) : 1-15.
27. Biedermann, T., Zimmermann, S., Himmelrich, H., Gumy, A., Egeter, O., Sakrauski, A.K., Seegmüller, I., Voigt, H., Launois, P., Levine, A.D., Wagner, H., Heeg, K., Louis, J.A., Röcken, M. (2001). IL-4 instructs TH1 responses and resistance to *Leishmania major* in susceptible BALB/c mice. Nat Immunol. **2** (11): 1054-60.
28. Reiner, S.L., Zheng, S., Wang, Z.E., Stowring, L., Locksley, R.M. (1994). Leishmania promastigotes evade interleukin 12 (IL-12) induction by macrophages and stimulate a broad range of cytokines from CD4+ T cells during initiation of infection. J Exp Med. **179** (2): 447-456.
29. Matthews, D.J., Emson, C.L., Mckenzie, G.J., Jolin, H.E., Blackwell, J.M., Mckenzie, A.N.J. (2000). IL-13 is a susceptibility factor for *Leishmania major* infection. J Immunol. **165** (3): 1458-1462.
30. Le Gros, G., Ben-Sasson, S.Z., Seder, R., Finkelman, F.D., Paul, W.E. (1990). Generation of interleukin 4 (IL-4)-producing cells in vivo and in vitro: IL-2 and IL-4 are required for in vitro generation of IL-4-producing cells. J Exp Med. **172** (3): 921-929.
31. Launois, P., Conceicao-Silva, F., Himmerlich, H., Parra-Lopez., C., Tacchini-Cotter, F., Louis, J.A. (1998). Setting in motion the immune mechanisms underlying genetically determined resistance and susceptibility to infection with *Leishmania major*. Parasite Immunology. **20** (5): 223-230.
32. Launois, P., Maillard, I., Pingel, S., Swihart, K.G., Xénarios, I., Acha-Orbea, H., Diggelmann, H., Locksley, R.M., MacDonald, H., Louis, J.A. (1997). IL-4 Rapidly produced by Vβ4 Vα8 CD4+ T cells instructs Th2 development and susceptibility to Leishmania major in BALB/c mice. Immunity. **6** (5): 541-549.

33. Gjorgjevikj, M. (1996). Transmembrane and intracellular signalling by interleukin-4: receptor dimerization and beyond. Eur Cytokine Netw. **7** (1): 37-49.
34. Nelms, K., Keegan, A.D., Zamorano, J., Ryan, J.J., Paul, W.E. (1999). The IL-4 Receptor: Signalling Mechanisms and Biologic Functions. Annual Review of Immunology. **17** (1): 701-738.
35. LaPorte, S.L., Juo, Z.S., Vaclavikova, J., Colf, L.A., Qi, X., Heller, N.M., Keegan, A.D., Garcia, K.C. (2008). Molecular and structural basis of cytokine receptor pleiotropy in the interleukin-4/13 system. Cell. **132** (2): 259-272.
36. Pillemer, B.B., Qi, Z., Melgert, B., Oriss, T.B., Ray, P., Ray, A. (2009). STAT6 activation confers upon T helper cells resistance to suppression by regulatory T cells. J Immunol. **183** (1): 155-163.
37. Tony, H.P., Shen, B.J., Reusch, P., Sebald, W. (1994). Design of human interleukin-4 antagonists inhibiting interleukin-4-dependent and interleukin-13-dependent responses in T-cells and B-cells with high efficiency. European Journal of Biochemistry. **225** (2): 659-665.
38. Zurawski, S.M.,Vega, F., Huyghe, B., Zurawski, G. (1993). Receptors for interleukin-13 and interleukin-4 are complex and share a novel component that functions in signal transduction. The EMBO Journal. **12** (7): 2663-2670.
39. Mohrs, M., Holscher, C., Brombacher, F. (2000). Interleukin-4 receptor alpha-deficient BALB/c mice show an unimpaired T helper 2 polarization in response to Leishmania major infection. Infection and Immunity. **68** (4): 1773-1780.
40. Nagy, A. (2000). Cre recombinase: The universal reagent for genome tailoring. Genesis. **26** (2): 99-109.
41. Ehrchen, J.M., Roebrock, K., Foell, D., Nippe, N., von Stebut, E., Weiss, J.M., Münck, N.A., Viemann, D., Varga, G., Müller-Tidow, C., Schuberth, H.J., Roth, J., Sunderkötter, C. (2010). Keratinocytes determine Th1 immunity during early experimental leishmaniasis. PLoS Pathog. **6** (4): 1-16.
42. Govender, M., Hurdayal, R., Martinez-Salazar, B., Gqada, K., Pillay, S., Gcanga, L., Passelli, K.,Nieuwenhuizen, N.E., Tacchini-Cottier, F., Guler, R., Brombacher, F. (2018). Deletion of Interleukin-4 Receptor Alpha-Responsive Keratinocytes in BALB / c Mice Does Not Alter Susceptibility to Cutaneous Leishmaniasis. Infection and Immunity. **86** (12): 1-16.
43. Descatoire, M., Hurrell, B.P., Govender, M., Passelli, K., Martinez-Salazar, B., Hurdayal, R., Brombacher, F., Guler, R., Tacchini-Cottier, F. (2017). IL-4Ralpha Signaling in Keratinocytes and Early IL-4 Production Are Dispensable for Generating a Curative T Helper 1 Response in Leishmania major-Infected C57BL/6 Mice. Front Immunol. **8** (1265): 1-12.
44. Ribeiro-Gomes, F.L., Moniz-de-Souza, M.C.A., Alexandre-Moreira, M.S., Dias, W.B., Lopes, M.F., Nunes, M.P., Lungarella, G., Dosreis, G.A. (2007). Neutrophils activate macrophages for intracellular killing of *Leishmania major* through recruitment of TLR4 by neutrophil elastase. J Immunol. **179** (6): 3988-3994.
45. Hölscher, C., Arendse, B., Schwegmann, A., Myburgh, E., Brombacher, F. (2006). Impairment of Alternative Macrophage Activation Delays Cutaneous Leishmaniasis in Nonhealing BALB/c Mice. J Immunol. **176** (2): 1115-1121.
46. Rochael, N.C., Guirmaraes-Costa., A.B., Nascimento, M.T.C., Desouza-Viera, T.S., Oliveira, M.P., Garcia-Souza, L.F., Oliveira, M.F., Saraiva, E.M. (2015). Classical ROS-dependent and early/rapid ROS-independent release of neutrophil extracellular traps triggered by *Leishmania* parasites. Scientific Reports. **5** (4): 1-11.
47. Herbert, D.R., Hölscher, C., Mohrs, M., Arendse, B., Schwegmann, A., Radwanska, M., Leeto, M., Kirsch, R., Hall, P., Mossmann, H., Claussen, B., Förster, I., Brombacher, F. (2004). Alternative macrophage activation is essential for survival during schistosomiasis and downmodulates T helper 1 responses and immunopathology. Immunity. **20** (5): 623-635.

48. Pulendran, B., Smith, J.L., Caspary, G., Brasel, K., Pettit, D., Maraskovsky, E., Maliszewski, C. R. (1999). Distinct dendritic cell subsets differentially regulate the class of immune response *in vivo*. Proc. Natl. Acad. Sci. **96** (3): 1036-1041.
49. De Trez, C., Magez, S., Akira, S., Ryffel, B., Carlier, Y., Muraille, E. (2009). iNOS-producing inflammatory dendritic cells constitute the major infected cell type during the chronic *Leishmania major* infection phase of C57BL/6 resistant mice. PLoS Pathog. **5** (6): 1-13.
50. Woelbing, F., Kostka, S.L., Moelle, K., Belkaid, Y., Sunderkoetter, C., Verbeek, S., Waisman, A., Nigg, A.P., Knop, J., Udey, M.C., von Stebut, E. (2006). Uptake of *Leishmania major* by dendritic cells is mediated by Fcgamma receptors and facilitates acquisition of protective immunity. J Exp Med. **203** (1): 177-188.
51. Miles, S.A., Conrad, S.M., Alves, R.G., Jeronimo, S.M., Mosser, D.M. (2005). A role for IgG immune complexes during infection with the intracellular pathogen Leishmania. J Exp Med. **201** (5): 747-754.
52. Harris, D.P., Haynes, L., Sayles, P.C., Duso, D.K., Eaton, S.M., Lepak, N.M., Johnson, L.J, Swain, S.L., Lund, F.E. (2000). Reciprocal regulation of polarized cytokine production by effector B and T cells. Nature Immunology. **1** (6):475-482.
53. Harris, D.P., Goodrich, S., Mohrs, K., Mohrs, M., Lund, F.E. (2005). Cutting edge: the development of IL-4-producing B cells (B effector 2 cells) is controlled by IL-4, IL-4 receptor alpha, and Th2 cells. J Immunol. **175** (11): 7103-7107.
54. Hoving, J.C., Kirstein, F., Nieuwenhuizen, N.E., Fick, L.C., Hobeika, E., Reth, M., Brombacher, F. (2012). B cells that produce immunoglobulin E mediate colitis in BALB/c mice. Gastroenterology. **142** (1): 96-108.
55. Hurdayal, R., Ndlovu, H.H., Revaz-Breton, M., Parihar, S.P., Nono, J.K., Govender, M., Brombacher, F. (2017). IL-4-producing B cells regulate T helper cell dichotomy in type 1- and type 2-controlled diseases. Proc Natl Acad Sci **114** (40): E8430-E8439.
56. Scott, P., Natovitz, P., Coffman, R.L., Pearce, E., Sher, A. (1988). Immunoregulation of cutaneous leishmaniasis. T cell lines that transfer protective immunity or exacerbation belong to different T helper subsets and respond to distinct parasite antigens. J Exp Med. **168** (5): 1675-1684.
57. Swain, S.L., Weinberg, A.D., English, M., Huston, G. (1990). IL-4 directs the development of Th2-like helper effectors. J Immunol. **145**: 3796-3806.
58. Zurawski, G., and de Vries, J.E. (1994). Interleukim 13, an interleukin 4-like cytokine that acts on monocytes and B cells, but not on T cells. Immunology Today **15** (1): 19-26.
59. Radwanska, M., Cutler, AJ., Hoving, J.C., Magez, S., Holscher, C., Bohms, A., Arendse, B., Kirsch, R., Hunig, T., Alexander, J., Kaye, P., Brombacher, F. (2007). Deletion of IL-4Ralpha on CD4 T cells renders BALB/c mice resistant to *Leishmania major* infection. PLoS Pathog. **3** (5): 0619-0629.
60. Dewals, B., Hoving, J.C., Leeto, M., Marillier, R.G., Govender, U., Cutler, A.J, Horsnell, W.G.C., Brombacher, F. (2009). IL-4Ralpha responsiveness of non-CD4 T cells contributes to resistance in *Schistosoma mansoni* infection in pan-T cell-specific IL-4Ralpha-deficient mice. Am J Pathol. **175** (2): 706-716.
61. Sakaguchi, S., Yamaguchi, T., Nomura, T., Ono, M. (2008). Regulatory T cells and immune tolerance. Cell. **133** (5): 775-787.
62. Yun, T.J., and Bevan, M.J. (2001). The Goldilocks conditions applied to T cell development. Nature Immunology. **2** (1): 13-14.
63. Li, M.O., and Rudensky, A.Y. (2016). T cell receptor signalling in the control of regulatory T cell differentiation and function. Nat Rev Immunol. **16** (4): 220-233.
64. Baecher-Allan, C., Brown, J.A., Freeman, G.J., Hafler, D.A. (2001) CD4+CD25high regulatory cells in human peripheral blood. J Immunol. **167** (3): 1245-1253.

65. Sakaguchi, S., Miyara, M., Costantino, C.M., Hafler, D.A. (2010). FOXP3+ regulatory T cells in the human immune system. Nat Rev Immunol. **10** (7): 490-500.
66. Hori S., Nomura T., Sakaguchi S. (2003). Control of regulatory T cell development by the transcription factor Foxp3. Science. **299** (3):981-985.
67. Fontenot, J.D., Gavin, M.A., Rudensky, A.Y. (2003). Foxp3 programs the development and function of CD4+CD25+ regulatory T cells. Nat Immunol. **4** (4): 330-336.
68. Roncador, G., Brown, P.J., Maestre, L., Hue, S., Martinez-Torrecuadrada, J.L., Ling K.L., Pratap, S., Toms, C., Fox, B.C., Cerundolo, V., Powrie, F., Banham, A.H. (2005). Analysis of FOXP3 protein expression in human CD4+CD25+ regulatory T cells at the single-cell level. Eur J Immunol. **35** (6): 1681-1691.
69. Bennett, C.L., Yoshioka, R., Kiyosawa, H., Barker, D.F., Fain, P.R., Shigeoka, A.O., Chance, P.F. (2000). X-Linked syndrome of polyendocrinopathy, immune dysfunction, and diarrhea maps to Xp11.23-Xq13.3. Am J Hum Genet. **66** (2): 461-468.
70. Campbell, D.J., and Ziegler, S.F. (2007). FOXP3 modifies the phenotypic and functional properties of regulatory T cells. Nat Rev Immunol. **7** (4): 305-310.
71. Lopes, J.E., Torgerson, T.R., Schubert, L.A., Anover, S.D., Ocheltree, E.L., Ochs, H.D., Ziegler, S.F. (2006). Analysis of FOXP3 reveals multiple domains required for its function as a transcriptional repressor. J Immunol. **177** (5): 3133-3142.
72. Brunkow, M.E., Jeffery, E.W., Hjerrild, K.A., Paeper, B., Clark, L.B., Yasayko, S.A., Wilkinson, J.E., Galas, D., Ziegler, S.F., Ramsdell, F. (2001). Disruption of a new forkhead/winged-helix protein, scurfin, results in the fatal lymphoproliferative disorder of the scurfy mouse. Nature Genetics. **27** (1): 68-73.
73. Bennett, C.L., Christie, J., Ramsdell, F., Brunkow, E., Ferguson, P.J., Whitesell, L., Kelly, T.E., Saulsbury, F.T., Chance, P.F., Ochs, H.D. (2001). The immune dysregulation, polyendocrinopathy, enteropathy, X-linked syndrome (IPEX) is caused by mutations of FOXP3. Nature Genetics. **27** (1): 20-21.
74. Asseman, C., Mauze, S., Leach, M.W., Coffman, R.L., Powrie, F. (1999). An essential role for interleukin 10 in the function of regulatory T cells that inhibit intestinal inflammation. J Exp Med. **190** (7): 995-1004.
75. Kursar, M., Koch, M., Mittrucker, H.W., Nouailles, G., Bonhagen, K., Kamradt, T., Kaufmann, S.H.E. (2007). Cutting Edge: Regulatory T cells prevent efficient clearance of *Mycobacterium tuberculosis*. J Immunol. **178** (5): 2661-2665.
76. McGeachy, M.J., and Cua, D.J. (2007). T cells doing it for themselves: TGF-beta regulation of Th1 and Th17 cells. Immunity. **26** (5): 547-549.
77. Joetham, A., Takeda, K., Taube, C., Miyahara, N., Matsubara, S., Koya, T., Rha, Y.H., Dakhama, A., Gelfand, E.W. (2007). Naturally occurring lung CD4(+)CD25(+) T cell regulation of airway allergic responses depends on IL-10 induction of TGF-beta. J Immunol. **178** (3): 1433-1442.
78. Gondek, D.C., Lu, L.F., Quezada, S.A., Sakaguchi, S., Noelle, R.J. (2005). Cutting edge: contact-mediated suppression by CD4+CD25+ regulatory cells involves a granzyme B-dependent, perforin-independent mechanism. J Immunol. **174** (4):1783-1786.
79. Zhao, D.M., Thornton, A.M., Dipaolo, R.J., Shevach, E.M. (2006). Activated CD4+CD25+ T cells selectively kill B lymphocytes. Blood. **107** (10): 3925-3932.
80. Cao, X., Cai, S.F., Fehniger, T.A., Song, J., Collins, LI., Piwnica-Worms, D.R, Ley, T.J. (2007). Granzyme B and perforin are important for regulatory T cell-mediated suppression of tumor clearance. Immunity. **27** (4): 635-646.
81. Zheng, S.G., Wang, J.H., Stohl, W., Kim, K.S., Gray, J.D., Horwitz, D.A. (2006). TGF-beta requires CTLA-4 early after T cell activation to induce FoxP3 and generate adaptive CD4+CD25+ regulatory cells. J Immunol. **176** (6): 3321-3329.

82. Mellor, A.L., Chandler, P., Baban, B., Hansen, A.M., Marshall, B., Pihkala, J., Waldmann, H., Cobbold, S., Adams, E., Munn, D.H. (2004). Specific subsets of murine dendritic cells acquire potent T cell regulatory functions following CTLA4-mediated induction of indoleamine 2,3 dioxygenase. Internatonal Immunology. **16** (10): 1391-1401
83. Xu, H., Zhang G.X., Ciric, B., Rostami A. (2008). IDO: a double-edged sword for T(H)1/T(H)2 regulation. Immunol Lett. **121** (1): 1-6.
84. Campanelli, A.P., Roselino, A.M., Cavassani, K.A., Pereira, M.S.F., Mortara, R.A., Brodskyn, C.I., Gonçalves, H.S., Belkaid, Y., Barral-Netto, M., Barral, A., Silva, J.S. (2006). CD4+CD25+ T Cells in Skin Lesions of Patients with Cutaneous Leishmaniasis Exhibit Phenotypic and Functional Characteristics of Natural Regulatory T Cells. The Journal of Infectious Diseases. **193** (9): 1313-1322.
85. Xu, D., Liu, H., Komai-Koma, M., Campbell, C., McSharry C, Alexander, J., Liew, F.Y. (2003). CD4+CD25+ regulatory T cells suppress differentiation and functions of Th1 and Th2 cells, *Leishmania major* infection, and colitis in mice. J Immunol. **170** (1): 394-399.
86. Mendez, S., Reckling, S.K., Piccirillo, C.A., Sacks, D., Belkaid, Y. (2004). Role for CD4+ CD25+ regulatory T cells in reactivation of persistent leishmaniasis and control of concomitant immunity. J Exp Med. **200** (2): 201-210.
87. Suffia, I., Reckling, S.K., Salay, G., Belkaid, Y. (2005). A role for CD103 in the retention of CD4+CD25+ Treg and control of *Leishmania major* infection. J Immunol. **174** (9): 5444-5455.
88. Belkaid, Y., Piccirillo, C., Mendez, S., Shevach, E.M., Sacks, D.L. (2002). CD4+CD25+ regulatory T cells control *Leishmania major* persistence and immunity. Nature. **420** (12): 502-507.
89. Abdel Aziz, N., Nono, J.K., Mpotje, T., Brombacher, F. (2018). The Foxp3+ regulatory T-cell population requires IL-4Ralpha signaling to control inflammation during helminth infections. PLoS Biol. **16** (10): 1-30.
90. Wan, Y.Y., and Flavell, R.A. (2007). Regulatory T-cell functions are subverted and converted owing to attenuated Foxp3 expression. Nature. **445** (7129): 766-770.
91. Williams, L.M., and Rudensky, A.Y. (2007). Maintenance of the Foxp3-dependent developmental program in mature regulatory T cells requires continued expression of Foxp3. Nature Immunology. **8** (3): 277-284.
92. Chapoval, S., Dasgupta, P., Dorsey, N.J., Keegan, A.D. (2010). Regulation of the T helper cell type 2 (Th2)/T regulatory cell (Treg) balance by IL-4 and STAT6. Journal of Leukocyte Biology. **87** (6): 1011-1018.
93. Wei, J., Duramad, O., Perng, O.A., Reiner, S.L., Liu, Y., Qin, F.X. (2007). Antagonistic nature of T helper 1/2 developmental programs in opposing peripheral induction of Foxp3+ regulatory T cells. Proc Natl Acad Sci. **104** (46): 18169-18174.
94. Belkaid, Y., Kamhawi, S., Modi, G., Valenzuela, J., Noben-Trauth, N., Rowton, E., Ribeiro, J., Sacks, D.L. (1998). Development of a natural model of cutaneous leishmaniasis: Powerful effects of vector saliva and saliva preexposure on the long-term outcome of *Leishmania major* infection in the mouse ear dermis. Journal of Experimental Medicine. **188** (10): 1941-1953.
95. Aljanabi, S.M, and Martinez, I. (1997). Universal and rapid salt-extraction of high quality genomic DNA for PCR-based techniques. Nucleic Acids Research. **25** (22): 4692-4693.
96. Rodgers, M.R., Popper, S.J., Wirth, D.F. (1990). Amplification of kinetoplast DNA as a tool in the detection and diagnosis of *Leishmania*. Experimental Parasitology. **71** (3): 267-275.
97. Ranasinghe, S., Wickremasinghe, R., Hulangamuwa, S., Sirimanna, G., Opathella, N., Maingon, R.D.C., Chandrasekharan, V. (2015). Polymerase chain reaction detection of Leishmania DNA in skin biopsy samples in Sri Lanka where the causative agent of cutaneous leishmaniasis is *Leishmania donovani*. Mem Inst Oswaldo Cruz. **110** (8): 1017-1023.

98. Wenchao, A., Haishan, L., Naining, S., Lei, L., Huiming, C. (2013). Optimal method to stimulate cytokine production and its use in immunotoxicity assessment. Int. J. Environ. Res. Public Health. **10** (9): 3834-3842.
99. Mollenhauer, H.H., Morré, J.D., Rowe, L.D. (1990). Alteration of intracellular traffic by monensin; mechanism, specificity and relationship to toxicity. Biochimica et Biphysica Acta. **1031** (2): 225-246.
100. Modolell, M., Corraliza, I.M., Link, F., Soler, G., Eichmann, K. (1995). Reciprocal regulation of the nitric oxide synthase/arginase balance in mouse bone marrow-derived macrophages by Th1 and Th2 cytokines. European Journal of Immunology. **25** (4): 1101-1104.
101. Streit, J.A., Donelson, J.E., Agey, M.W., Wilson, M.E. (1996). Developmental changes in the expression of *Leishmania chagasi* gp63 and heat shock proteins in a human macrophage cell line. Infection and Immunity. **64** (5): 1810-1818.
102. Lowenthal, J.W., Castle, B.E., Christiansen, J., Schreurs, J., Rennick, D., Arai, N., Hoy, P., Takebe, Y., Howard, M. (1988). Expression of high affinity receptors for murine interleukin 4 (BSF-1) on hemopoietic and nonhemopoietic cells. J Immunol. **140** (2): 456-464.
103. Zheng, S.G., Wang, J.H., Gray, J.D., Soucier, H., Horwitz, D.A. (2004). Natural and induced $CD4^+CD25^+$ cells educate $CD4^+CD25^-$ cells to develop suppressive activity: the role of IL-2, TGF-beta, and IL-10. J Immunol. **172** (9): 5213-5221.
104. Cassatella, M.A., Meda, L., Bonora, S., Ceska, M., Constantin, G. (1993). Interleukin 10 (IL-10) inhibits the release of proinflammatory cytokines from human polymorphonuclear leukocytes. Evidence for an autocrine role of tumor necrosis factor and IL-1 beta in mediating the production of IL-8 triggered by lipopolysaccharide. J Exp Med. **178** (6): 2207-2211.
105. Baldwin, T.M., Elso, C., Curtis, J., Buckingham, L., Handman, E. (2003). The site of *Leishmania major* infection determines disease severity and immune responses. Infection and Immunity. **71** (12): 6830-6834.
106. Belkaid, Y., Mendez, S., Lira, R., Kadambi, N., Milon, G., Sacks, D. (2000). A natural model of *Leishmania major* infection reveals a prolonged "silent" phase of parasite amplification in the skin before the onset of lesion formation and immunity. J Immunol. **165** (2): 969-977.
107. Parihar, S.P., Hartley, M., Hurdayal, R., Guler, R., Brombacher, F. (2016). Topical Simvastatin as Host-Directed Therapy against Severity of Cutaneous Leishmaniasis in Mice. Scientific Reports. **6** (1): 1-10.
108. Makala, L.H.C., Baban, B., Lemos, H., El-Awady, A.R., Chandler, P.R., Hou, D.Y., Munn, D.H., Mellor, A.L. (2011). *Leishmania major* attenuates host immunity by stimulating local indoleamine 2,3-dioxygenase expression. Journal of Infectious Diseases. **203** (5): 715-725.
109. Makala, L. (2012). The role of indoleamine 2, 3 dioxygenase in regulating host immunity to *Leishmania* infection. Journal of Biomedical Science. **19** (1): 1-8.
110. Baban, B., Chandler, P.R., Johnson, B.A., Huang, L., Li, M., Sharpe, M.L., Francisco, L.M., Sharpe, A.H., Blazar, B.R., Munn, D.H., Mellor, A.L. (2011). Physiologic control of IDO competence in splenic dendritic cells. J Immunol. **187** (5): 2329-2335.
111. Munn, D.H., and Mellor, A.L. (2016). IDO in the Tumor Microenvironment: Inflammation, Counter-Regulation, and Tolerance. Trends Immunol. **37**(3): 193-207.
112. Grohmann, U., Orabona, C., Fallarino, F., Vacca, C., Calcinaro, F., Falorni, A., Candeloro, P., Belladonna, M.L., Bianchi, R., Fioretti, M.C., Puccetti, P. (2002). CTLA-4-Ig regulates tryptophan catabolism *in vivo.* Nature Immunology. **3** (11): 1097-1101.
113. Fallarino, F., Grohmann, U., Vacca, C., Bianchi, R., Orabona, C., Spreca, A., Fioretti, M.C., Puccetti, P. (2002). T cell apoptosis by tryptophan catabolism. Cell Death and Differentiation. **9** (10): 1069-1077.

114. Okwor, I., and Uzonna, J. (2008). Persistent parasites and immunologic memory in cutaneous leishmaniasis: implications for vaccine designs and vaccination strategies. Immunol Res, **41** (2): 123-36.
115. Von Stebut, E., Ehrchen, J.M., Belkaid, Y., Kostka, S.L., Mölle, K., Knop, J., Sunderkötter, C., Udey, M.C. (2003). Interleukin 1alpha promotes Th1 differentiation and inhibits disease progression in *Leishmania major*-susceptible BALB/c mice. . J Exp Med, **198** (2): 191-199.
116. Lyon, M. (1961). Gene Action in the X-chromosome of the Mouse *(Mus musculus L.).* Nature. **190**: 372-373.
117. Nagase, H., Jones, K.M., Anderson, C.F and Noben-Trauth, N. (2007). Despite increase CD4+Foxp3+ cells within the infection site BALB/c IL-4 receptor-deficient mice reveal CD4+Foxp3- negative T cells as a source of IL-10 in *Leishmania major* susceptibility. The Journal of Immunology. **179** (4): 2435-2444.
118. Nabavi, N.S., Pezeshkpoor, F., Valizadeh, N., Ahmadi Ghezeldasht, S., Rezaee, S.A. (2018). Increased Th17 functions are accompanied by Tregs activities in lupoid leishmaniasis. Parasite Immunology. **40** (1): 1-6.
119. Meiler, F., Klunker, S., Zimmermann, M., Akdis, C.A., Akdis, M. (2008). Distinct regulation of IgE, IgG4 and IgA by T regulatory cells and toll-like receptors. Allergy. **63** (11): 1455-1463.
120. Loeuillet, C., Bañuls, A.L., Hide, M. (2006). Study of *Leishmania* pathogenesis in mice: experimental considerations. Parasites and Vectors. **9**: 144.
121. Rani, R., Jordan, M.B., Divanovic, S., Herbert, D.R. (2012). IFN-γ-driven IDO production from macrophages protects IL-4Rα-deficient mice against lethality during *Schistosoma mansoni* infection. American Journal of Pathology. **180** (5): 2001-2008.
122. Mellor, A.L., and Munn, D.H. (2004). IDO expression by dendritic cells: tolerance and tryptophan catabolism. Nat Reviews Immunology. **4** (10): 762-774.
123. Sharma, M.D., Hou, D.Y, Liu, Y., Koni, P.A., Metz, R., Chandler, P., Mellor, A.L., He, Y., Munn, D.H. (2009). Indoleamine 2,3-dioxygenase controls conversion of Foxp3+ Tregs to TH17-like cells in tumor-draining lymph nodes. Blood. **113** (24): 6102-6111.
124. Rodriguez-Pinto, D., Navas, A., Blanco, V.M., Ramirez, L., Garcent, D., Cruz, A., Craft, N., and Saravia, N.G. (2012). Regulatory T cells in the pathogenesis and healing of chronic human dermal leishmaniasis caused by *Leishmania* (*Viannia*) species.PLoS Negl Trop Dis. **6** (4): 1-11.

6. Appendix

List of Flow Cytometry Antibodies used

Antibody	Company	Clone	Catalogue Number	Dilution
CD3	BD Pharmingen	500A2	557984	1:320
CD4	BD Pharmingen	RM4-5	553052	1:640
CD19	BD Pharmingen	1D3	551001	1:320
IL-4Rα (CD124)	BD Pharmingen	mIL4R-M1	552509	1:160
PD-1	Biolegend	29F.1A12	135208	1:320
Ki67	BD Pharmingen	B56	51-36525X	1:50
GATA3	BD Pharmingen	L50-823	560405	1:40
T-bet	eBioScience	eBio4B10	12-5825-82	1:40
RoRγt	BD Pharmingen	Q31-378	562683	1:40
Foxp3	BD Pharmingen	MF23	560401	1:100
IFN-γ	BD Pharmingen	XMG1.2	554412	1:50
IL-4	BD Pharmingen	11B11	560700	1:50
IL-13	eBioScience	eBio13A	53-7133-82	1:50
IL-10	eBioScience	JES5-16E3	12-7101-82	1:50
CD11c	BD Pharmingen	HL3	560583	1:320
CD11b	BD Pharmingen	M1/70	560455	1:640
MHC-II	eBioScience	M51114.15.2	17-5321-82	1:640
B220	BD Horizon	RA3-6B2	561226	1:640
CD80	BD Pharmingen	16-10A1	553769	1:320
PD-L1	Biolegend	10F.9G2	124311	1:320
IDO	eBioScience	mIDO-48	11-9473-82	1:100
Streptavidin	BD Horizon		562284	1:1000

List of ELISA Antibodies

Cytokine Antibody		Company	Clone/Catalogue number	Final Concentration
IL-4	Primary	BD Biosciences	11B11	2 µg/ml
	Standard	BD Biosciences	550067	100 ng/ml
	Secondary	BD Biosciences	BVD6-24G2	0.5 µg/ml
IL-10	Primary	WhiteSci	MAB417-500	1 µg/ml
	Standard	WhiteSci	417-ML-005	100 ng/ml
	Secondary	Biocom Biotech	504906	0.5 µg/ml
TGF-β	Primary	BD Biosciences	555052	1:500
	Standard	WhiteSci	240-B-002	100 ng/ml
	Secondary	BD Biosciences	555053	1:250
IFN-γ	Primary	Lab-made (UCT)	AN18KL6	1 µg/ml
	Standard	BD Biosciences	554587	500 ng/ml
	Secondary	BD Biosciences	XMG1.2	0.5 µg/ml

Supplementary Figures

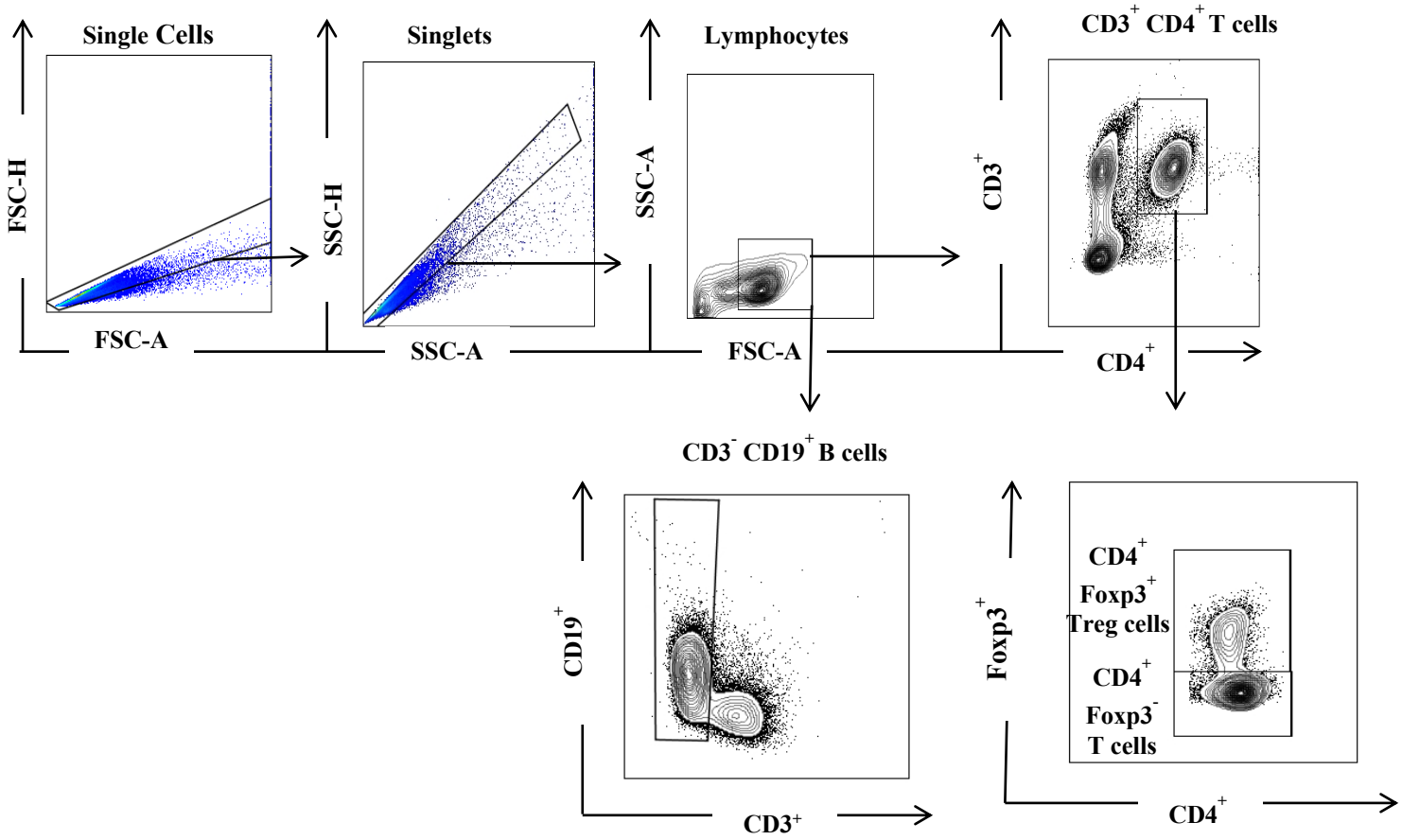

Supplementary Figure 1: Gating strategies used to analyse $CD19^+$ B cell, $CD4^+$ $Foxp3^+$ and $CD4^+Foxp3^-$ T cell populations. Experimental mice were subcutaneously infected with $2x10^6$ stationary phase *L. major* LV39 promastigotes into the left hind footpad. Popliteal lymph node cells were isolated from *L. major* infected experimental mice, stained and gated for B cell ($CD3^-CD19^+$) and T cell populations ($CD3^+CD4^+$). The Treg cell population was identified as $CD4^+$ $Foxp3^+$. The following analyses are representative of 4 independent experiments with 5 mice per group.

Female

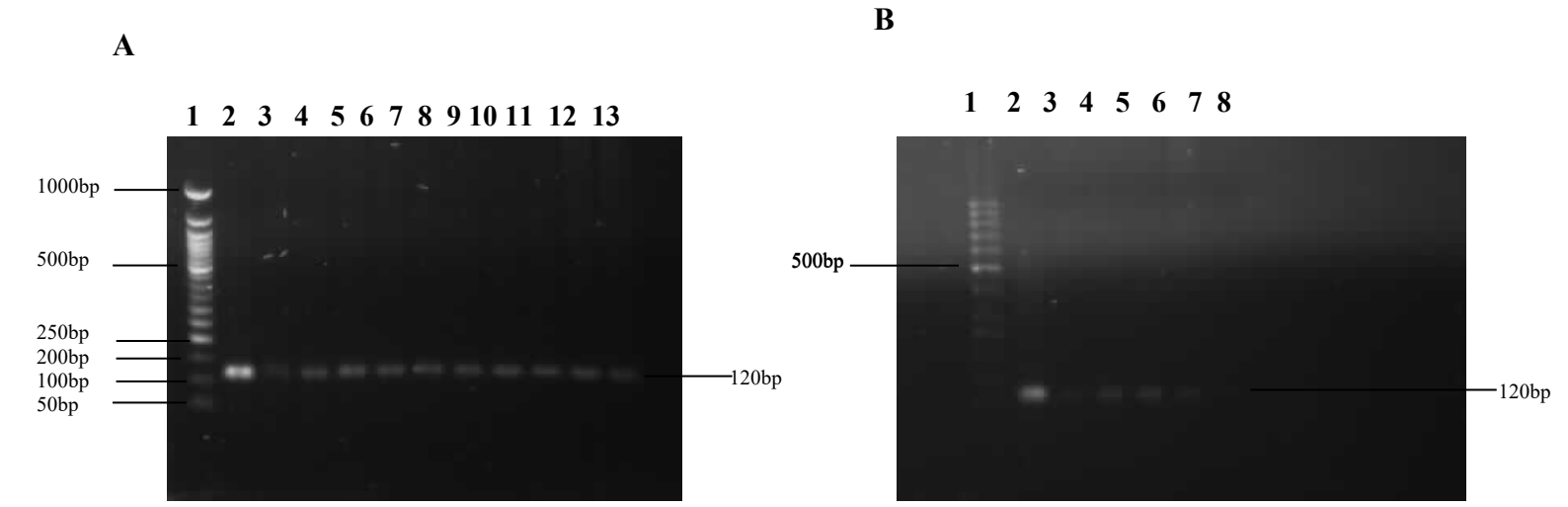

Male

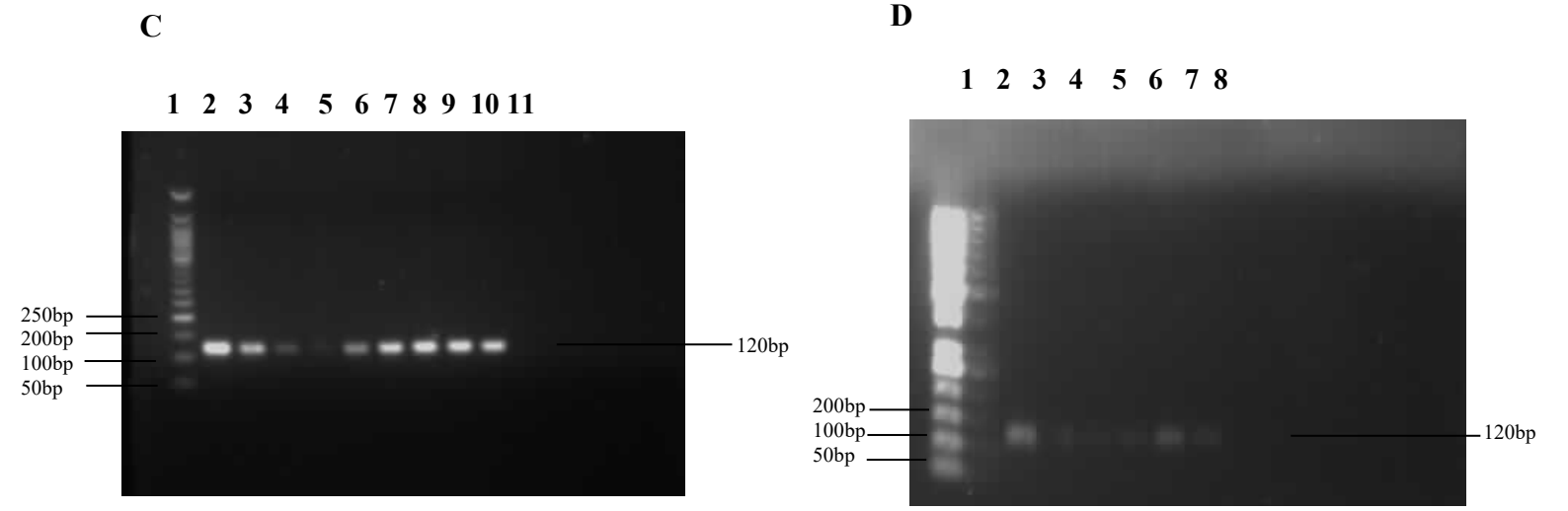

Supplementary Figure 2: *Leishmania* parasite DNA is significantly increased in Foxp3^{cre}IL-4Rα$^{-/lox}$ male mice. Experimental mice were subcutaneously infected in the left hind footpad with 2x10^6 stationary phase *L. major* LV39 promastigotes. At 8 weeks post infection, amastigote kinetoplast DNA extracted from infected footpads was amplified via PCR with JW11/JW12 primers. The final 120 bp PCR products were electrophoresed on 1.5% agarose gels and visualized following ethidium bromide staining under UV illumination. (A) Lane 1: 50 bp DNA ladder; Lane 2: *L. major in vitro* culture; Lanes 3-7: Female IL-4Rα$^{-/lox}$ samples; Lanes 8-12; Female Foxp3^{cre}IL-4Rα$^{-/lox}$ samples; Lane 13: Negative Control (No DNA). (B) Lane 1: 50bp DNA ladder; Lane 2: *L. major in vitro* culture; Lanes 3-7: Female C57BL/6 samples; Lane 8: -ve control. (C) Lane 1: 50 bp DNA ladder; Lane 2: *L. major in vitro* culture; Lanes 3-6: Male IL-4Rα$^{-/lox}$ samples; Lanes 7-10: Male Foxp3^{cre}IL-4Rα$^{-/lox}$ samples; Lane 11: -ve control. (D) Lane 1: 50bp DNA ladder; Lane 2: *L. major in vitro* culture; Lanes 3-6: Male C57BL/6 samples; Lane 8: -ve control. Results are representative of one independent experiment.

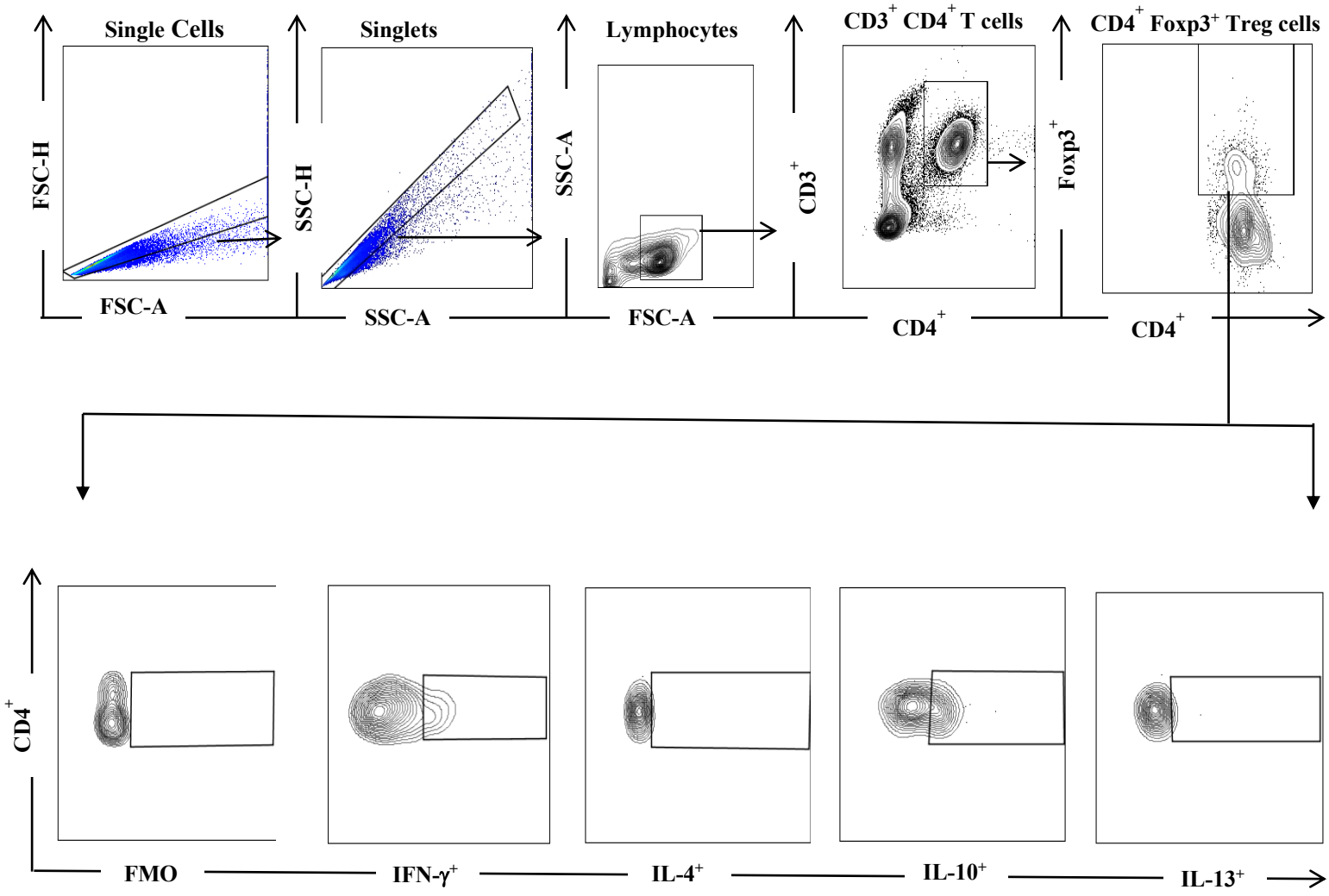

Supplementary Figure 3: Gating strategies used to identify cytokine-producing Treg cell populations. Experimental mice were subcutaneously infected with $2x10^6$ stationary phase *L. major* LV39 promastigotes into the left hind footpad. Popliteal lymph node cells were isolated from *L. major* infected experimental mice, stained and gated for Treg cell populations ($CD4^+Foxp3^+$). Cytokine secreting Treg cells were gated for the production of IFN-γ, IL-4, IL-10 and IL-13, within the popliteal lymph node following PMA/Ionomycin stimulation in the presence of monensin. The following analyses are representative of 2 independent experiments with 5 mice per group.

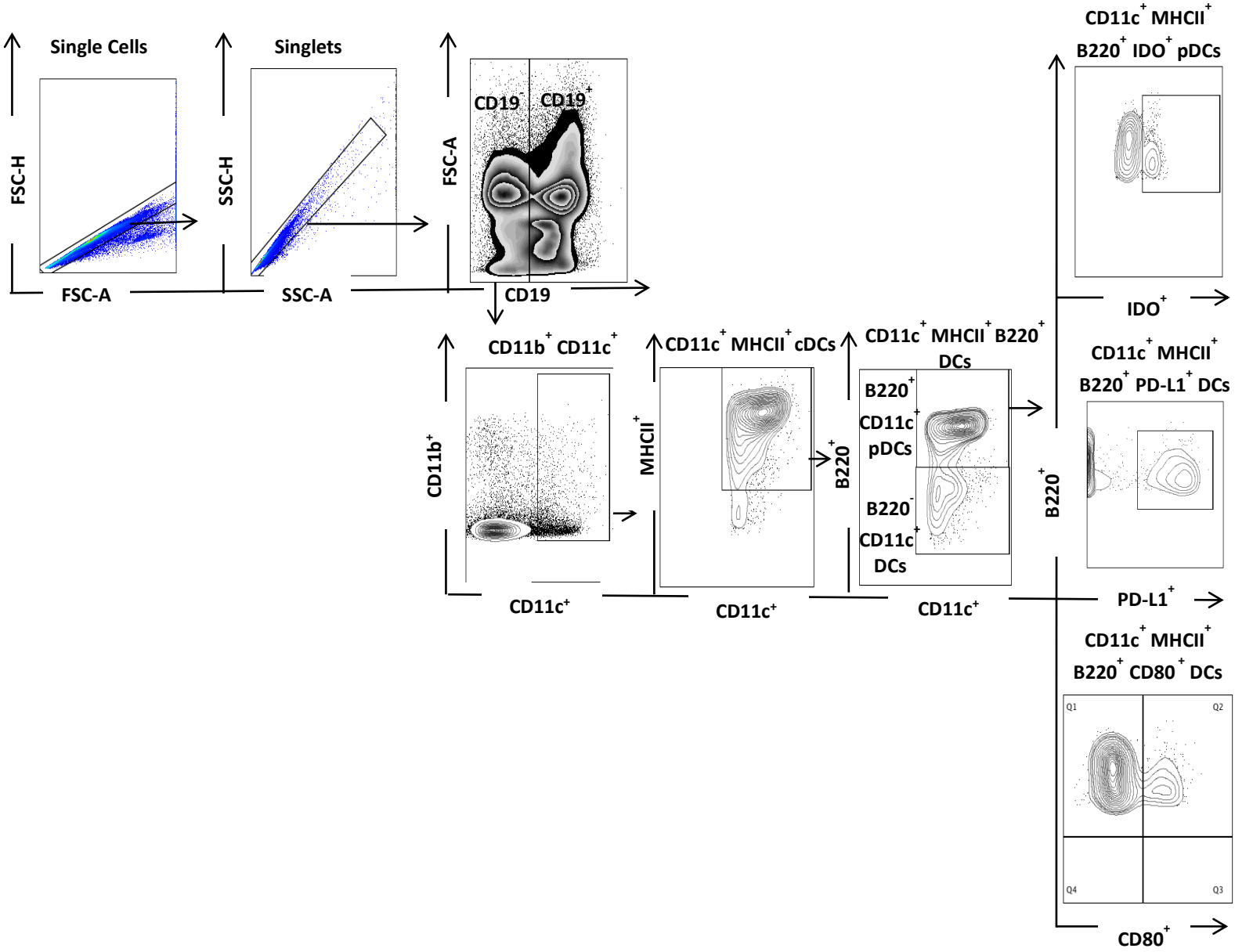

Supplementary Figure 4: Gating strategies used to CD11c$^+$ dendritic cell populations. Experimental mice were subcutaneously infected with 2x10^6 stationary phase *L. major* LV39 promastigotes into the left hind footpad. Popliteal lymph node cells from Foxp3^{cre}IL-4Rα and their littermate control mice were stained and gated to identify various dendritic cell populations. Dendritic cells populations were differentiated according to the following markers: conventional dendritic cells (cDCs; CD19$^-$CD11b$^+$CD11c$^+$MHCII$^+$), plasmacytoid DCs (pDCs; CD11c$^+$MHCII$^+$B220$^+$) and dendritic cells expressing CD80, PD-L1 and IDO. The following analyses are representative of 1 independent experiment with 5 mice per group.

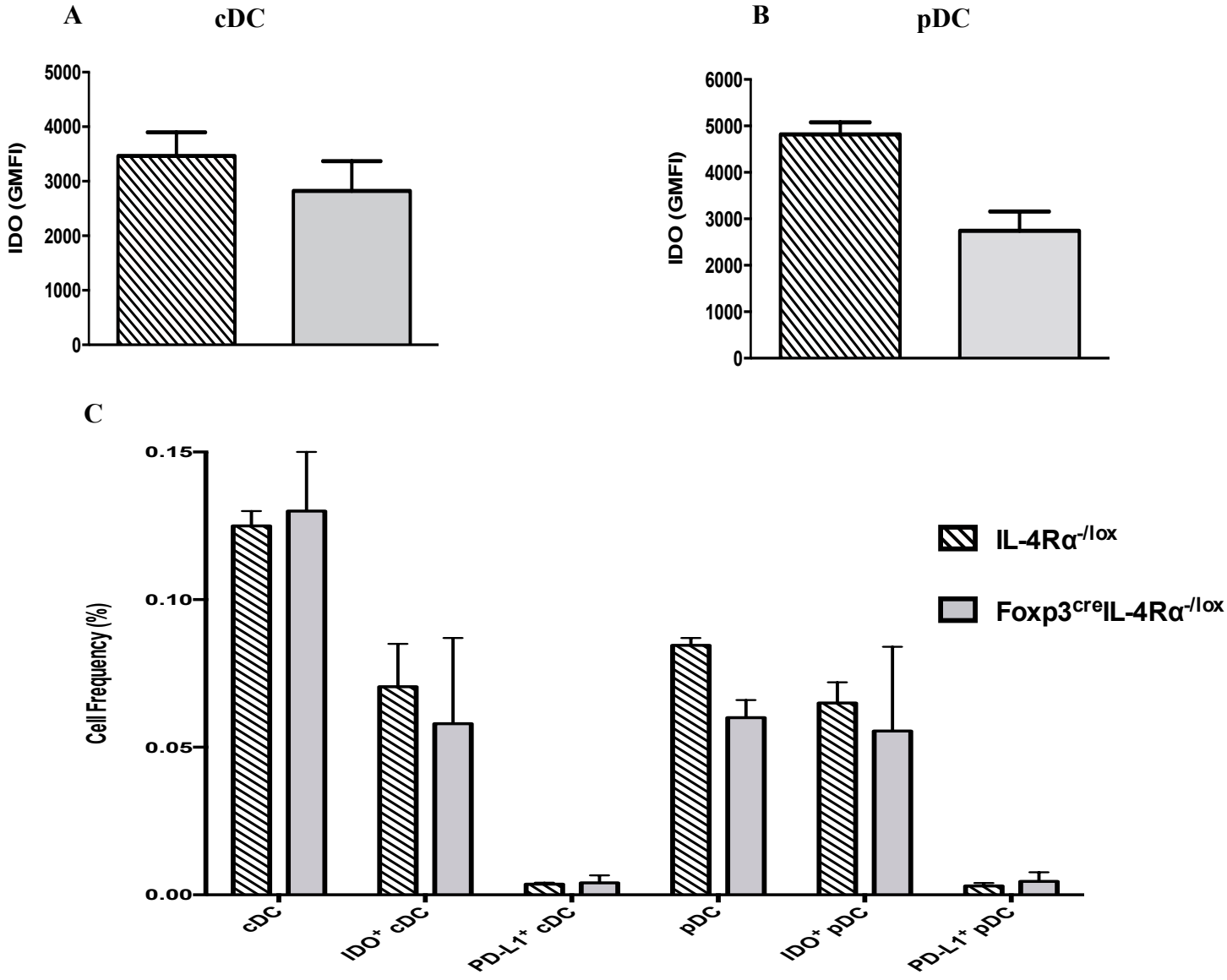

Supplementary Figure 5: Dendritic cell populations expression of IDO and PD-L1 in naïve experimental mice. Geometric mean fluorescent intensity (GMFI) of IDO expression was determined by flow cytometry analysis from the popliteal lymph nodes of naïve IL-4Rα$^{-/lox}$ and Foxp3^{cre}IL-4Rα$^{-/lox}$ male mice. (A) IDO GMFI in conventional dendritic cells (cDCs; CD19^{-}CD11b^{+}CD11c^{+}MHCII^{+}), (B) IDO GMFI in plasmacytoid DCs (pDCs; CD11c^{+}MHCII^{+}B220^{+}), (C) Frequency of IDO expressing or PD-L1 expressing dendritic cell subpopulations from the popliteal lymph nodes of naïve mice**.** The following analyses are representative of 1 independent experiment with 5 mice per group expressed as mean±SEM.

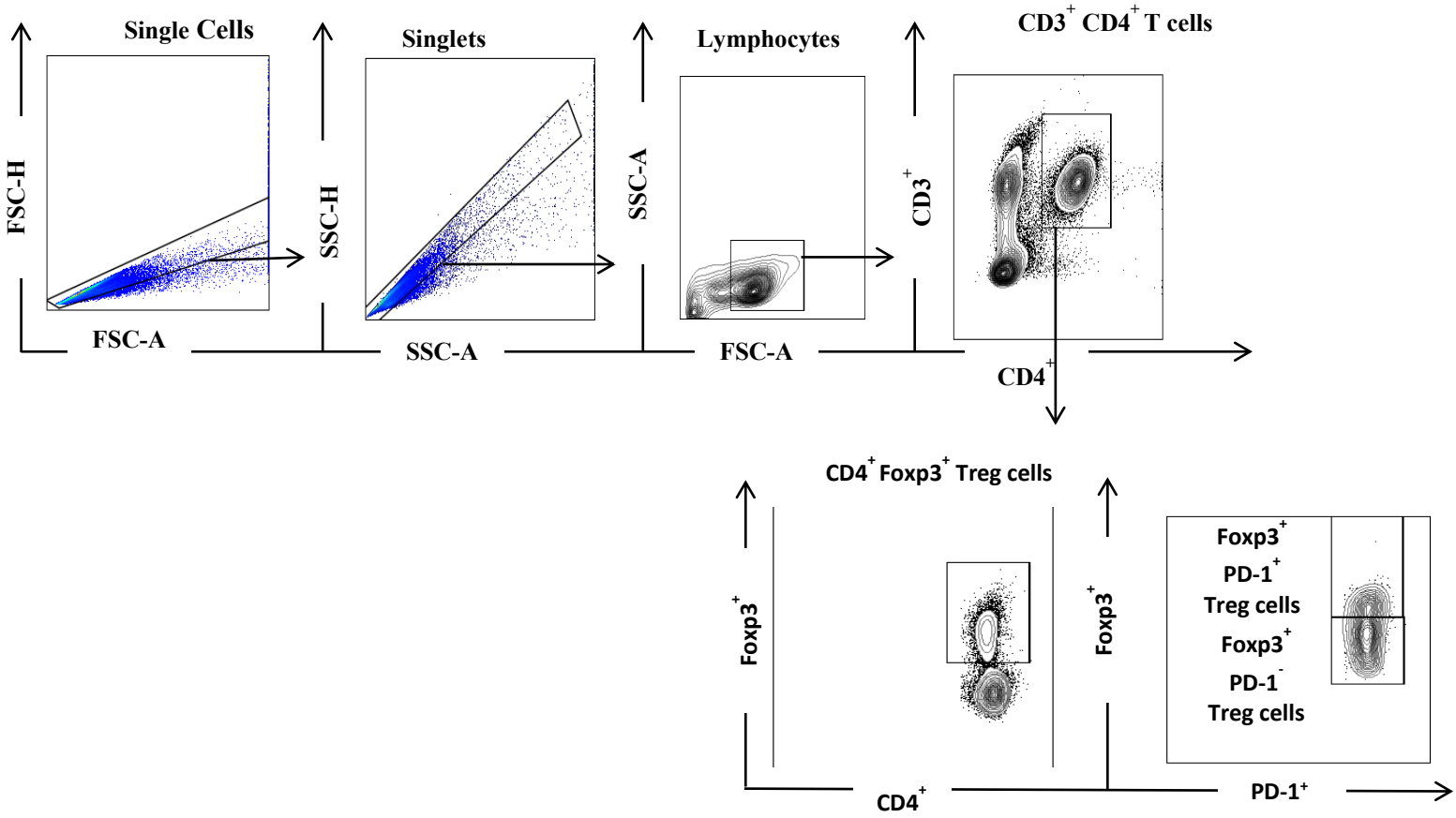

Supplementary Figure 6: Gating strategies used to identify PD-1 expressing Foxp3$^+$ Treg cells Experimental mice were subcutaneously infected with 2x10^6 stationary phase *L. major* LV39 promastigotes into the left hind footpad. Popliteal lymph node cells were isolated from Foxp3^{cre}IL-4Rα and their littermate control mice stained and gated for expression of PD-1 on the Treg cell population (CD4$^+$ Foxp3$^+$). The following analyses are representative of 1 independent experiment with 5 mice per group.

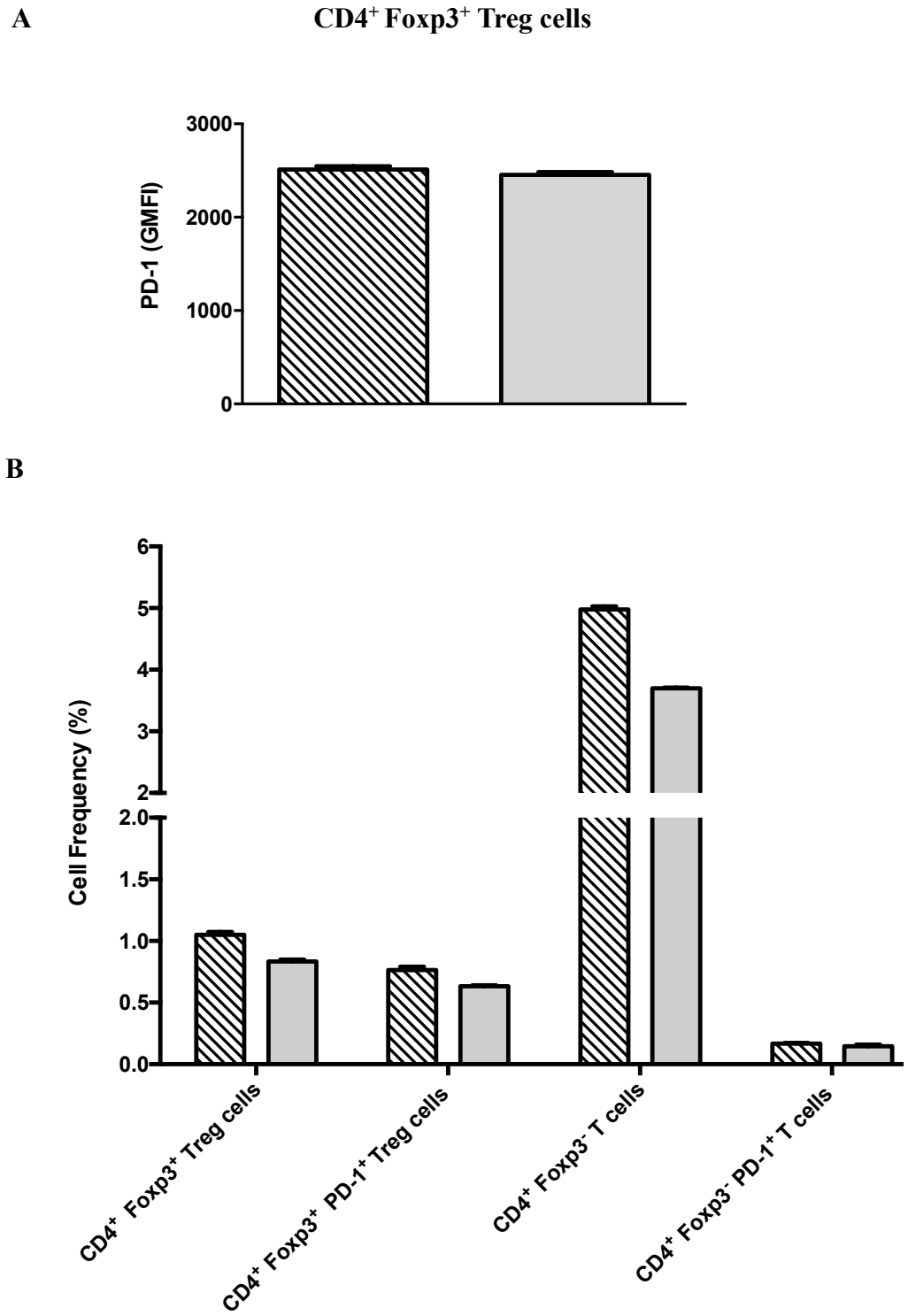

Supplementary Figure 7: Treg cell population expression of PD-1 in naïve experimental mice. Geometric mean fluorescent intensity (GMFI) of PD-L1 expression was determined by flow cytometry analysis from the popliteal lymph nodes of naïve IL-4Rα$^{-/lox}$ and Foxp3^{cre}IL-4Rα$^{-/lox}$ male mice. (A) PD-1 GMFI in CD4^{+}Foxp3^{+} Treg cells (B) Frequency of PD-1 expressing T cell populations from the popliteal lymph nodes of naïve mice**.** The following analyses are representative of 1 independent experiment with 5 mice per group expressed as mean±SEM.

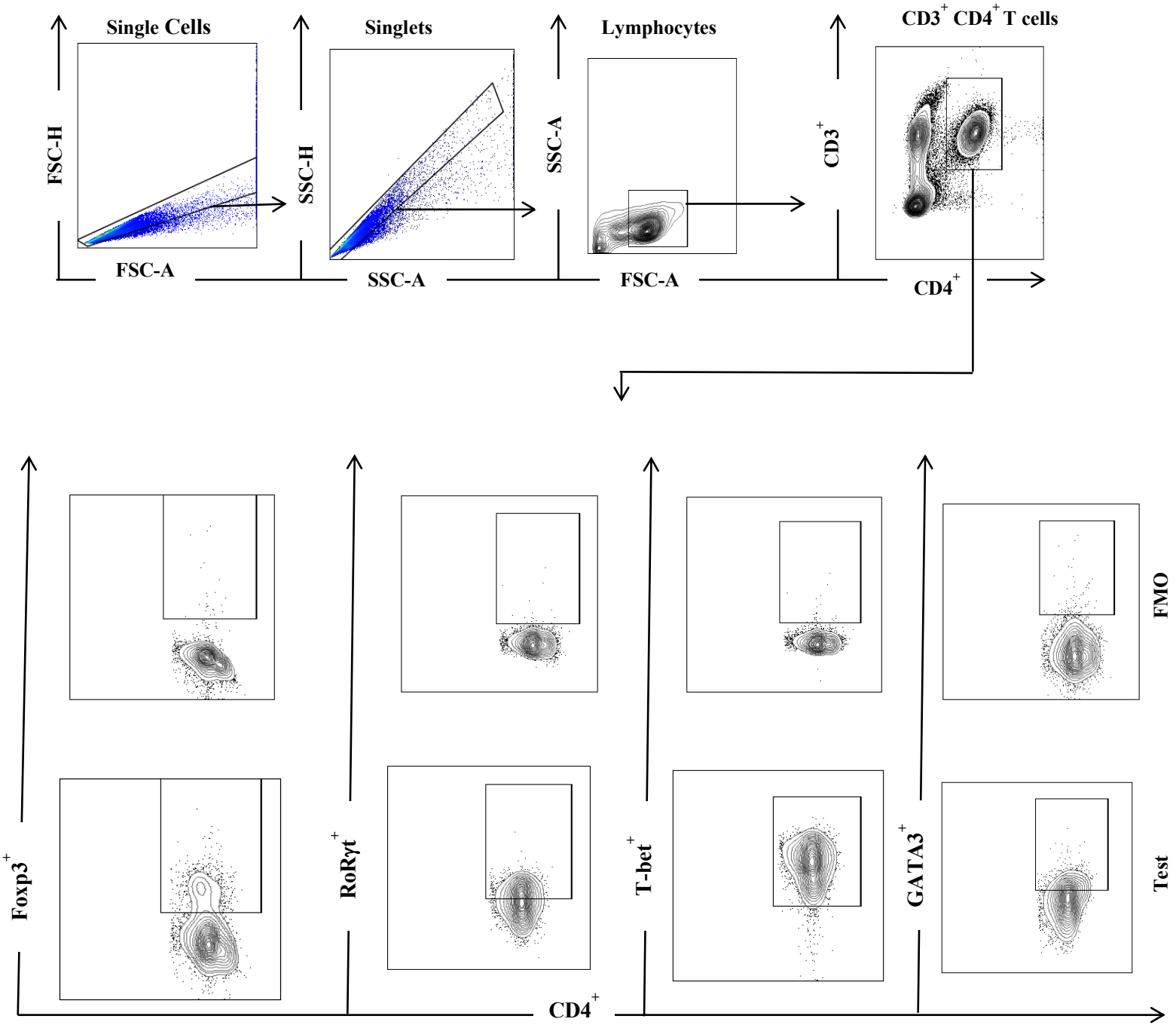

Supplementary Figure 8: Gating strategies used to identify transcription factor expressing T cell populations. Experimental mice were subcutaneously infected with $2x10^6$ stationary phase *L. major* LV39 promastigotes into the left hind footpad. Popliteal lymph node cells were isolated from *L. major* infected experimental mice, stained and gated for T cell populations ($CD3^+CD4^+$). Treg cells were identified as $CD4^+$ $Foxp3^+$, Th17 cells were identified as $CD4^+RoR\gamma t^+$, Th1 cells were identified as $CD4^+$T-bet^+ and Th2 cells were identified as $CD4^+GATA3^+$. FMO: Fluorescence minus one. The following analyses are representative of 2 independent experiments with 5 mice per group.